Experimental Investigation of the Effects of Coagulant Dose and Permeate Flux on Membrane Fouling in a Moving Bed Biofilm Reactor - Membrane Process

by

Masoomeh Karimi

A thesis

presented to the University of Waterloo

in fulfillment of the

thesis requirement for the degree of

Master of Applied Science

in

Chemical Engineering

Waterloo, Ontario, Canada, 2012

AUTHOR'S DECLARATION

I hereby declare that I am the sole author of this thesis. This is a true copy of the thesis, including any required final revisions, as accepted by my examiners.

I understand that my thesis may be made electronically available to the public.

Abstract

The application of membrane bioreactors (MBRs) to wastewater treatment is increasing due to their ability to operate at high biomass concentrations and to deliver effluents of high quality. The major challenges associated with the application of MBRs is fouling which can shorten the useful life of the membrane, increase in the amount of energy consumed, and the cost for membrane cleaning. The main reasons for fouling are the deposition of solids as a cake layer, pore plugging by colloidal particles, adsorption of soluble compounds and biofouling. Fouling is a particular problem for activated sludge membrane bioreactors (AS-MBRs) since this process deals with liquors having a high concentration of total solids as well as dissolved compounds such as extracellular polymeric substances (EPS). The combination of a moving bed biofilm reactor and a membrane reactor (MBBR-MR) has significant potential. It may be considered as a compact wastewater treatment process which can compensate for the drawbacks of AS-MBRs. Readily biodegradable COD is removed in the MBBR while particulate matter is separated by the membrane. To further reduce the membrane fouling the effects of adding an intermediate coagulation stage was investigated critically on membrane fouling.

The present study includes an overall assessment of the performance of a combined MBBR-MR system, based on the chemical oxygen demand (COD) removal efficiency and membrane fouling mechanism. The required test runs were conducted using pilot-scale MBBR and ultra filtration membrane. The pilot MBBR had a working volume of 1.8 m^3 with a 60% carrier fill fraction. The MBBR was operated with loading rate of 78 ± 21 $g/m^2/d$ (HRT of 4 h). The ultra-filtration was spiral wound and composed of polyethersulfone (PES) with a pore size of 0.03 microns. The MBBR feed was obtained from a final treated wastewater effluent in a food processing plant located in SW Ontario. In this research, ferric chloride was also employed as a coagulant and influences of different coagulant doses and permeate fluxes on membrane fouling were studied.

Based on the experimental results, it was found that the combination of MBBR with membrane filtration can produce a constant high quality permeate that is appropriate for water reuse purposes. The composition analysis of permeate showed that the stream is free of suspended solids and the average COD turns to 75 ± 25 mg/l. In addition, the

MBBR had a SCOD removal of 76% ± 7% which is considered as a reasonable efficiency for a single reactor.

Operating the membrane without adding coagulant caused rapid fouling in a short time period and the Trans Membrane Pressure (TMP) reached the maximum allowable pressure of 10 psi. However, addition of coagulant was found to decrease the fouling of the membrane as well as increasing the filtration time. The extent of the pre-coagulation effect on membrane fouling was found to strongly depend on the dosage of the coagulant and the MBBR effluent characteristics. A coagulant dose of 400 mg/l with a permeate flux of 7.6 LMH performed the best at reducing membrane fouling. Colloidal fouling was found to be a significant fouling mechanism at low coagulant dose (e.g. 200 mg/l), while cake formation appeared to be mainly responsible for fouling at higher coagulant doses.

Permeate flux was found to have a significant effect on the fouling of the membrane. The presence of colloidal matters at low fluxes and TSS at higher fluxes were responsible for fouling of the membrane by blocking the pores and formation of the cake layer on the membrane surface, respectively. Then later addition of Dissolved Air Flotation (DAF) inside the factory had a noticeable effect on wastewater characteristics and consequently on fouling of the membrane. A 22% and 31% improvement in TCOD and TSS in the wastewater was observed leading to reduction in the fouling.

Acknowledgements

I would also like to acknowledge all my friends, who are also my family. If I were to mention everyone by name, it would take a few pages. I am thankful for all of them who stood behind me every step of the way.

Last, but indeed not least, I am very grateful to my husband, Sohrab Zendehboudi, my parents. They have all done so much I know that I cannot possibly thank them properly. In particular, thank them for the stabilizing role in the winding road that has lead to the completion of my M.Sc. This dissertation is a greater product for the continued role they have played in the life of its author.

Dedication

Dedicated to my lovely son, Daniel who is everything in my life.

Table of Contents

List of Figures

List of Tables

Nomenclature

Acronyms

AGTS	Attached Growth Total Solids
AS	Activated Sludge
BOD5	Biological Oxygen Demand for 5 days
CFF	Cross Flow Filtration
CFV	Cross Flow Velocity
COD	Chemical Oxygen Demand
DAF	Dissolved Air Flotation
DO	Dissolve Oxygen
DOC	Dissolve Organic Matter
EPS	Extracellular Polymeric Substances
HMS	Hydrolyzing Metal Salt
HRT	Hydraulic retention time
MBBR	Moving Bed Biofilm Reactor
MBR	Membrane Bioreactor
MF	Micro-Filtration
MLSS	Mixed Liquor Suspended Solids
MR	Membrane Reactor
MWCO	Molecular Weight Cut-Off
NF	Nano-Filtration
NOM	Natural Organic Matter
NTU	Nephlometric Turbidity Unit
PACl	Poly-Aluminium Chloride
PAFC	Polyaluminium Ferric Chloride
PES	Polyethersulfone
PLC	Programmable Logic Controller
PS	Polysulfone
PVDF	Polyvinylidene Fluoride
RAS	Return Activated Sludge
RO	Reverse Osmosis

SCOD	Soluble Chemical Oxygen Demand
SMP	Soluble Microbial Products
SP	Soluble Phosphorous
SS	Suspended Solids
TCF	Temperature Correction Factor
TCOD	Total Chemical Oxygen Demand
TFF	Tangential Flow Filtration
TKN	Total Kjeldahl Nitrogen
TMP	Trans Membrane Pressure
TOC	Total Organic Carbon
TP	Total Phosphorous
TSS	Total Suspended Solids
UF	Ultra-Filtration
VSS	Volatile Suspended Solids

Symbols: Latin, then Greek

GPM	Flow rate unit (gallon per minute)
SCFM	Air flow rate unit (standard cubic feet per minute sft^3/m)
LMH	Flux unit (L/m^2h)
μ	Dynamic viscosity (Pa.s)

Variables

Ac	Cross sectional area (m^2)
Flux	Flows through a unit area per unit time (L/m^2h)
J	Filtration flux (L/m^2h)
Q	Volumetric flow rate (m^3/s)
Q_P	Permeate flow rate (m^3/s)
R	Resistance (1/m)
R_t	Total resistance of the membrane (1/m)
U	Cross flow velocity (m/s)

CHAPTER 1

INTRODUCTION

1.1 The Growing Need for Water and Wastewater Treatment

The 21st century is called the "water century" where the aim is to find the most cost and effective process for the treatment of water by allowing reuse of the treated effluent (zero discharge concept) to protect the environment and water resources for the future (Li *et al*., 2008). Clearly, water is the most precious resource in the world when considering the limited water resources and large increases anticipated in water demand due to an increasing world population.

Every community or industry produces both liquid and solid waste. Industrial activities generate a large amount and variety of wastes products. The nature of industrial waste depends primarily on the industrial processes from which they originate. Some sources of industrial wastewater includes: agricultural waste, iron and steel industries, mines and quarries, food industries, complex organic chemicals industries and the nuclear industry. In industrial wastewater, the following substances are of major importance: (i) absorbable organic halogen compounds (AOX), (ii) chlorinated and halogenated hydrocarbons, (iii) hydrocarbons (benzene, phenol, and other derivatives), (IV) heavy metals, in particular mercury, cadmium, chromium, copper, nickel, and zinc, and (V) cyanides (Jördening and Winter, 2005).

Wastewater generated from agricultural and food operations have distinctive characteristics that set it apart from municipal wastewater. This includes that it is biodegradable and nontoxic, but that it has high concentrations of biochemical oxygen demand (BOD) and suspended solids (SS) (EEA, 2001). Processing of food produces wastes generated from cooking which are often rich in plant organic material and may also contain salt, flavouring, colouring material and acid or alkali. Very significant quantities of oil or fats may also be present. When untreated wastewater accumulates, the

decomposition of the organic matter it contains will lead to nuisance conditions including the production of aromatic gases (Tchobanoglous *et al.*, 2003). Wastewater also contains nutrients which can stimulate the growth of aquatic plants. For these reasons, the immediate removal of wastewater from its source of generation, followed by treatment and disposal, is not only desired but also necessary in an industrialized society (Tchobanoglous *et al.*, 2003). In this study, the potential reuse of water from a food processing factory was investigated by examining the use of a combined MBBR and membrane system.

1.2 Research Objectives

The primary goal of this study was to evaluate the benefits of integrating a moving bed biofilm reactor (MBBR) with a spiral wound membrane filter (MR) unit to determine the potential of producing a compact cost-efficient treatment facility that may be capable of generating treated effluents suitable for water reuse. The main objectives of this thesis are:

- Perform an overall assessment of the performance of a combined MBBR-MR system with respect to effluent quality
- Assess membrane fouling and COD removal efficiency in a MBBR-MR system during the treatment of industrial wastewater from a food manufacturer
- Optimize pre-coagulation requirements by determining suitable coagulant dosages based on membrane fouling and COD removal efficiency
- Evaluate membrane fouling mechanisms resulting from different operational conditions
- Compare the fouling reduction potential of different pre-treatment approaches in the upstream process

1.3 Research Approach

The experimental approach for this study was divided into two phases:

Phase I:

- Installation of a moving bed biofilm reactor (MBBR) in the industrial facility, establishment of the biofilm in the MBBR and detailed characterization of the wastewater. TSS, VSS, TCOD, SCOD, ammonia and phosphorous of the inlet and effluent streams of the MBBR were measured periodically to investigate the performance of the MBBR.
- Installation of the membrane pilot plant in the industrial facility with a coagulation stage and pre-treatment primary settling stage. Characteristics of the wastewater at different locations were measured as well as transmembrane pressure (TMP) and permeate flow rate of the membrane unit to investigate the effect of different coagulant dosages and permeate fluxes on membrane fouling.

Phase II: Operation of the pilot facility with enhanced primary settling following the addition of a dissolved air flotation (DAF) unit in the factory. The effect of changing the upstream pre-treatment on membrane fouling was conducted by comparing data from phase I.

CHAPTER 2

LITRATURE REVIEW

2.1 Background on Membrane Treatment

In 1920 micro-porous membranes were patented and employed for the first time (Belfort *et al.*, 1994) although their applications were limited to laboratory scale until 1950. Membranes were originally utilized to enumerate bacteria and remove microorganisms and particles from liquid and gas streams. They were employed for fractionating and sizing macro-molecules like proteins (MWH, 2005). Industrial applications started in the 1950's with the integration of membrane filtration into the pharmaceutical industry mainly for the sterilization of liquid pharmaceuticals and intravenous solutions. Industry gradually moved to the application of membranes in the removal of oils, fats, acids and brine from waste streams as an approach for wastewater treatment (MWH, 2005).

Membranes fall into four main groups including: microfiltration (MF), ultrafiltration (UF), nanofiltration (NF) and reverse osmosis (RO). Membrane classification is commonly based on pore size, molecular weight cut-off (MWCO) and the required pressure difference. MWCO indicates the removal characteristics of a membrane in terms of atomic weight or mass, usually expressed in Daltons (AWWA, 2005). A summary of various membrane types, their specifications and also applications is presented in Table 2-1.

Membranes currently have a variety of applications that include environmental, chemical, food, beverage, pharmaceutical and different separation processes. The application of membrane processes in water and wastewater treatment is rapidly growing in areas related to clarification and disinfection (Sethi and Wiesner, 2000).

Table 2-1 Specific removal capacities for various membrane categories

(Adapted from Taylor and Wiesner, 1999)

Type	Pore sizes (microns)	Operating pressure (kPa)	Primary application	Microbes removed
MF	≥ 0.1	30-50	Removal of particles and turbidity	Protozoa , algae and most bacteria
UF	≥ 0.01	30-50	Removal of small colloids	Protozoa, algae, most bacteria and viruses
NF	≥ 0.001	500-1000	Removal of divalent ions (Ca^{+2}, Mg^{+2}) and dissolved organic matter	Protozoa, algae, most bacteria and viruses
RO	≥ 0.0001	1000-5000	Removal of monovalent ions (Na^+, Cl^-)	Protozoa, algae, most bacteria and viruses

Since the 1990's MF and UF membrane processes have started to play a very important role in the production of drinking water and in the treatment of wastewater (Bruggen *et al*., 2003). UF membranes are particularly useful in eliminating turbidity. The source of turbidity in water is suspended matter that can include clay, silt, organic matter, plankton etc. Turbidity is considered as a key cause of water impurities in drinking and surface waters, therefore there is always interest in this parameter. UF membranes are capable of producing a permeate stream with a turbidity less than 0.1 NTU (Pilutti and Nemeth, 2003).

The extensive growth in the use of low pressure membrane systems in large scale applications has occurred for several reasons. The main reason is changes in the regulations for drinking water in Canada, requiring lower turbidity and removal of chemical disinfectant-tolerant micro-organisms such as *Cryptosporidium* (AWWA, 2005). Figure 2-1 shows the growth in membrane applications in North America since 1987.
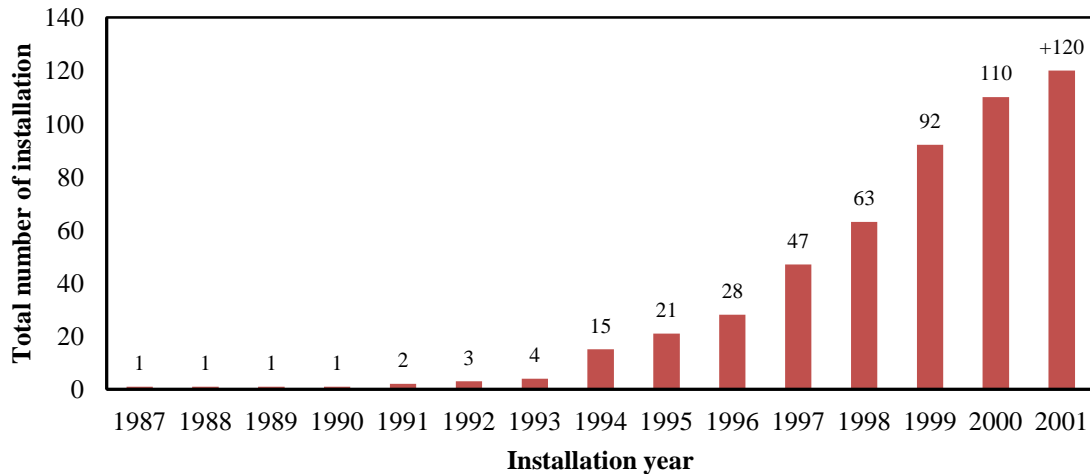
Figure 2-1 Growth of membrane technology (Adopted from AWWA, 2005)

The broad applicability of membrane technology compared to conventional drinking water treatment is another reason for the rapid growth in the use of membrane-basedprocesses. MF and UF systems are particulate filters and unlike nano-filtration (NF) and reverse osmosis (RO), do not remove dissolved constituents. Therefore, they can be more appropriate options for use as replacement to conventional filters. The increase in low pressure membrane approaches can be attributed to their low capital and operating costs. The capital cost for MF and UF facilities are usually 1/2-1/3 of the cost for NF and RO plants (Farahbakhsh *et al.*, 2004). Furthermore, backwashing or cleaning schemes lower the operational cost in MF and UF by decreasing the possibility of the occurrence of fouling on the membrane surface and inside the membrane pores.

Membranes can be used in combination with other treatment technologies to achieve higher removal efficiencies. Pre-filtration, pH adjustment, coagulation, bio-filtration adsorption and pre-oxidation are examples of the pre-treatment techniques available that can be used in combination with MF or UF membranes (Kimura *et al.*, 2005).

2.2 Cross-Flow Microfiltration

2.2.1 General Concepts

Membrane filtration is defined as a separation of elements from a feed flow using a membrane in which the separation is mainly based on size differences (Taylor and Weisner, 1999). In a membrane-based process, the liquid stream passing through the membrane or permeate stream, contains the particles with a size smaller than the membrane pores. The liquid flow leaving the membrane or retentate will have a higher concentration of retained particles. In cross-flow (CFF) or tangential flow (TFF) filtration influent enters the membrane tangentially to the membrane. In this case due to the movement of the feed streams, the deposited components are reduced due to a reduction in the accumulation of feed constituents on the membrane surface. Due to the reduction in build-up on the membrane surface, the permeate flow resistance is reduced in comparison to dead-end filtration. A schematic for cross-flow filtration is shown in Figure 2-2.
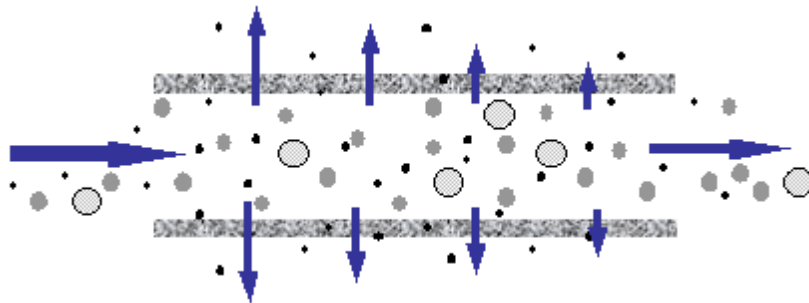
Figure 2-2 Schematic of cross-flow filtration

Trans-membrane pressure (TMP) is the driving force for separation in membrane-based filtration systems. TMP refers to the pressure drop across the membrane and is expressed as the pressure difference between the upstream side (the average pressure between the influent pressure (P_f) and the retentate pressure (P_r) at the inlet and outlet of the membrane) and the downstream side (permeate pressure, P_p) (Zeman and Zydney, 1996).

$$TMP = \Delta P = \frac{P_f + P_r}{2} - P_p \tag{2.1}$$

The velocity in the flow channel of the membrane or the cross-flow velocity U is taken to be proportional to the volumetric flow rate Q,

$$U = \frac{Q}{A_c} \tag{2.2}$$

where A_c represents the cross-sectional area of the fibres. The flow rate of permeate is indicated as Jp or just flux (J) and is often given in units of $Lm^{-2} h^{-1}$ or LMH. It refers to the permeate flow rate Q_p per membrane area A:

$$J = \frac{Q_p}{A} \tag{2.3}$$

The permeate flux is described as a function of TMP, permeate viscosity and total resistance and is based on the Darcy's Law.

$$J = \frac{TMP}{\mu_p \times R_t} \tag{2.4}$$

The total resistance R_t is divided into two parts, namely intrinsic membrane resistance (R_m) and resistance of a fouling layer (R_f).

$$R_t = R_m + R_f \tag{2.5}$$

Fouling is usually defined as the interaction of feed elements with the membrane that leads to changing in membrane characteristics.

2.2.2 Membrane Materials

Membranes vary based on their construction materials and pore sizes. Traditional materials include organic polymers (Mulder, 1996). For UF the most frequently used materials are polysulfone (PE), polyethersulfone (PES), polyvinylidene fluoride (PVDF), and cellulosics such as cellulose acetate and polyether imide. Polymer blends are commonly used to increase the hydrophilicity of the membranes (Bruggen *et al*., 2003).

The choice of the membrane to be used depends on the characteristics of the influent and filtration performance requirements. For example, low protein-binding membranes are suitable for the removal of high value proteins with low concentrations since unlimited protein transfer through the membrane is required (Bowen and Hughes, 1990; Bowen and Gan, 1991). One of the major problems associated with hydrophobic membranes is

protein adsorption because adsorption onto the walls of the membrane leads to a reduction in membrane permeation rate and a change in the rejection properties of the membrane. Hydrophilic membranes result in an increase in protein removal and diminish the fouling by proteins and corresponding decline in filtration efficiency (Defrise and Gekas, 1988). Polysulfone (PS) and polyvinylidene fluoride (PVDF) are both hydrophobic naturally but their hydrophilicity can be increased by the use of various surface treatments. Ceramic and regenerated cellulose membranes are also fairly hydrophilic (Russotti and Goklen, 2001).

Kabsch-Korbutowicz *et al*. (1999) confirmed that the most hydrophilic of the membranes tested (regenerated cellulose) had the lowest susceptibility to fouling by organic colloids. These findings were further supported by Tu *et al*. (2001) who showed that membranes with a higher negative surface charge and greater hydrophilicity were less prone to fouling due to fewer interactions between the chemical groups in the organic solute and the polar groups on the membrane surface. Cherkasov *et al*. (1995) also showed that hydrophobic membranes had a thicker irreversible adsorption layer than hydrophilic membranes.

2.2.3 Operation Mode

Cross-flow filtration can be operated under either constant TMP or constant permeate flux conditions. Depending on the fouling behaviour of the influent for the constant TMP mode, the permeate flux will vary versus filtration time (Figure 2-3 A). During operation at constant TMP, a high initial membrane flux is observed which then rapidly decreased as membrane fouling occurs. The high initial permeate flux causes rapid particle deposition, leading to a rapid build-up of a layer at the membrane surface and an increase in the flow resistance. If the membrane is operated at a TMP corresponding to a flux rate which is smaller than the high initial flux, rapid particle deposition will be avoided. An appropriate selection of TMP is very important to control fouling and the compressibility layer for the process. As the TMP increases, the higher permeation drag and compressive forces exerted on the cake layer will favour a denser packed cake layer. Consequently, a

faster reduction in the permeate flux will be observed (Frenander and Jonsson, 1996; Faibish *et al.*, 1998).
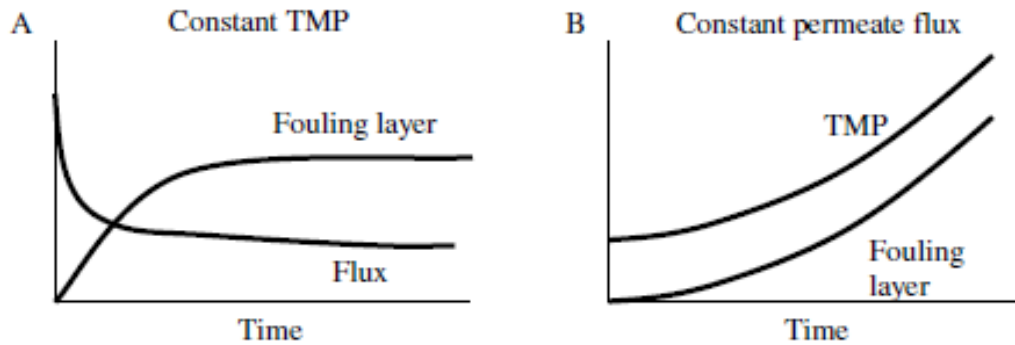
Figure 2-3 Typical permeate flux, TMP profiles and membrane fouling layer for crossflow filtration: (A) constant TMP and (B) constant permeate flux. (Adapted from Newcombe and Dixon, 2006)

A constant permeate flux can maintained during membrane filtration by connecting a permeate pump to the permeate line to withdraw the liquid phase at a constant pumping rate. Based on equations (2.4) and (2.5), the TMP parameter depends on the resistance of the fouling layer (R_f) while the process is under a constant permeate flux. Upon formation of a fouling layer and an increase in the hydraulic resistance, the TMP will increase with filtration time. In this case, the TMP value is strongly dependent on the filtration conditions such as the permeate flux (Berthold and Kempken, 1994; Tardieu *et al.*, 1999) and the influent characteristics (Maiorella *et al.*, 1991). Figure 2-3 B shows the TMP profile versus time. As shown to maintain a steady flux a gradual increase in the required TMP will be required if fouling occurs. As in the case of constant TMP, the permeate flux values should be carefully chosen. Berthold and Kempken (1994) investigated effect of different permeate fluxes for the filtration of hybridoma cell suspensions. According to their study, high permeate flux causes a rapid increasing TMP, while TMP remained constant for low permeate fluxes. The filtration performance was affected considerably by the operating conditions.

Harscoat *et al.* (1999) compared the fouling resistance for constant TMP (1 bar) and constant flux (45 LMH) filtration with a 0.5 μm tubular ceramic membrane for filtrations aimed at the recovery of glucuronane polysaccharides. They found that fouling reduction was considerably higher when operating at a constant permeate flux rather than constant TMP. The reversible fouling resistance obtained was 42.7 E+11 (1/m) compared to the 65.8 E+11 (1/m) for constant TMP mode. However, both modes had almost the same values for irreversible fouling resistance at 9.3E+11 (1/m) and 8.2E+11 (1/m) for constant flux and TMP, respectively. The average fluxes when operating at constant permeate flux can be higher than that constant pressure particularly if the filtration process takes a long time (Frenander and Jonsson, 1996).

Defrance and Jaffrin (1999) also investigated whether it would be better to have a constant TMP or permeate flux in terms of fouling reduction of ceramic membranes used in a MBR. According to their findings, operating in constant flux mode resulted less fouling.

Vyas *et al.* (2002) explored the performance of various scenerios of constant pressure and constant flux crossflow microfiltration for lactalbumin suspensions and found that operating under constant flux above the critical flux followed by constant TMP operation caused rapid fouling. In contrast, constant TMP operation followed by a very low constant flux was found to reduce fouling by reducing the convective forces towards the membrane. Although fouling in constant flux operation is observed to be slower, there is some evidence that deposition under these conditions may be more irreversible since the dominate mechanism would be internal fouling by macromolecular species (Le-Clech *et al*., 2006).

2.2.4 Permeate Flux

A critical flux refers to a permeate flux lower than that at which fouling is decreased appreciably or even completely eliminated (Field *et al*., 1995). Therefore, particle deposition does not exist at the membrane if the permeate flux is lower than the critical value and particle deposition increases if the permeate flux is set on or above this critical flux (Li *et al*., 1998). Kwon *et al*. (2000) conducted some tests using particle suspensions

with various sizes. They obtained an average TMP for this system which was close to the TMP measured in the filtration of clean water and remained constant over the time tested. Once the permeate flux was increased, the TMP started to increase with time and a significant difference was observed between the TMP and that for the clean water stream. The particle deposition rate increased when the particle size was reduced for a given permeate flux. Also, for a specific particle size, the particle deposition rate increased with an increase in the permeate flux.

Choi *et al*. (2005) investigated the effect of permeate flux and tangential flow (cross flow) on membrane fouling in a process for the treatment of a synthetic paper mill wastewater. They were able to show that permeate flux declined faster with increasing feed concentration or by reducing the tangential flow. They found that the main reason for the reduced flux in the MBR was biological suspensions (i.e., *activated sludge*) including mixed liquor suspended solids (MLSS) and dissolved organic carbon (DOC). Determination of critical flux values is not theoretically predictable, but requires experimental determination. Critical flux depends on various factors, such as hydrodynamics, particle size, interaction between colloid material and the membrane and suspension properties (pH, salinity, and conductivity) (Howell, 1995).

2.3 Membrane Fouling

One of the main constraints in applications of membranes to drinking water or wastewater treatment is high energy consumption attributed to membrane fouling. Membrane fouling causes a reduction in the permeate flux through the membrane. The main reason for this decline is the accumulation of particles on the surface, creation of a cake layer, or the adsorption of particles inside the membrane pores (AWWA, 2005).

Membrane fouling can fall into two categories: reversible and irreversible fouling. Reversible fouling can be recovered through backwash cycles; however, chemical cleaning is required to diminish the irreversible fouling. Four important mechanisms have been proposed for the fouling phenomenon that affects membrane performance: inorganic fouling (scaling), particulate/colloidal fouling, microbial/biological fouling (biofouling) and organic fouling (Li *et al*., 2008).

Inorganic fouling or scaling occurs by accumulation of inorganic precipitates, such as metal hydroxides and scales, on the membrane surface or within the pores. This happens when the concentration of the substances is very high at the membrane surface and exceeds their saturation concentration. Scaling is major concern for RO and NO since these membranes reject inorganic species and form a concentrated layer in the vicinity of membrane which is referred to as concentration polarization (Li *et al*., 2008). For MF and UF, inorganic fouling due to concentration polarization is much less profound but can exist likely due to interaction between ions and other fouling materials (i.e., organic polymers) via chemical bonding. Some pre-treatment process such as coagulation, if not performed properly, may introduce metal hydroxides on the membrane surface or within the pores (Li *et al*., 2008). In colloidal and particulate fouling, accumulation of the particles on the membrane surface or inside the pores causes membrane flux reduction. Algae, bacteria, and some natural organic matter fall into the size range of particles and colloids. Biofouling is a result of the formation of biofilms on the membrane surface and microbial growth on the surface or inside the pores of a membrane. Such films release biopolymers (polysaccharides, proteins and amino sugars) as a result of microbial activity resulting in a reduction in the permeate flux and ultimately fouling. Dissolved and suspended particles that enter inside the pores and sit on the surface of the membrane are the main causes for organic fouling. Several studies have shown that NOM is a major UF membrane foulant in water treatment.

Hlavacek and Bouchet (1993) developed four mechanistic fouling models for constant permeate flux filtration; pore blockage, pore constriction, intermediate blockage, and cake filtration. Four different types of fouling are presented in Figure 2-4. Pore blockage (Figure 2-4A) is described as the deposition of particles at the entrance of the membrane pores with no superposition of particles; thus, completely blocking the flow through those pores. Pore constriction applies when particles enter the pores and along the surface of the pores which reduces the effective diameter of the pores (Figure 2-4B). The intermediate pore blockage model is similar to the complete pore blockage model and accounts for the possibility of particles settling on other particles that have previously are already blocking some of the pores (Figure 2-4C). Cake filtration basically reflects

external membrane fouling where particles accumulate on the membrane surface and form a cake layer (Figure 2-4D).
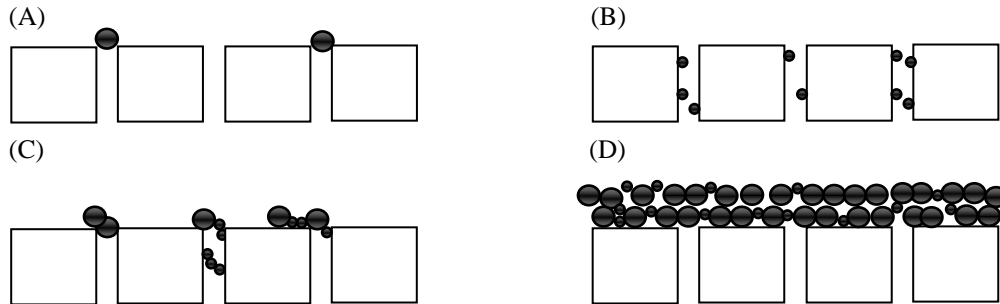
Figure 2-4 Membrane fouling mechanisms: (A) pore blockage, (B) pore constriction, (C) intermediate blockage and (D) cake filtration (Adapted from Field, 2010)

Howe and Clark (2002) documented that the presence of small colloidal matter with a diameter of about 3-20 nm is responsible for the fouling most of the time in water treatment. They concluded that the majority of the DOM by itself is not the reason for membrane fouling; however, the actual foulant is a relatively small fraction of bulk DOM. Combe *et al.* (1999) proposed that NOM enters into the pores and coats the membrane surface. They also reported that NOM creates a gel layer, which thickens over time reducing the overall flux through the membrane.

2.3.1 Fouling Mechanisms in MBRs

Municipal and industrial wastewaters are often treated biologically, such as by an activated sludge (AS) process or an alternative technology such as a membrane bioreactor (MBR). The nature and extent of fouling in MBRs is strongly influenced by three factors: the membrane characteristics, operating conditions and biomass characteristics (MLSS constituents) (Chang *et al.*, 2002). The effects of membrane characteristics (e.g. material, pore size) and operating conditions (e.g. CFV, constant TMP) on fouling of membrane have been discussed earlier. The composition of the mixed liquor suspended solids (MLSS) is known to have a significant effect on membrane fouling (Chang *et al.*, 2002).

14

MLSS includes suspended solids and dissolve organic matter (DOC). DOC of MLSS mainly includes biopolymers such as EPS, humic substances, low-molecular weight acids and low molecular weight neutrals (Haberkamp *et al*., 2007). MLSS also includes residual DOC from the feed water. A number of studies have identified the different fractions of MLSS and their role as a major contributor to membrane fouling for different wastewater treatment approaches (Table 2-2).

Table 2-2 Major MBR foulants for various wastewater sources

Source	MR type	Pore size	Major foulant	Reference
Synthetic waste water (dairy effluent)	Hollow fibre (MBR)	0.1 µm	Colloidal fraction	Bouhabila *et al*., 2001
Sewage plant	Tubular ceramic (MBR)	0.1 µm	SS	Defrance *et al*., 2000
Activated sludge mixed liquor	Cellulose acetate UF (MBR)	35-300 kDa (MWCO)	SS	Bae and Tak, 2005
Synthetic wastewater	MF (MBR)	0.2 µm	EPS	Wisniewsli and Grasmick, 1998
Municipal wastewater	Hollow fibre (MBR)	0.1 µm	EPS	Li *et al*., 2005
Synthetic simulated municipal wastewater	Tubular ceramic (MBR)	300 kDa (MWCO)	Organic compound below 0.1 µm	Cicek *et al*., 2003
Synthetic wastewater (industrial and municipal)	Tubular (MBR)	0.05-0.4µm	Submicron particle below 0.1 µm	Pollice *et al*., 2005
Municipal wastewater	Hollow fibre (MR+ MBBR)	0.04µm	Organic matter below 1.2µm	Leiknes *et al*., 2006

As MBRs are generally operated under constant flux conditions, fouling phenomena can self-accelerate and eventually cause a sharp increase of TMP (Judd, 2011). Several studies have investigated the fouling behaviour for long-term MBR filtration conducted at sub-critical flux. However, these experiments have shown considerable fouling for MBRs operated at sub-critical flux (Ognier *et al*., 2001, Pollice *et al*., 2005, Brookes *et al*., 2006). A detailed analysis of the mechanisms and factors involved in the fouling has been reported by Zhang *et al*. (2006) (Figure 2-5).
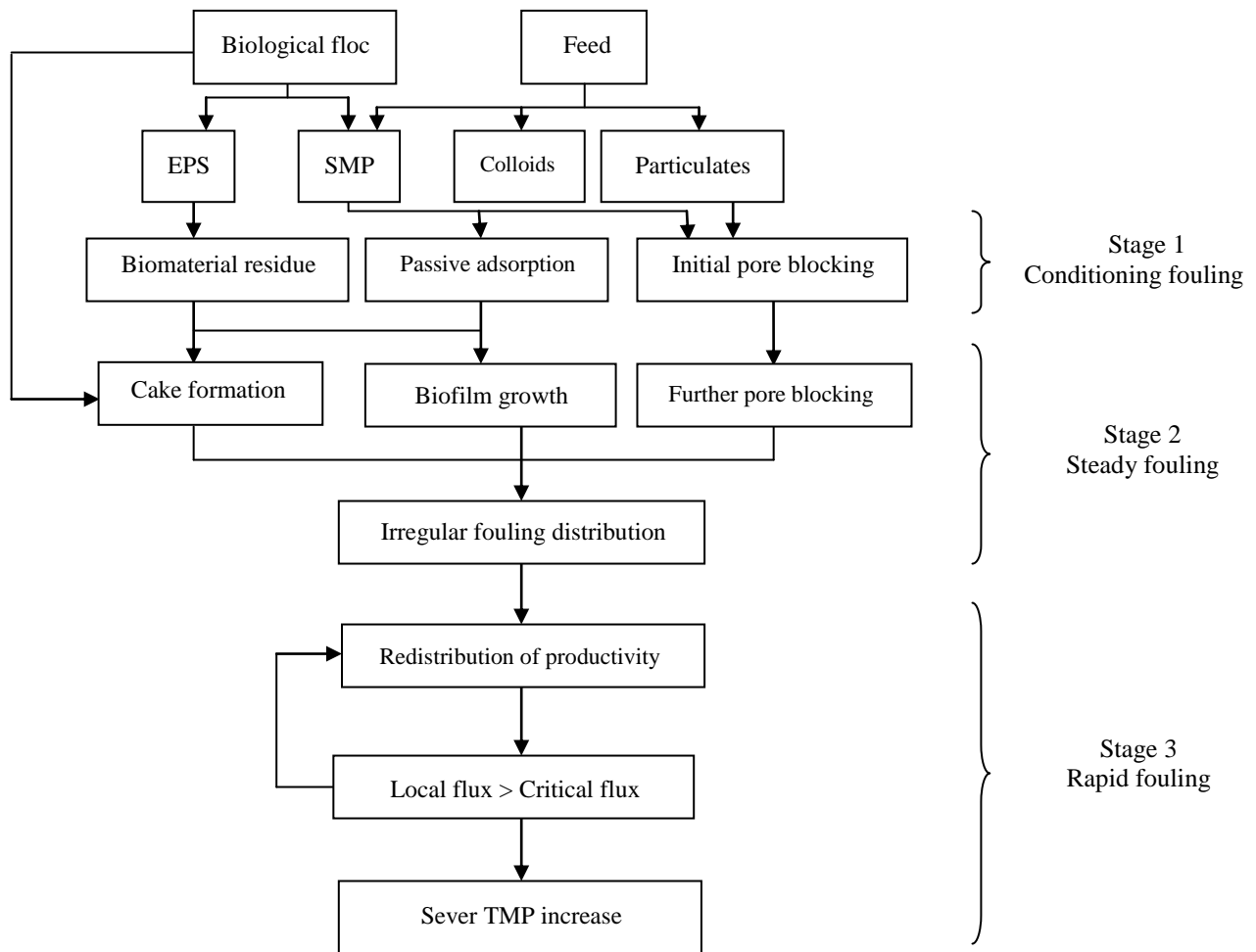
Figure 2-5 Fouling mechanisms for MBR operated at constant flux (adapted from Zhang *et al*., 2006).

According to Zhang *et al*. (2006), there are three stages of fouling: conditioning fouling, steady fouling and severe fouling. They found strong interactions between the EPS present in the mixed liquor of a concentrated simulated municipal wastewater and the membrane surface which they proposed is probably responsible for the initial stage of fouling during constant flux operation. Passive adsorption of organics and colloids was observed before any deposition mechanism was initiated. Biomass is able to attach easily to the membrane surface even if the MBR is operated below the critical flux because settling will occur and contribute to stage 2 fouling. Further adsorption, pore blocking and deposition of organics on the membrane surface may occur. Biological flocs may

initiate formation of a cake layer at this stage without a direct effect on permeability. However by the time the flux has decreased significantly overall permeate redistributes to the fouled membrane area or pores which are not as fouled and cause an increasing in local flux. As a result, a rapid rise in TMP will be observed (Stage 3).

2.4 Membrane Cleaning

Membrane cleaning is very important for maintenance and extension of membrane life. There are several ways that a membrane can be maintained including physical and chemical cleaning.

2.4.1 Physical Cleaning

Physical cleaning of the membrane includes membrane relaxation where the filtration process is paused and the membrane backwashed, that is the permeate flow is reversed through the membrane. Backwashing has proven successful for removing most of the reversible fouling by dislodging the loosely attached filter cake from the membrane surface. In some cases, clogging near the membrane surface may also be partially removed by backwashing (Bouhabila *et al*., 2001, Psoch and Schiewer, 2006, Le- Clech *et al*., 2006). Most commercial low pressure membrane systems are set-up with automatic backwash cycles operating with different frequencies.

Key parameters in the design of backwashing are: frequency, duration, and the ratio between these two parameters. Jiang *et al*. (2005) concluded that less frequent but longer backwashing was more efficient than more frequent backwashing for a municipal wastewater treatment system. Although more foulants are expected to be removed by increasing backwashing frequency and duration, optimization of the backwashing protocol requires minimizing energy and permeate consumption. Increasing the backflush flux (which is usually 1-3 times the operational flux) leads to a loss in permeate and reduces the net permeate flux (Judd, 2011).

Membrane relaxation is known to improve considerably membrane efficiency. During the relaxation period non-irreversibly attached foulants can diffuse away from the

membrane surface through the concentration gradient at the surface of the membrane. The fouling removal efficiency of this method can be enhanced when air scouring is applied during relaxation (Hong *et al*., 2002). Membrane backwashing and relaxation effectiveness tends to decrease with operation time, since more irreversible fouling accumulates on the membrane surface.

2.4.2 Chemical Cleaning

Chemical cleaning is used to target the contaminants that cause irreversible fouling of the membrane. The frequency is different from the backwashing as it ranges from a few days to several months, depending on the membrane characteristics and the wastewater quality. When foulants cannot be removed from the membrane surface by backwashing then chemical cleaning is required. There are different types of chemical cleaning which include: chemically enhanced backwash (daily), maintenance cleaning with higher chemical concentration (weekly), and intensive chemical cleaning (once or twice a year) (Le-Clech *et al*., 2006). Maintenance cleaning is performed in order to maintain design permeability of the membranes and reduce the frequency of intensive cleaning. Intensive cleaning is usually performed when TMP is so high and further filtration is not easily achievable.

The chemicals used for membrane cleaning are usually recommended by the membrane manufacturer. Alkaline cleaning is often used to remove organic foulants from the membrane surface and from the membrane pores while acid cleaning removes precipitated salts (Schäfer *et al*., 2005). Acid cleaning is used largely for RO since the scaling occurs in connection with salt retention (Schäfer *et al*., 2005). Generally under normal conditions an effective cleaning agent is sodium hypochlorite (for organic foulants) and citric acid (for inorganic foulants). Sodium hypochlorite hydrolyzes the organic molecules and therefore loosens the particles and biofilm attached to the membrane (Le-Clech *et al*., 2006).

In addition, a combination of a low pH cleaning followed by a solution with a high pH is extremely effective in removing organics for all type of water treatment membranes. The low pH cleaning helps break the bridge between the organic and the membrane, the high

pH solution then causes the foulant to detach from the membrane surface. This is reason there is sometimes a colored discharge when using high pH cleaning approaches. Kimura *et al.* (2005) reported that alkaline cleaning was more effective than the use of a chelating agent and acid solutions in recovering membrane permeability.

2.5 Background on Coagulation

Coagulation occurs when small particles in an aqueous solution are destabilized (Bratby, 2006) due to the addition of a chemical agent and aggregation occurs. Coagulation serves to remove particles through four primary mechanisms: (1) electrical double layer (EDL) compression, (2) adsorption and charge neutralization, (3) adsorption and bridging, and (4) enmeshment in a precipitate resulting in sweep flocculation (Howe and Clark, 2002).

EDL compression can be accomplished by addition of an electrolyte to increase the ionic strength of the solution. Adsorption and charge neutralization occurs when the positively charged counter ions adsorb to the surface of negatively charged particles until the charge is neutralized, once the surface charge is neutralized, particles can collide and aggregation can occur. Adsorption and bridging often occurs with coagulants which have long polymer chains that can absorb to the surface of two colloids and form a polymer bridge (Howe and Clark, 2002). If metal salts (e.g. alum) are added in sufficient quantities to exceed the solubility products of metal hydroxide a "sweep floc" can form. Colloids become enmeshed in the settling sweep floc and as a result are removed from suspension (Howe and Clark, 2002).

Enhanced coagulation or low pH coagulation is often used in order to increase the elimination of TOC and other particulate substances. This enhancement is usually achieved by lowering the pH of the raw water to an optimum value. For example, the pH value for iron-based coagulants is in on the range of 4.5-5.5 while the optimum for aluminum-based coagulants ranges between 5.5 and 6.5 (Sharp *et al.*, 2006).

The most widely used coagulants (for water treatment) in North America are inorganic metal ions such as aluminum sulphate (alum), polyaluminum chloride (PACl), ferric sulphate and ferric chloride (Howe and Clark, 2002). Ferric chloride and alum are two widely used coagulants that have important applications in the drinking and wastewater

treatment plants. Both coagulants are known as hydrolyzing metal salt (HMS) coagulants with active metals (AWWA, 1999). In solution, these small, positively charged ions form a strong bond with oxygen atoms of six surrounding water molecules such as $M(H_2O)_6^{3+}$ in solution where M is the active metal. The hydrogen-oxygen bond is subsequently weakened, and the hydrogen ions are released into solution. This reaction is called hydrolysis and the resulting active metal hydroxide species are known as hydrolysis products. Hydrolysis of such ions is often described as a replacement of the water molecules by hydroxyl ions (Gregory and Duan, 2001) and can also be thought of as a progressive de-protonation of water molecules in the primary hydration shell (Richens, 1997). The simplest representation for Al^{3+} for such a process is presented in Equation (2.6). As each step involves the loss of a proton, an increase in pH causes the reaction to be shifted to the right and forms the soluble aluminate ion (Gregory and Duan, 2001). A similar sequence can be written for the Fe^{3+}.

$$Al^{3+} \leftrightarrow Al(OH)^{2+} \leftrightarrow Al(OH)_2^+ \leftrightarrow Al(OH)_3(s) \leftrightarrow Al(OH)_4^- \tag{2.6}$$
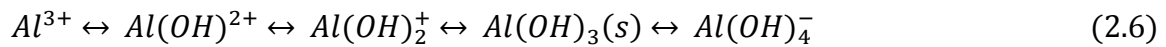
Hydrolyzing coagulants remove particles in two ways: charge neutralization and sweep flocculation. NOM and other particles can be destabilized by small quantities of hydrolyzing coagulant. Suitable destabilization is related to the neutralization of particle charge that then results in aggregation of the neutral particles (Gregory and Duan, 2001). It should be noted here that over dosing of the positive charged coagulants can lead to charge reversal, leaving the particles positively charged and thus re-stabilized. When charge neutralization is the leading mechanism, the coagulant dose required is proportional to the concentration of the particles in solution. The required doses can still be affected by the type of NOM in the water and not simply the concentration.

Jiang (2001) reported that a high coagulant dose was more efficient in some cases due to extensive hydroxide precipitation and sweep flocculation. Sweep flocculation can be used to overcome two main disadvantages of destabilization by charge neutralization: (1) very accurate control of the coagulant dose is required to give optimum destabilization; (2) coagulation rate depends on the particle concentration which can be extremely low for dilute solutions. Sweep flocculation prevents the occurrence of both problems if high doses of coagulant are used. The high doses form large amounts of amorphous hydroxide

precipitates. The target particles are trapped in this growing precipitate and can then be eliminated by sedimentation. The sweep floc happens when the pH of water rises above the zero point of charge for the dissolved substances that are produced from coagulants such as alum.

2.5.1 Coagulation Performance

Although coagulation is a well known mechanism (Erbil, 2000) the advanced application of coagulants in wastewater treatment is relatively recent with the application of aluminum sulphate and ferric chloride as coagulants in large scale treatment units. A systematic investigation on the removal of NOM using different real surface and synthetic water samples was conducted to optimize coagulation performance since the 1980's (Jiang, 2001). In the 1990's, NOM and other precursors of the disinfection by-products were still considered as a main concern in water and wastewater treatment.

2.5.2 Impact of the Use of Coagulant on Membrane Fouling

Combining UF with coagulation leads to removal of significant amounts of contaminants which cause fouling resulting in improved permeation rates and permeate quality (Kim *et al*., 2005). Kim *et al.* showed that organics were more important for membrane fouling than particulates during membrane filtration of surface water, suggesting that coagulation should target the removal of organic rather than material attributed to turbidity. The coagulation pH was also found to be an important parameter. When pH was too low, more fouling was observed due to changes in the particle characteristics.

Dong *et al*. (2007) studied the effect of fouling by NOM and reported that high molecular weight hydrophobic compounds reduced the flux significantly; however, the flux was recovered by employing a coagulant by removing large hydrophobic compounds. Figure 2-6 presents the effect of coagulation on membrane fouling. When water treated with coagulants is filtered the flocs accumulate on the membrane surface and form a cake layer that can absorb a fraction of the NOM. The cake can be easily removed by backwashing and flushing.
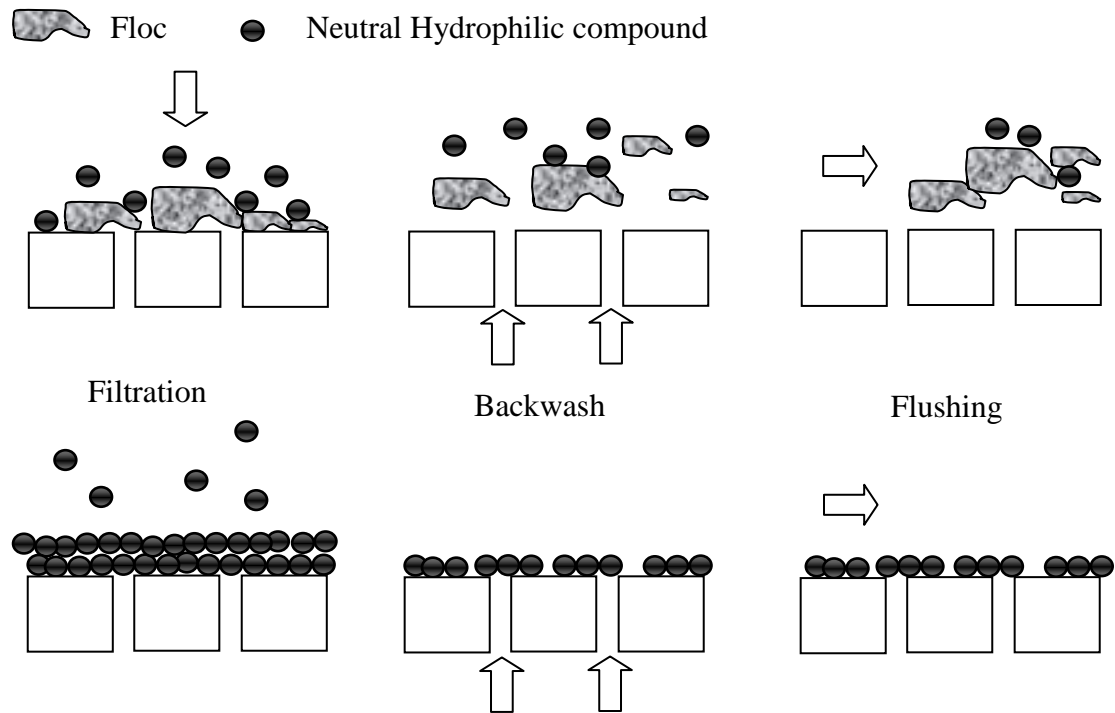
Figure 2-6 Mechanism of preventing membrane from fouling by coagulation treatment (Adapted from Dong *et al*., 2007)

Among the various particle characteristics, particle size was found to be the most important factor for membrane fouling (Kim *et al*., 2005). Coagulation increases the particle size which leads to a reduction in fouling. Kim *et al*. (2005) examined the effect of different coagulant dosages to determine what the exact role of coagulation is in fouling reduction. It was found that by adding low alum doses, membrane fouling reduction occurred due to changes in the particle characteristics. However, improvement in membrane performance was achieved at high alum dosages through both a change in particle characteristics and contaminant loading reduction.

Kerry J *et al*. (2006) found that the main component of membrane foulants for natural surface water were NOM components in particular the fraction between 1 μm and 100 kDa. Components smaller than 100 kDa had relatively little effect on fouling during filtration of either raw or coagulated water. Choo *et al*. (2007) investigated the effect of organic and inorganic coagulants on fouling during crossflow UF and observed that an organic (polymeric) coagulant aggravated membrane fouling, while an inorganic

coagulant mitigated the fouling. Among the inorganic coagulants tested PACl showed the best performance in fouling reduction even at small doses (1.0 mg/l as Al).

Not only has pre-coagulation of the membrane feed water been widely studied in water treatment, it has been studied to a lesser extent in wastewater treatment for removal of the colloids that are formed in bioreactors. Coagulation can effectively remove undesirable inorganic and organic colloids (protein viruses, polysaccharide with acidic groups in EPS and SP) by incorporating them into larger flocs (Ivanovic *et al*., 2008) which would be rejected by a membrane or by sweep flocculation and sedimentation. As a result membrane performance with respect to fouling reduction and contaminant removal efficiency may increase. Yoon and Collins (2006) investigated the addition of a modified cationic polymer coagulant to full-scale and pilot-scale municipal MBRs using flat sheet submerged membrane units. The membrane was operated at a flux 39% higher than the critical flux and a constant, low rate of fouling was observed. However, operation without the coagulant at a flux that was 35% higher than the critical flux increased fouling significantly. For long term filtration, the MBR could be operated with a 50% higher flux and the flux duration increased from 22 days to more than 30 days by employing coagulant.

Yoon *et al*. (2005) also investigated the use of pre-coagulation in lab scale and pilot scale MBR with submerged flat sheet membranes. In this study, a proprietary cationic polymer (referred to as membrane performance enhancer (MPE)) was used as coagulant. The MBR was seeded with sludge from a sewage wastewater treatment plant and acclimated with a high strength synthetic feed (COD of 10,500 mg/l) for a month in order to create high fouling conditions. Fouling was reported to be reduced significantly, as a result of reducing SMP level by 50% (from 41 to 21 mg/l) by coagulant addition. They were also able to operate the membrane for longer intervals between cleaning.

Ivanovic *et al*. (2008) investigated the effect of adding a flocculant zone (F-zone) to a pilot scale biofilm membrane reactor (BF-MBR) with a submerged hollow fibre membrane unit for treatment of municipal wastewater. The reactor was modified to include the F-zone by extending the bottom and placing the inlet to the membrane reactor under the membrane aeration system. The HRT of the MBBR was about 4 hours and the

23

membrane unit was operated with a constant flux of 50 LMH with 96% recovery. The membrane performance was evaluated by monitoring the TMP over time. They found that introducing flocculant zone resulted in a reduction of the number of submicron particles and of the SS concentrations around the membrane area and consequently observed an improvement in the membrane performance in terms of lower fouling rates.

Chen and Liu (2012) studied the possibility and applicability of coagulation in a MBR hybrid system with the multiple flat sheet membrane units targeted at the reclamation of dairy wastewater. HRT of the MBR was kept at 10 hours and the filtration and relaxation time of the membrane were set at 8 and 2 minutes. It was observed that PACl (among the other coagulants tested, e.g. alum, aluminum sulphate, ferric chloride, polyacrylamide) was effective resulting in turbidity removal of 98.95% at the optimum dosage of 900 mg/l. Liu *et al*. (2011) also studied domestic wastewater treatment using a coagulation-MBR system in combination with a hollow fibre membrane unit (pore size of 0.2 μm). Results showed that the coagulation MBR had showed improved performance over a traditional MBR as COD and ammonia removal efficiency increased from 90.26% to 91.74% and 92.04% to 96.55%, respectively. Membrane fouling was also improved after adding PAFC as a coagulant.

2.6 Membrane and Moving Bed Biofilm Reactors

Membrane bioreactors (MBRs) are increasingly being employed for wastewater treatment due to their potential to operate at a very high biomass concentrations and ability to generate high quality effluents (Judd, 2011). This approach employs both a biological stage and a membrane module to treat wastewater. Biological degradation of organic compounds is carried out in the bioreactor by acclimatized microorganisms while the separation of the microorganisms from the treated wastewater is performed by membrane filtration. In some industrial applications, MBRs can produce effluents with quality that allows direct discharge (Judd, 2011) or reuse as an industrial process streams.

There are two configurations for the MBR: the membrane can be placed either submerged inside or placed outside of the bioreactor (Figure 2-7). For the submerged configuration, the filtration occurs in the aeration basin by suction removal of effluent

while for the outside configuration, the mixed liquor is filtered under pressure in a specific membrane module.
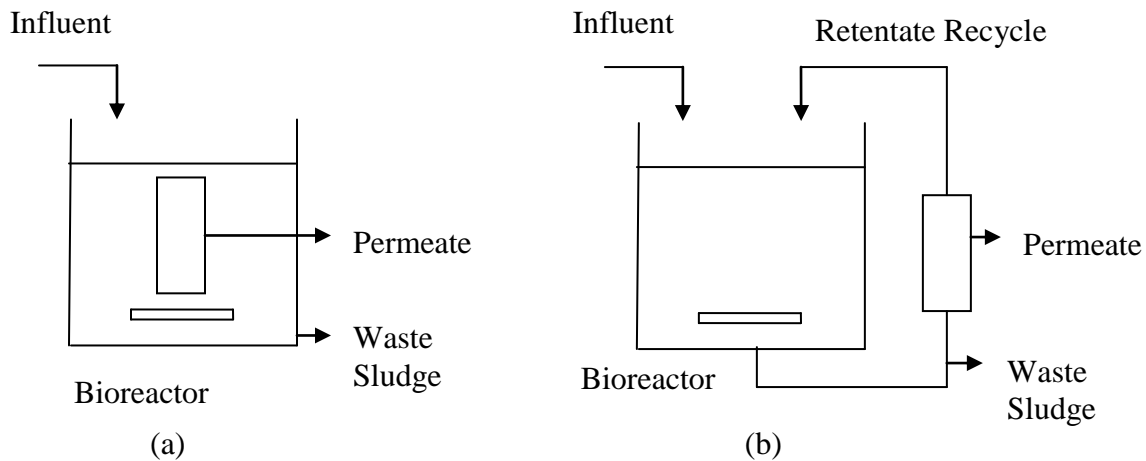
Figure 2-7 (a) Submerge and (b) Side-stream membrane bioreactors (adapted from Judd, 2011)

In the submerged configuration (Figure 2-7a), the permeate flux generally varies from 15 to 50 LMH and the TMP is about 0.5 bar. In the external configuration (Figure 2-7b), the permeate flux varies between 50 and 120 LMH and the TMP is in the range of 1-4 bar (Huang *et al*., 2001). The submerged configuration is more economical based on energy consumption due to milder operational conditions (low value of TMP and tangential velocities) and does not require an additional recycle pump (Huang *et al*., 2001). Compared with traditional activated sludge (RAS) systems, the MBR has some advantages: the traditional clarifier is replaced by a membrane module which is more compact; the biomass concentrations can be higher than the RAS. In the MBR up to 30 g/L biomass concentrations can be accommodated (Yamamoto *et al*. 1989 and Jefferson *et al*., 2000); whereas, in the conventional process the biomass concentrations required is less than 5 g/L to avoid problems inherent to floc settling; and there is a reduction in the production and disposal of sludge by a factor of 2 to 3 (Gander *et al*., 2000) resulting in a reduction of the overall operating cost.

Jefferson *et al*. (2000) compared the performance of a MBR and aerated biological filters for gray water recycling and concluded that the MBR system was the most efficient process for the removal of biochemical oxygen demand (BOD_5) and turbidity. As

discussed earlier using a MBR for industrial wastewater treatment is a very attractive technology that offers several advantages compared with conventional treatment processes. However, membrane fouling is a challenging phenomenon which can increase energy requirements and costs associated with membrane cleaning and restoration. The high biomass concentration in these systems is mainly responsible for membrane fouling (Le-Clech *et al*., 2006). Fouling in the MBR system can be due to filter cake formation which is reversible by backwashing or accumulation of extracellular polymeric substances which is irreversible and requires chemical cleaning. An alternative configuration to conventional activated sludge MBRs is combining a fixed film biological process such as moving bed biofilm reactors (MBBRs) with a membrane process. MBBRs are now being used in more than 300 wastewater treatment plants in 22 countries for both municipal and industrial wastewater for various treatment purposes (BOD/COD removal, nitrification and denitrification) (Odegaard, 2006; Odegaard *et al*., 2000). Interest in biofilm-based process has increased over the past decade and has been found to be more favourable than activated sludge processes for removal of organic carbon and nutrients. The advantages of biofilm systems over activated sludge systems are a reduced footprint, higher concentration of microorganisms, flexibility to in the selection of the biomass separation method and no need for sludge recirculation (Odegaard *et al*., 1994). In addition, the effluent from MBBRs has a lower solids concentration (e.g., typically 100-200 mg/l) than activated sludge systems (Odegaard, 2006). The suspended solids that are produced by fixed film bioreactors will likely have significantly different properties than those generated by a suspended growth system (Grady *et al*., 1999).

In most biofilm reactors the whole tank volume is used for biomass growth. Biomass grows on the carriers (primarily on the inside of carriers depending on the carrier configuration) which move freely in the reactor by pneumatic agitation or mechanical mixing in aerobic. Since the carriers are retained in the reactor using an outlet sieve sludge recycle is not required as conducted in for activated sludge processes. Furthermore, a high SRT (i.e., *sludge age*) is achievable in the MBBR configuration leading to a lower rate of sludge generation compared with conventional activated sludge

processes. This is an important advantage as it is vital in relation to the cost for sludge disposal.

The effect of various carrier sizes and shapes on performance has been investigated for MBBRs used in treating municipal wastewater and it has been concluded that shape and size of the carrier may not have significant effects on organic carbon removal as long as the effective surface area is the same (Odegaard *et al*., 2000). It appears that the biofilm area is the key parameter in the MBBR design; therefore, an effective surface area (g/m^2d) in terms of carrier fill fraction should be considered (Odegaard *et al*., 1999). In order to have free movement of carriers, a filling fraction of below 70% is recommended (Odegaard, 2006) The most frequently employed carrier is a small cylinder made of high density $(0.95\ g/cm^3)$ polyethylene with a cross on the inside and fins on the outside (K1 type from AnoxKaldnes^{TM}) (Odegaard, 2006).

Several studies have reported that MBBRs and activated sludge processes have the same concentration of biomass in both attached and suspended forms $(2-5\ kg/m^3$ volume of the tank); however, the removal efficiency of the MBBR is much greater than that for activated sludge processes. According to Rusten *et al.* (1998), MBBRs have higher SS concentrations in the effluent while employing higher organic loading rates.

The efficiency of MBBRs can be enhanced by increasing the HRT or by the utilization of multiple MBBR compartments (Leiknes and Odegaard, 2007). Melin *et al*. (2005) studied the effect of organic loading rate on MBBR performance. Despite operating the MBBR at different organic loading rates (4.1 and 26.6 g COD/ m^2d) the average COD removal efficiency was reduced from 87% to 83% by decreasing the HRT.

In spite of the potential benefits of the MBBR-MRs there have been relatively few studies on the integration of these processes. Melin *et al*. (2005) compared high and low organic loading rate operation of combined MBBR-MR systems that had membranes with a pore size of 0.1 μm. They reported that MBBR loading had little effect on membrane fouling based on the development of TMP under constant flux operation. The submerged design of the membrane reactor (MR) allowed accumulation of a significant concentration of suspended solids in the reactor which may affect the rate of the fouling. Ahl *et al*. (2006) and Leiknes *et al*. (2007) studied a pilot scale MBBR using Kaldnes media and a

submerged membrane reactor with a pore size of 0.04 μm to treat settled (with a small pre settler, HRT< 10 min) municipal wastewater. Two different loading rates were used and fouling was assessed by measuring TMP at constant flux operation. Low rate operation produced a greater fraction of submicron particles which was expected to increase fouling by colloidal fraction. However, enhanced flocculation from increased particles was more evident for low loading rates which resulted in reduced fouling.

Lee *et al*. (2006) reported results for a bench scale membrane-coupled moving bed biofilm reactor (M-CMBBR) system where hollow fibre membranes were submerged in the MBBR tank. The carriers employed consisted of activated carbon impregnated polyurethane cubes and a synthetic soluble wastewater. Fouling was found to be less than that of conventional activated sludge due to collision of the carriers with the membrane surface which resulted in reduced accumulation of the biofilm on the membranes.

Rahimi *et al*. (2011) examined a pilot plant MBBR apparatus using poly propylene carries with 70% fill fraction and a hollow fibre membrane module with the pore size of 0.1 μm to treat a synthetic wastewater without fluctuation in the feed concentration. The effect of aeration rate of the MBBR on membrane fouling was assessed. They concluded that aeration rate significantly affected membrane fouling as well as nutrient removal in the MBBR. At both low and high aeration rates, the foulant concentration increased resulting in a reduction of permeability. At high aeration rates, despite the fact that little or no excess filamentous bacteria were observed, floc breakage resulted in higher fouling.

Previssian *et al*. (2011) evaluated the effect of using different coagulants on MBBR effluent and its effect on fouling using a dead-end bench scale UF. The addition of coagulant improved membrane permeability and all coagulants decreased reversible fouling and depended on the type and dosage of coagulant. Ferric chloride performed the best compared with alum and a coagulant blend. The literature clearly indicates that performance of MBBR-MR systems will be impacted by the wastewater characteristics as well as the design and operating conditions of both the bioreactor and membrane processes.

CHAPTER 3

EXPERIMENTAL PLAN, MATERIALS AND METHODS

3.1 Experimental Plan

One of the main objectives of this research project was to evaluate the performance of an integrated moving bed biofilm reactor and a pilot plant ultra-filtration membrane system (MBBR-MR). Such configuration has the potential to lead to a compact cost-efficient treatment facility that is capable of producing treated effluents which are suitable for water reuse. The pilot testing was conducted in a food processing factory located in Cambridge, Ontario, Canada.

The characteristics of the influent and effluent of the MBBR were regularly monitored for more than an eight month period. In addition, the effect of pre-coagulation on the fouling of the membrane was investigated. A series of jar test experiments was also performed to estimate the coagulant dose for pilot plant operation. Ferric chloride was selected in this study as it has been shown that this coagulant is very effective on mitigating membrane fouling (Laboussine-Turcaud *et al.*, 1990; Pervissian *et al.*, 2011). Laboussine-Turcaud *et al.* (1990) reported that iron coagulation of surface water is very efficient for reducing fouling phenomena when flocculation conditions produce particles with a zeta potential close to zero. Due to fluctuations in the quality of the wastewater, jar tests were performed daily during the operation of the pilot plant.

The pilot plant was operated for three continuous days for each of the different conditions in relation to the coagulant dosage and permeate flux. The effect of each variable on membrane fouling was investigated based on the magnitude of the total membrane resistance changes during the three days of operation. In order to determine whether the coagulation resulted in improved membrane performance the pilot plant was run both with and without the coagulant and the results of the two runs compared. The results are presented and discussed in Chapter 4.

3.2 Characteristics of the Industrial Wastewater

This research project involved a study of the treatment of the final wastewater effluent from a food processing industry located in Cambridge, ON. Some of the effluent from the pH adjustment tank, prior to being released into the municipal sewer, was diverted to the pilot plant. The quality of the effluent from the MBBR varied as a result of fluctuations of the influent quality. A brief description of the water treatment process before the pH adjustment tank is presented to understand the reasons behind the fluctuations in the waste stream.

The variations observed in the MBBR feed quality was caused by equipment failures, bypass of several of the clarifiers, and/or changes in conditions of the process flow at the factory. All the wastewater steams (about 300 GPM) in the factory were processed through a mechanical screen to remove solids larger than 0.1cm (Figure 3-1). Although the mechanical screen should have always been running, it was often shut off. As a result, there was often the presence of pieces of corn and other particles in the influent stream; sometimes, clogging the flow meter and stopping the flow of wastewater to the pilot plant. After the screen, wastewater is processed through three clarifiers with a HRT of 30 minutes. Only one clarifier was working during this research. Overflow of the clarifiers then flows to the pH adjustment tank prior to discharge into the city sewer stream. The solids that have accumulated at the bottom of the clarifiers are drained to the scum tank. After passing through a mulch and strainer, the solids are processed in a centrifuge for separation of the solids from the liquid. The resulting liquid phase is passed to the clarifier for further treatment (Figure 3-1).
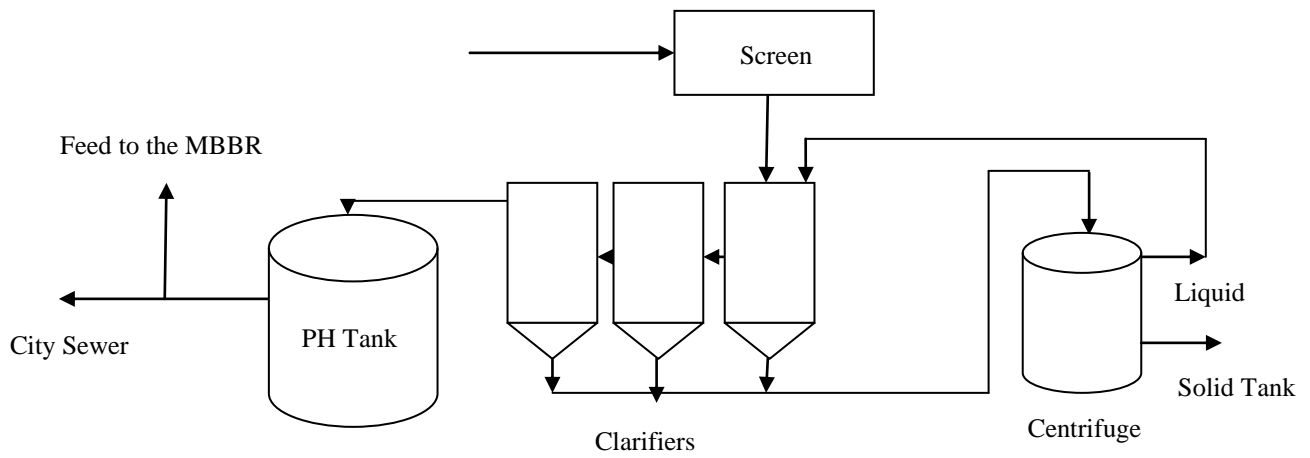
Figure 3-1 A schematic of pre-treatment process prior to the upgrade at the plant
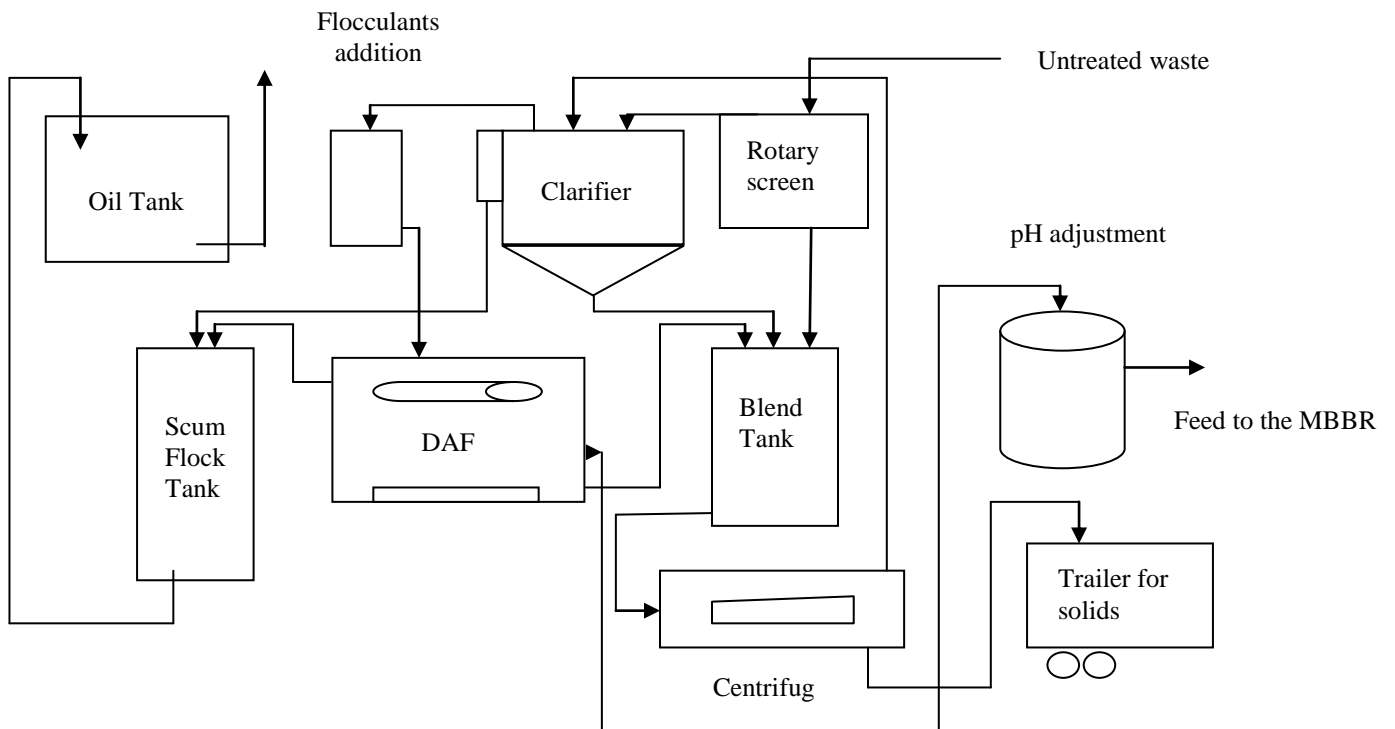
Figure 3-2 A schematic of the pre-treatment process after the upgrade at the plant

The plant's wastewater treatment system was upgraded by the addition of a Dissolved Air Flotation (DAF) unit to remove free and emulusifed oil from the wastewater. Following the rotary screen, the wastewater is directed into a large clarifier to remove the solids. The overflow line empties to a flocculant tank and the oil content is removed by the DAF. No flocculant is added to wastewater during the week but it is usually used during the weekend when the amount of oil and grease is high due to the cleaning process at the plant. The oil that is separated from the aqueous phase is collected in the oil tank and the treated wastewater flows to the pH adjustment tank where the pH is adjusted to 5.5-9.5 by using sulfuric acid and sodium hydroxide. The solids that have accumulated in the clarifier and DAF go to the blend tank and then are processed through a centrifuge to separate the solids from water phase. The solids are collected in a trailer and water is bypassed to the rotary screen to begin a cycle (Figure 3-2).

3.3 Moving Bed Biofilm Reactor

This research was carried out using a pilot-scale moving bed biofilm reactor. The pilot MBBR had a working volume of 1.8 m^3 and the volume fraction of the reactor with carriers was 60%. The MBBR was supplied by the Headworks Bio Canada Inc., Victoria, BC.

The biofilm carriers (Fig. 3-3) possess a specific gravity slightly less than water and mixing in the reactor is accomplished using three air diffusers installed at the bottom of the tank. The carriers are made from polyethylene in the form of small cylinders with diameter of 22 mm and a length of 15 mm. They were designed to provide a large protected surface for biofilm development and optimal conditions for biofilm growth. Approximately 110,000 carriers (around 1 m^3) were employed, so with each carrier having an internal protected surface area of 0.00365 m^2 this results in 402 m^2 of total protected area. The carriers were retained in the reactor using a screen sieve just before the effluent stream.

The amount of attached growth biomass (AGTS) was determined during first few months of the MBBR operation to ensure sufficient biomass had developed on the carriers.
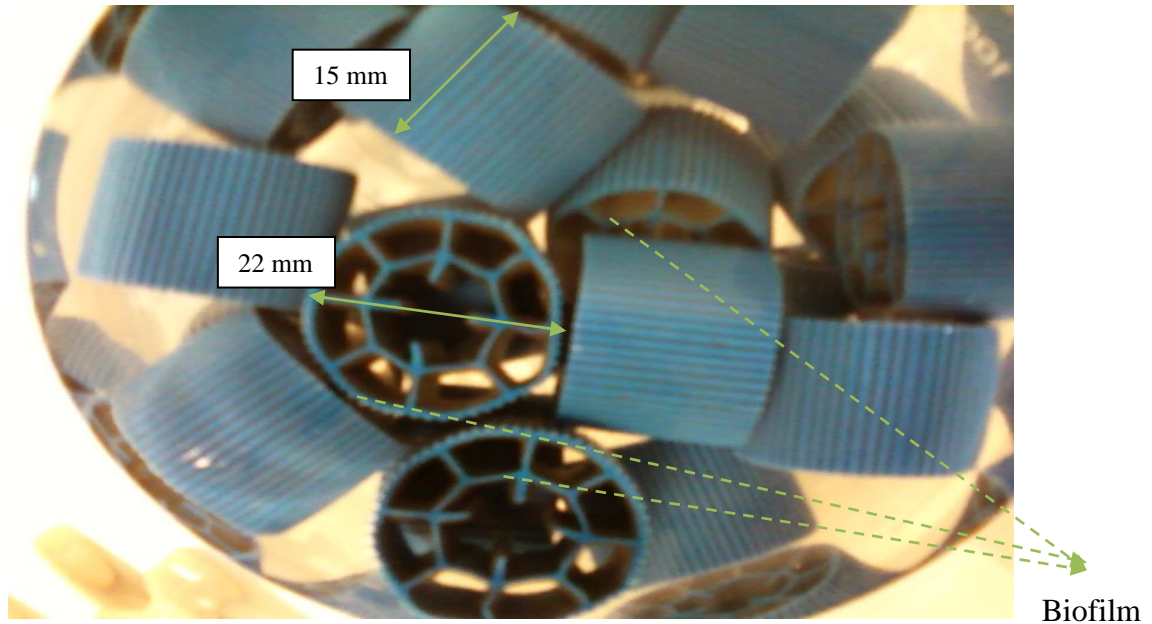
Figure 3-3 Active cell biofilm carriers

For start-up and acclimation of the carries in the reactor, a batch acclimation was performed using 200 litres of return activated sludge (RAS) from the Waterloo waste water treatment plant and 500 litres of the wastewater from the plant. pH and DO of the bioreactor were monitored and the pH value was found to be between 6.5 and 8.5. The air flow was also controlled to maintain a DO greater than 3 mg/l. Two days after addition of the RAS to the bioreactor, the batch process moved to continuous acclimation. Continuous flow of influent wastewater to the bioreactor was set initially at 20% of design influent flow (2 GPM design, 0.4 GPM initial). Initial influent feed at a low rate was recommended by Headworks to provide additional seeding time for the carriers and also to minimize any potential toxicity effects during the acclimation process. Samples were collected regularly and analysed in a sampling protocol. The flow rate was gradually increased by from 0.4 to 0.6, 0.9, 1.3, and finally 2 GPM (10.9 m^3/d).

The feed to the MBBR was accomplished by a T-connection from the city sewer pipeline flow that exits from the pH adjustment tank. Prior to the MBBR, a flow meter (F-40750L,

Blue-White Industries Ltd.) was installed to manually control the influent flow rate into the MBBR. MBBR used during the first month of operating is shown in Figure 3-4.
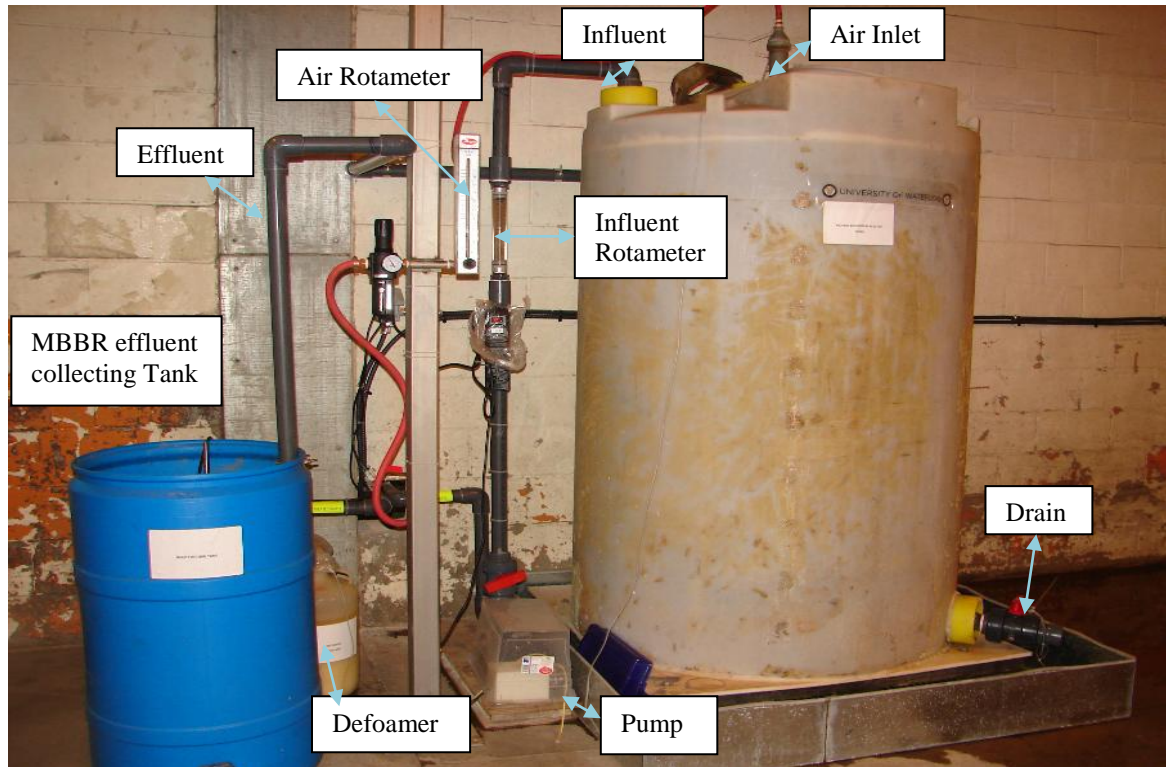
Figure 3-4 The MBBR installed and operated in the plant

During start-up stabilization of the biofilm on carriers took around two months. Therefore, the ultra-filtration pilot plant was not installed in the pilot plant at that time. Some fluctuations in the composition were observed in the influent wastewater (MBBR feed) due to variations in the products produced and the types of the potatoes utilized.

The MBBR was operated at a HRT equal to 4 h. The organic loading rates depend on the HRT and the influent COD concentration which fluctuated frequently. However, an average loading rate of approximately 78 ± 21 g/m^2/d was obtained. It should be noted here that the loading rate decreased by 20% to reach 63 ± 12 g/m^2/d when the new wastewater facility was installed at the factory.

The influent and effluent wastewater characteristics were regularly monitored for over 9 months based on a comprehensive sampling protocol as presented in Table 3-1. The influent samples were obtained from a sampling valve on the MBBR influent line and the effluent samples were taken from the open end of the effluent line. The influent and effluent samples were analysed in the wastewater laboratory of the University of Waterloo. The parameters measured during the course of this study are given in Table 3-1.

Table 3-1 Sampling and analysis protocol used in this research project

Location	Unit	MBBR Influent	MBBR Effluent
Water/Air flow	GPM/scfm	2/day	2/day
DO	mg/l		2/day
pH		1/day	1/day
Alkalinity	mg $CaCO_3$/l	2/week	2/week
TCOD	mg/l	3/week	3/week
SCOD	mg/l	3/week	3/week
TSS	mg/l	3/week	3/week
VSS	mg/l	3/week	3/week
NH3	mg N/l	2/week	2/week
SP	mg Po_4^{-3}/l	2/week	2/week
TKN	mg N/l	1/week	1/week

The samples were analyzed twice a week for alkalinity, TSS, VSS, TCOD, SCOD, ammonia, TKN, and phosphorous based on Standard Methods (APHA, 1996). The samples were completely mixed and homogenized prior to each analysis. COD was measured according to a method modified from section 5220D (closed reflux, colorimetric method) of Standard Methods. In this modified method, potassium dichromate and concentrated sulphuric acid were used as oxidants and the reflux time

was extended from 2 to 3.5 hours to ensure a complete reaction. For soluble COD, ammonia, and soluble phosphorous analysis, the samples were filtered through a Whatman® glass microfibre filters with nominal pore size of 1.2 μm (934-AHTM, Whatman Inc., Clifton, NJ). The pH was measured in duplicate by using a VWR sympHony pH/Dissolved Oxygen Meters 1246001 SP80PD. For TKN measurements, the samples were digested with a digestion solution of sulphuric acid at 220°C for 1.5 h and then at 380 °C for 2.5 h in order to convert organic nitrogen to ammonia. This procedure was developed at the Water Technology Center located in Burlington, ON, Canada. In order to prepare the digestion solution, 40 grams of potassium sulfate and 2 ml Selenium oxychloride (97%) were dissolved in 250 ml concentrated sulfuric acid. After the solution was allowed to cool it was diluted with deionized water to a volume of 500 ml. Ammonia was then measured by an alkaline phenate method (4500-NH3 F). The solids analysis for the TSS and VSS measurements was done in accordance with section 2540D and E, respectively of the Standard Methods (APHA, 1996). Furthermore, alkalinity and phosphorous measurements were carried out based up on sections 2320 and 4500-P C of the Standard Methods, respectively.

The objective of the MBBR influent and effluent analysis was to optimize the influent flow rate and operational conditions to meet the effluent quality of interest with respect to soluble COD removal. For instance, the influent flow rate would be decreased if the soluble COD was lower than the targeted soluble COD removal.

Ammonia and phosphorous concentrations were measured to ensure that there were sufficient nutrients available for biomass growth. A correct ratio of influent concentrations of BOD:N:P of 100:5 1 was required as well as effluent concentrations of residual ammonia above 2 mg/l and residual ortho-phosphate above 0.5 mg/l (Headworks Bio Inc., Victoria. BC).

Continuous aeration was performed by using three coarse bubble diffusers as aperture sizes underneath the MBBR varied between 6.350 and 9.525 mm. It was recommended by the Headworks Bio Inc. to keep the DO of the MBBR above 2 mg/l. The average DO of the MBBR was 3.2 mg/l; however, DO was varied from 7.3 to 0.2 mg/l due to flunctuations in influent characteristics which affected the DO. The DO was manually

measured on site using a SympHony DO meter (SP80PD) twice per day. Higher COD loading rates in the plant, especially when a defoamer was employed, led to a low DO during the pilot plant operation.

After installation of a sprinkler system and an airline to disrupt the foam instead of using defoamer, DO was no longer the limiting factor and the DO remained within a reasonable range. This was attributed to the additional airline at the top of the MBBR, or the removal of the defoamer from the system. The defoamer and the fat and oil in the aerobic treatment process could limit oxygen transfer into the biomass through the building up an oil film at the air/water interface decreasing oxygen transfer. Also, grease adsorption to bacterial flocs can have a similar effect decreasing the DO level (Lefebvre *et al.*, 1998).

Foaming of the MBBR proved to be challenging. Foaming normally occured during the start-up of the MBBR system when there was a high COD load and aeration. However, due to fluctuations in the influent quality during this research project, excessive foaming occurred frequently. A non-toxic defoamer (KFO TM 6450 FL, Emerald Performance Material LLC, Cuyahoga Falls, OH) was employed. A small peristaltic pump was used with a flow of ≈ 3 ml/min. Approximately 4 litres of defoamer was required each day during the first few months of the pilot plant operation. It should be noted that there was still some over foaming even if the sprinkler system was used. However, no over foaming occurred after installation of the new wastewater treatment facility since the influent characteristics changed.

3.4 Coagulation

In order to determine proper dosage for the subsequent membrane trials, a series of coagulation jar tests were carried out. Ferric chloride was used a coagulant based up on a previous study (Pervissian *et al.*, 2011). This coagulant was found to perform the best as a pre-treatment coagulant when compared to alum and the coagulant blend with reduction in both reversible and irreversible fouling (43-86% and 51-71%, respectively).

A number of jar tests were performed with samples collected for different days to cover a range of MBBR effluent characteristics. Figure 3-5 shows a jar test unit. The coagulant was provided by the Control Chem /Inc, Burlington, ON. Two jar test units were

employed. Each jar was dosed with a different quantity of coagulant and pH and turbidity were measured and recorded after the experiment. The rapid mixing phase of all of the jar test trials was performed for 2 min at 100 rpm, representing a velocity gradient of 70 s^{-1}. The slow mixing phase of all the trials was performed for 20 min at 20 rpm representing a velocity gradient of 10 s^{-1} (Randtke, 1988). The settling period lasted for 45 min. The mixing speeds and time intervals were obtained from standard jar test practices that have been employed for both water and waste water treatment (AWWA, 2005). Once the settling period was complete, samples were collected from the supernatant near the top of the beaker and turbidity of the supernatant and pH then was recorded. Turbidity of the samples was measured in triplicate with a portable hand held Hach turbiditimeter model 2100P (Hach Co., Loverland, CO).

The coagulant dosage that yielded the lowest turbidity in the settled water or the lowest dosage above which the decrease of residual turbidity was insignificant, was deemed the optimal dose.

Figure 3-5 The jar test unit implemented in this study

3.5 MBBR Coagulation and MR Apparatus

A process flow diagram (PFD) for the entire membrane pre-treatment system is shown in Figure 3-6.
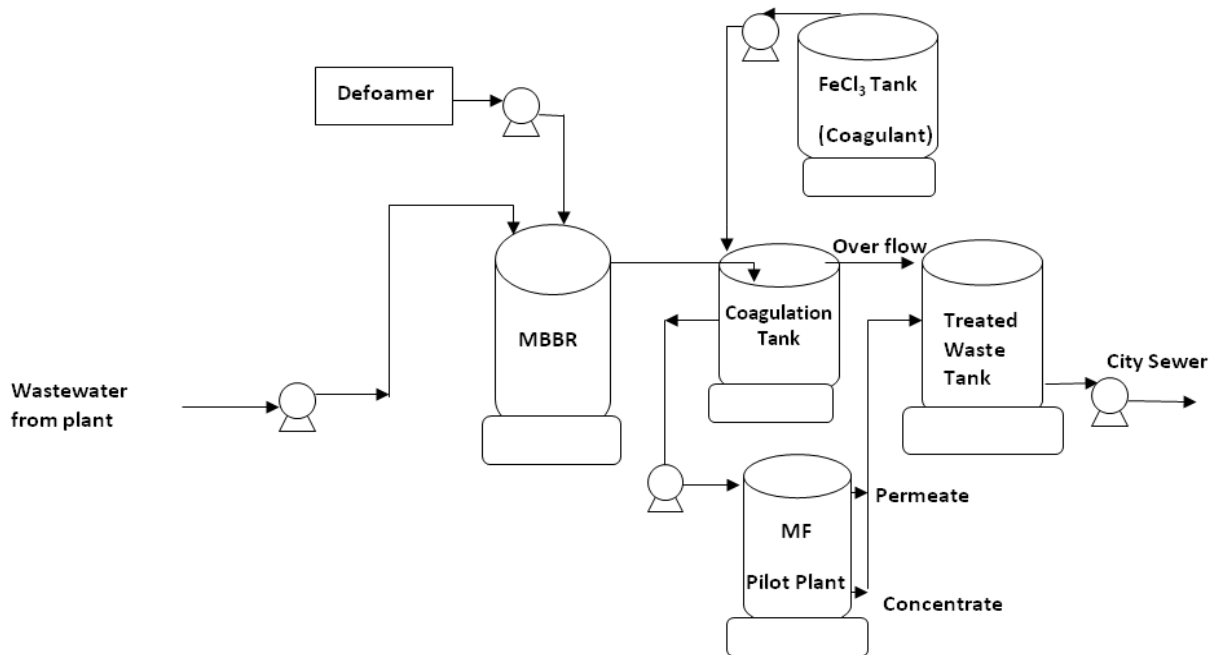
Figure 3-6 Schematic of the MBBR-MR pilot

Raw feed was introduced to the MBBR using a laundry tub pump (Burke Group, model: 300315W, Laval, Canada) with the flow of 2 GPM (10.9 m^3/d). Effluent from the bioreactor was fed by gravity to a coagulation tank and coagulant was added via an adjustable positive displacement pump (Masterflex). A mixer was utilized to mix the coagulant with the wastewater, ensuring a uniform mixture for waste throughout the duration of all membrane trials. Speed of the mixer was adjusted so that it was high enough to prevent the flocs from settling but not too high to cause disruption of the flocs. A U tube shape was employed to direct the excess feed to the waste tank to control the hydraulic retention time (HRT) of coagulation at 15 min and to prevent overflow of the waste. The coagulation tank was cleaned after each trial as a substantial amount of floc was found to accumulate at the bottom of the tank.

Coagulated feed was added to the membrane process tank with a centrifugal pump (Goulds pumps Inc, model 4101007403, HP ½, rpm 1725, Hz 60), and the filtrated stream was directed into a permeate storage tank where overflow was collected in the waste tank to be discharged into the municipal sewer. The concentrate stream, which was high in solids concentration, was also pumped with an adjustable pump (Master flex, model 7529-30) into the waste tank. Figure 3-7 shows a picture of the pilot plant as installed and operated at the factory.

Figure 3-7 A picture of the pilot plant as installed and operated at the factory

After the MBBR was run for several weeks, the MR was installed in the pilot plant. During the operation a rapid fouling occurred and the resulting fouling caused an increase in the suction pressure of the membrane exceeding the maximum allowable pressure (~ -9 psi or -62.1 Kpa). Different operational conditions with respect to permeate and air flow rates, backwash duration etc. were then investigated, but fouling was still observed after a few hours of treatment.

The membrane supplier, Trisep Corporation, suspected the rapid fouling could be due to either the presence of oil and grease in the wastewater or an issue with the silicone-based defoamer used at the factory. Samples of bioreactor influent and effluent were collected on 3 different days and analyzed for oil and grease content. The oil and grease concentrations were found to be in the range of 13.5-59.5 mg/l and 82.9-248 mg/l for the influent and effluent, respectively. This high level of oil and grease in the effluent line was attributed to the silicone-based defoamer that was added to the bioreactor to reduce foaming. The use of defoamer was therefore stopped and a sprinkler system that disrupted the foam mechanically was introduced. A sump pump (Mastercraft) was installed to utilize the MBBR fluid to run through the sprinkler so that no additional liquid would be introduced into the system.

3.6 Ultra-Filtration Process

The spiral wound membrane unit consists of an immersed, negative-pressure ultra-filtration (UF) membrane which removes suspended solids, turbidity, viruses, bacteria, and some organic compounds. The UF membrane consists of a spiral wound element with a pore size of 0.03 μm, submerged inside a process tank. The membrane element is attached to a permeate header pipe which in turn is connected to the UF membrane. A vacuum is generated by the suction of a centrifugal pump, creating the necessary net drive pressure to pull water through the UF membrane. Air is bubbled up through the membrane element via a diffuser, creating shear forces on the membrane surface to help remove any suspended solids. Periodically, permeate water was backwashed through the membrane to further help remove accumulated suspended solids. The membrane can also be chemically cleaned through one of the following two processes: a Periodic Flux Enhancement (PFE) or the Clean In-Place (CIP) procedure.

Feed to the UF process was separated into two streams: permeate and concentrate. Approximately 10% of the feed entering the membrane tank was removed as concentrate via a concentrate drain valve. An automated ball valve is employed to turn the concentrate flow on or off via the PLC. A concentrate removal pump was installed to

pump the solid stream out to the waste tank. Permeate is drawn through the membrane with a centrifugal pump.

3.6.1 Process Start-up

Feed was introduced to the membrane tank via a centrifugal pump controlled by the PLC. The feed control valve which controls the feed flow meter was manually set using a flow meter. Once the feed water was introduced to the membrane tank and triggers the high level switch (located at the top of the membrane tank) the blower turned on. The air flow was manually adjusted in order to provide a proper air flow rate to the element (5 scfm).

3.6.2 Permeate Production

Once the membrane tank is completely filled and triggers the high-high level switch, the PLC sends a command for turning on the permeate pump and to open the concentrate valve which must be set at a proper concentrate flow rate. When the permeate production started, timers for the backwash frequency and PFE were started. Permeate and feed pumps work based on the level switches and if at any time the level of the feed decreases the permeate pump is turned off and until the level recovers. Also, if the level rises too high and stays there for longer than 1 minute, the feed pump shuts off. In order to prevent solid accumulation in the membrane, water was continually drained from the process tank by a reject pump

3.6.3 Membrane Backwash and PFE

Permeate production and aeration was stopped every 10 min. The permeate water from the permeate storage tank was backwashed through the membrane for a period of about 30 seconds to further remove cake layer formation. Excess water that was introduced to the tank was removed via a tank overflow line. Once the backwash sequence expired, the backwash pump was automatically turned off. The blower was turned on and allowed to operate for 30 seconds (relaxation) before the production was restarted.

A PFE was performed for every four hours of production. When a PFE process was initiated then the production was stopped and the blower and feed pump were turned off.

The UF permeate and chemicals (sodium hypochlorite and sodium hydroxide) were then automatically backwashed through the membrane while still immersed in the feed water (membrane tank was not drained for this process).

Membrane Backwash

Frequency	10 min
Duration	30 sec
Relaxation time	30 sec
Backwash flow rate	3-4 GPM

Periodic Flux Enhancement (PFE)

Frequency	4 hour
PFE Backwash Length	10 min
PFE Static Soak Length	10 min
PFE Backwash Flow Rate	1.8-2 GPM
Sodium Hypochlorite PFE Dosage Concentration	100 mg/l
Sodium Hydroxide Concentration	0.1%

3.6.4 Clean-In-Process

A full-scale Clean-In-Process (CIP) was performed when the maximum TMP of the system (10 psi) was reached or between each run. After the feed water was drained from the membrane tank, permeate containing chemical (sodium hypochlorite and sodium hydroxide) was backwashed through the system until the membrane elements were fully submerged. Additional chemicals were then added to adjust the pH to 10.5 and chlorine concentration of 1000 ppm. The membrane was allowed to soak in the cleaning solution for a period of 1-3 hours. After the static soak, additional backwashing was performed in order to remove the additional solids and particulate matter. The cleaning solution was then drained and directed into the waste storage tank at the plant.

A rupture disc (1 inch, 150 ANSI, part number 4858K701) with a burst pressure of 15 psig ± 5 % was used in the permeate line. Therefore, under high pressure conditions, PSH would appear on the control panel and the alarm light on the front of the panel would flash fast indicating a need to do and immediate action by the operator (e.g., decrease the backwash flow rate) in order to prevent rupture.

The main control screen for the membrane pilot plant is presented in Figure 3-8. The operator can see the status of the entire system and control the START/STOP of the system. Also, the operator can navigate to all the remaining screens for Manual-Off-Auto control of all the devices. Since the program at the PLC was defined to open the concentrate line only during the production period, and no solids were removed at the time of backwash or PFE, it was set manually open all the time to remove the accumulated solids during the backwashes and PFE.
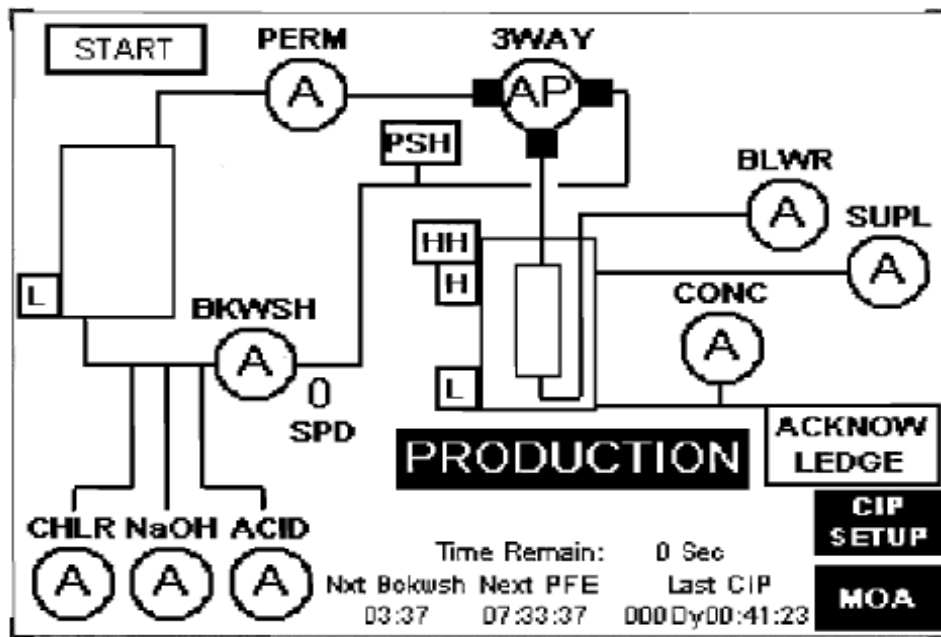
Figure 3-8 The main control screen of the membrane pilot plant used in the factory

3.6.5 Equipment Design and Specifications

Design and specifications of the equipment used during this research project are described on the text below.

Ultra filtration membrane

Model	SpiraSep 960
Chemistry	PES
Element diameter	9.38"
Element Length	43"
Membrane tank	100 gallon P.E.
Permeate storage tank	100 gallon P.E.
Chemical supply tank	10 gallon

Permeate pump

Pump type	Goulds GT10 self- priming centrifugal
Capacity	45 GPM @ 20 ft suction lift
Pump power	1 HP
Power	115/230 VAC, 1-phase, 60 Hz

Backwash pump

Pump type	Goulds NPO 1NS1C5F4SS centrifugal
Capacity	10 GPM @ 10.0 psi discharge
Pump power	1/2 HP
Power	230/460 VAC, 3-phase, 60 Hz

Chemical metering pump

Pump type	Positive Displacement
Model	LMI- Milton Roy
Capacity	0.21 GPH
Controller	Manual
Power	115/230 VAC, 1-phase, 60 Hz

Blower

Power	1 HP
Blower type	Regenerative (oil less)
Model	Atantic

Construction   Carbon steel

Process piping   sch 80 PVC changed to galvanized pipe

Control   Manual throttle valve

Capacity   75 cfm @ 2.55 psi discharge

Table 3-2 Manufacturer's specifications for the ultrafiltration membrane

Parameter	Specification
Diameter	9.38 inches (238 mm)
Length	40.0 inches (1,016 mm)
Active Membrane Area	225 ft^2 (20.9 m^2)
Membrane Chemistry	Polyethersulfone
Average Pore Size	0.03 micron
Maximum Chlorine Exposure	2,000 mg/l
Operating pH	2-11
Cleaning pH	2-12

3.7 Evaluation of Membrane Resistance and Flux

3.7.1 Temperature Correction Factor

Membrane permeate production is partially dependent on temperature. In order to estimate the effect of temperature on membrane flux, the following temperature correction factor (TCF) was used (reference temperature was 25 °C).

$$\text{TCF} = e^{1100(\frac{1}{298} - \frac{1}{T})} \qquad \textbf{3-1}$$

where the unit of T is °K.

To calculate the temperature corrected flux rate, the Equation 3-2 was used:

$$Q_{TCF} = Q_p / (A \times \text{TCF}) \qquad \textbf{3-2}$$

Where:

Q_p =   permeate flow rate (L/h)

A   =   membrane area (m^2) and

TCF   =   temperature correction factor

Also, Q_{TCF} is in L/m^2h or (LMH).

3.7.2 Membrane resistance

Performance of the membrane separation unit was evaluated based on the increase in membrane resistance (membrane fouling) and permeate COD. The permeate flow rate, temperature, and Transmembrane Pressure (TMP) were recorded by the data logger every 20 seconds during operation.

The permeate flux is proportional to the TMP and inversely proportional to the dynamic viscosity (μ) of permeate and total resistance (R) according to Darcy's law. Membrane resistance was determined using Eq. 3-3:

$$R= TMP / (Q_{TCF} \times μ) \hspace{3cm} \textbf{3-3}$$

R is in 1/m.

3.8 Ultra-Filtration Experimental Plan Design

A systematic analysis of the experimental design is provided in Table 3-3. A total of 16 trials were performed (including 3 replicate runs of) each lasting three days.

Table 3-3 Summary experimental design of the ultra-filtration experiments

Trial	Coagulant Dosage (mg/l)	Permeate flux (LMH)	Feed flow rate (GPM)	Concentrate flow rate (GPM)	Air flow rate (scfm)
1	600	7.6	2	0.2	5-6
2 (Two R)	600	8.7	2	0.2	5-6
3	600	9.8	2	0.2	5-6
4	800	7.6	2	0.2	5-6
5	800	9.8	2	0.2	5-6
6	1000	7.6	2	0.2	5-6
7	400	7.6	2	0.2	5-6
8	400	9.8	2	0.2	5-6
9 (R)	600	7.6	2	0.2	5-6
10	600	8.7	2	0.2	5-6
11	200	7.6	2	0.2	5-6
12	200	8.7	2	0.2	5-6
13	0	7.6	2	0.2	5-6

(R) = Replicate runs

The experimental work using the membrane was carried out by varying the coagulant dose and permeates fluxes; however, other variables were kept constant for all tests conducted. Flow rates of the membrane feed and concentrate streams were maintained at 2 and 0.2 GPM, respectively. Backwash frequency for all tests was 10 min, and membrane rinsing with permeate and relaxation took 30 sec. The PFE was performed every 4 hours of production without considering the backwash time. A chemical CIP was also implemented after each run to recover the membrane permeability. The intrinsic membrane resistance was not always totally recovered and some changes in the membrane pore size due to frequent cleaning were inevitable.

Replication of the experiments was conducted in order to assess the reproducibility of the results considering the fluctuations of the effluent characteristics. The first six tests were carried out before the wastewater treatment plant at the factory was upgraded. After

installation of the new waste water treatment plant, more runs were performed to investigate the effect of wastewater properties on membrane fouling.

Representative samples from 6 different ports are presented in Figure 3-9. From left to right: influent to MBBR, effluent of MBBR, coagulated feed to the membrane, membrane process tank, permeate, and concentrate streams, respectively.
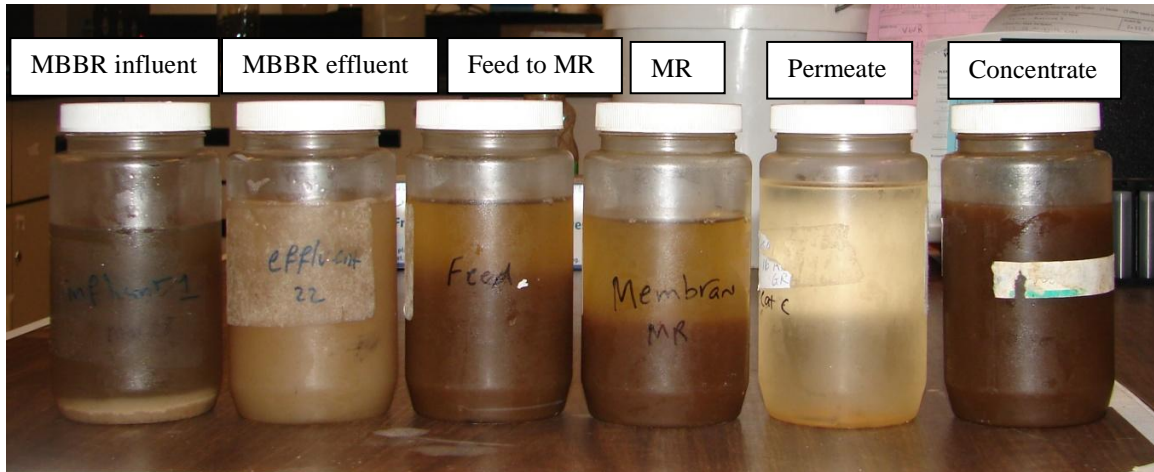
Figure 3-9 Wastewater samples from different sample port locations of the pilot plant

CHAPTER 4

ULTRA-FILTRATION TRIALS

4.1 Introduction and Objectives

The following chapter presents the results obtained through the series of membrane trials performed during phase I and II of the research. There were a total of 16 trials performed (including 3 runs of replicates), each lasting three days. As previously mentioned, all of the trials were carried out using the pilot scale UF membrane system described in Chapter 3. In each experimental test, different coagulant doses and fluxes were used and other variables, including feed and concentrate flow rate, aeration flow rate, backwash, PFE frequency and duration, were kept constant in order to examine the effects of each variable on membrane fouling. A chemical Cleaning In Process (CIP) was applied after each run to recover the membrane permeability.

During each trial period, trans-membrane pressure (TMP) values and permeate flow rates were recorded; comparative results presented in this chapter highlight how different coagulant doses in the form of pre-treatment to the UF membrane system were employed. Additionally, some samples of each trial were collected at six different locations: raw wastewater inlet, MBBR effluent, coagulated wastewater, membrane tank (top zone), permeate and concentrate line. Each of the six samples was analysed in duplicate for TCOD, SCOD, TSS and VSS. The permeate COD of each trial was measured to assess the treatment efficiency of the system. Some of the trials were repeated at least twice in order to ensure the reproducibility of the experiments.

The objectives of research were as follows:

- To assess the effects of coagulant dose on UF membrane fouling;
- To evaluate the impact of permeate flux on membrane fouling;
- To determine the impact of upstream pre-treatment on the performance of the MBBR and on the membrane fouling rate.

4.2 Characteristics of MBBR Influent and Effluent

This section describes the performance of the MBBR in phases I and II of the research. TSS, VSS, TCOD, SCOD, alkalinity, ammonia and phosphorous of the MBBR influent and effluent were measured three times per week based on the analytical methods mentioned in Chapter 3. The characteristics of the MBBR influent and effluent are presented in Table 4-1.

Table 4-1 Characteristics of MBBR influent and effluent before upgrade (n = 63)

Location	Parameter	pH	TCOD mg/l	SCOD mg/l	TSS mg/l	VSS mg/l	NH3-N mg N/l	TP mg PO_4^{-3}/l	TKN mg N/l
Influent	Mean	7.9	3196	2231	1313	1072	21.7	18.7	110.4
	Standard Deviation	1.0	785	554	1165	1034	11.6	7.8	46.5
	Minimum	6.2	1298	835	275	170	4.0	1.6	29.0
	Maximum	9.7	5148	3729	5720	5050	47.7	33.0	168.6
Effluent	Mean	7.5	2735	716	2056	1741	28.7	4.1	120.6
	Standard Deviation	0.4	922	287	1095	858	15.2	3.0	34.1
	Minimum	6.5	257	229	410	350	0.1	0.05	69.6
	Maximum	8.1	4685	1360	6450	4750	57.7	14.6	184.5

Table 4-1 presents pH, TCOD, SCOD, TSS, VSS, ammonia, TP and TKN in the influent and effluent of bioreactor. As shown in Table 4-1, no pH adjustment was required during the study as the values varied between 6.5 and 8.1 for the bioreactor effluent. The TCOD of the influent varied widely throughout the period of data collection, from 1298 to 5148 mg/l, with an average value of 3196 mg/l. These significant fluctuations of the stream were mainly due to operational variability in the factory and/or equipment failures in the upstream wastewater treatment plant. The average SCOD of the influent and effluent had values of 2231 ± 554 mg/l and 716 ± 287 mg/l, respectively which showed 72% SCOD removal by the MBBR.

As shown in table 4-1, higher TSS and VSS values were observed in the MBBR effluent as compared to the influent. An increase in TSS from an average of 1313 mg/l in the influent to an average of 2056 mg/l in the effluent (almost 36%) was observed. This increase can be explained by the fact that MBBR did not provide high particulate matter removal, however, there was biomass growth in the MBBR, therefore, higher particulate matter was observed in the effluent.

Table 4-1 also shows that concentrations of ammonia and phosphorous in the MBBR influent were in the range of 21.7 ± 11.6 mg/l and 18.7 ± 7.8 mg/l, respectively. As mentioned in Chapter 3, the ratio of bCOD: N: P ratio that has been reported in the literature to be necessary for good treatment is 100:5:1 and 250:5:1 for aerobic and anaerobic treatment, respectively (Tchobanoglous *et al.*, 2003). The nutrient concentrations in the wastewaters employed in this study (i.e., 116:5:0.8) were lower than those reported in the literature. However, the effluent concentrations of residual ammonia were above 2 mg/l (28.7 ± 15.2 mg/l) and the residual ortho-phosphate concentrations were above 0.5 mg/l (4.1 ± 3 mg/l) that were recommended by the MBBR vendor (Headworks Bio Inc.). Therefore no nutrient addition was required during this study. It should be noted that occasionally the amount of residual ammonia in the effluent was higher than in the influent. This was attributed to the time-varying nature of the influent stream and the relatively short HRT of the reactor that was about 4 hours.

Table 4-2 Characteristics of MBBR influent and effluent after upgrade (n = 15)

Location	Parameter	pH	TCOD	SCOD	TSS	VSS	NH3-N	TP	TKN
			mg/l	mg/l	mg/l	mg/l	mg N/l	mg PO_4^{-3}/l	mg N/l
Influent	**Mean**	7.3	2490	1761	903	727	16.7	15.5	57.0
	Standard Deviation	0.8	460	281	489	366	3.0	8.5	4.8
	Minimum	5.2	1716	1304	250	160	13.5	5.8	52.8
	Maximum	8.1	3341	2279	1960	1590	23.4	32	62.2
Effluent	**Mean**	7.6	1636	411	1341	1006	15.8	4.3	73.6
	Standard Deviation	0.2	274	110	312	225	7.0	1.8	24.4
	Minimum	7.1	1172	241	780	640	5.4	2.3	49.1
	Maximum	7.9	2179	652	2000	1520	26.1	7.8	98.0

Table 4-2 presents the characteristics of the influent and effluent of the MBBR after the upgrade of the upstream wastewater treatment plant (phase II). From Table 4-2, it can be seen that the pH values did not show significant variability, remaining between 7.1 and 7.9, which indicated pH adjustment was not required in this phase. It was noted that the pH value varied over a narrower range for phase II than phase I. However, there was not a significant difference between the values observed in the two phases (ANOVA is summarized in Tables B-1, Appendix B). The TCOD of the influent and effluent varied from 1716 mg/l to 3341 mg/l and 1172 to 2179 mg/l, respectively. The TCOD reduction indicate that some of the organic compounds (mainly readily biodegradable COD) were removed by the bioreactor. Although the bCOD:N:P ratio was approximately174:5:1.4, there was enough residual ammonia and phosphorous in the bioreactor and hence nutrient addition was not required (see Table 4.2). The concentrations of TKN in the MBBR effluent decreased by 35% through the enhancement of the wastewater treatment plant at the factory, reducing from 120.6 ± 34.1 mg/l to 73.6 ± 24.4 mg/l. An ANOVA test revealed that this difference was statistically significant (Table B-2, Appendix B). The high TKN concentrations of the wastewater suggest the presence of proteins. Proteins

can be one of the major polymer foulants (Jarusutthirak *et al*., 2002) that may affect the membrane fouling in the UF trials.

The carriers in the MBBR provided 420 m^2 of protected area for microbial growth and it was anticipated that the amount of attached biomass on the carriers would affect MBBR performance. The amount of attached biomass on carriers was measured by performing the attached growth total solid (AGTS) test (Appendix A). Figure 4-1 depicts the amount of biomass per carrier versus time. The plot indicates that there was a rapid increase in biomass growth on the carriers during the first month of operation. However, the trend became almost constant after steady state conditions were reached, achieving about 0.08 grams of biomass per unit of carrier. Hence, there was no net accumulation of solids on the carriers while the membrane testing trials were conducted.
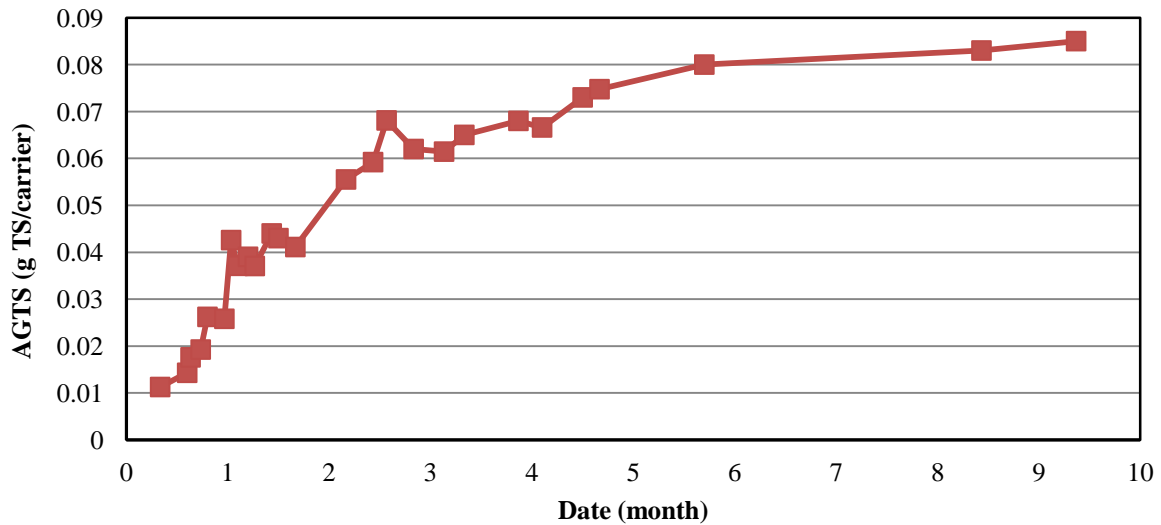
Figure 4-1 AGTS on carriers versus time

4.3 Effect of Upgrading WWTP on MBBR Performance

Dissolved air flotation (DAF) has been used with increasing frequency in the recent decades for the treatment of industrial wastewater (Ross *et al*., 2000). This process has gained widespread usage for the removal of suspended solids (TSS), oil and greases

(O&G) and biochemical oxygen demand (BOD) from wastewater and other industrial process streams. Therefore it is expected that upon installation of the DAF in the WWTP, solid, oil and grease (O&G) concentrations would be reduced, leading to reduction of membrane fouling.
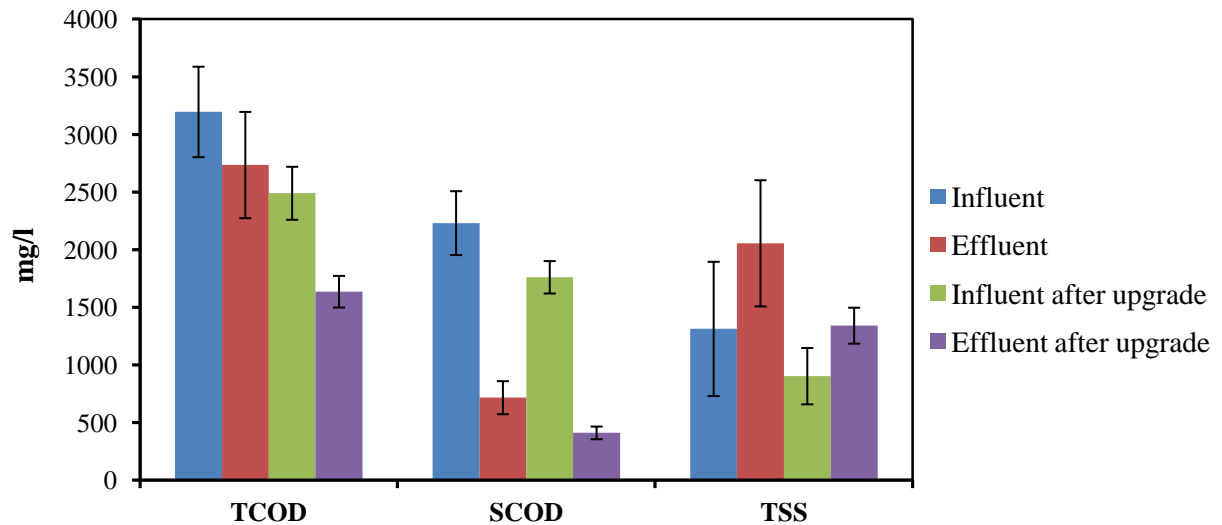
Figure 4-2 Characteristics of wastewater before and after upgrade

Figure 4-2 summarizes the characteristics of influent and effluent of the MBBR before and after the upgrade. As Figure 4-2 shows, the TCOD of the MBBR influent (raw wastewater) decreased from an average of 3196 mg/l to 2490 mg/l when the wastewater treatment plant (WWTP) was modified, a reduction of 22%. Also, a 31% decrease in the TSS of the raw wastewater was observed (from 1313 mg/l to 903 mg/l). The concentration of phosphorus remained relatively constant before and after plant upgrades; however the concentration of ammonia was reduced by 23% due to changes in the WWTP facility. These findings were analyzed through a one way ANOVA (Table B-3 through B-6, Appendix B) and found to be statistically correct. A decrease in organic compounds and solid concentrations (TCOD and TSS) of the wastewater stream could affect the UF performance during the test runs. The MBBR had a SCOD removal of 72% ± 8% which increased to 78% ± 7% for the new wastewater. An ANOVA test was performed and demonstrated that the removal efficiencies were significantly different

(see Table B-7 in Appendix B). The observed performance was considered as a good efficiency for a single reactor. It was anticipated that the more SCOD that was removed, the more colloidal particles would be eliminated and there would be a reduced loading of this material on the membrane. Therefore, it could reduce the membrane fouling in terms of irreversible fouling (pore blockage).

4.4 Preliminary Coagulation Jar Test Trials of MBBR Effluent

Preliminary coagulation tests were performed to determine a starting dose to operate the pilot plant and to evaluate if there was a correlation between the optimum doses in jar tests and the fouling of the membrane in the UF trials. In the jar test trials for ferric chloride, a range of dosages of ferric chloride were added to 1 litre samples of the MBBR effluent; the turbidity and pH at each dose were measured. Four trials were conducted before the upgrade (Bu-1, Bu-2, Bu-3 and Bu-4) and after the upgrade (Au-1, Au-2, Au-3 and Au-4) to the WWTP and are presented in this section. The wastewater characteristics and the optimal dosage of iron for turbidity removal are presented in Table 4-3. As mentioned in Chapter 3, the coagulant dose that yielded the lowest turbidity in the settled water was to be deemed the optimal dose for the purposes of this study (optimization was based on the standard jar test method).

Table 4-3 Wastewater characteristics for ferric chloride coagulation

Trial	DO (mg/l)	TSS (mg/l)	TCOD (mg/l)	SCOD (mg/l)	Initial pH	Optimum dose (mg/l)	pH at optimal dose	Turbidity at optimal dose (NTU)
Bu-1	4	1840	2967	1197	7.0	600	5.2	8.3
Bu-2	3.5	2030	3368	1035	6.9	800	5.1	8.0
Bu-3	1.5	2200	3566	704	7.5	850	5.0	2.9
Bu-4	4	1800	2377	737	6.7	600	5.5	4.6
Au-1	3.9	1000	1622	260	7.1	700	5.4	5.0
Au-2	4	1290	2041	511	7.8	600	6.0	5.6
Au-3	4.2	1600	2179	427	7.6	700	5.9	27.4
Au-4	2.9	1140	1679	652	7.7	800	5.9	15.8

Table 4-3 shows the values of DO, TSS, TCOD, SCOD and pH of the wastewater along with the optimum dose, pH and turbidity at optimal dose. The DO of the MBBR could not be kept stable during the experimental period and varied from 1.5 to 4.2 mg/l. In trial 3 (Bu-3) the optimal dose of ferric chloride was the highest dose tested (850 mg/l). This may have been due to the high concentration of solids and organic compounds in the Bu-3 sample (2200 and 3566 mg/l). The initial pH did not affect the coagulant efficiency and optimal dosage. The pH at optimal dosage was in the range of 5.0 - 6.0. Therefore, it is expected that the maximum turbidity and colloidal particles removal would occur in this pH range. The optimal dose ranged from 600 to 850 mg/l with an average of 700 ± 100 mg/l. This significant range might have been due to fluctuations in the wastewater characteristics. Overall, turbidity decreased from $515 - 1000$ NTU to $2.9 - 27.4$ NTU, yielding a 99% turbidity removal in these trials.
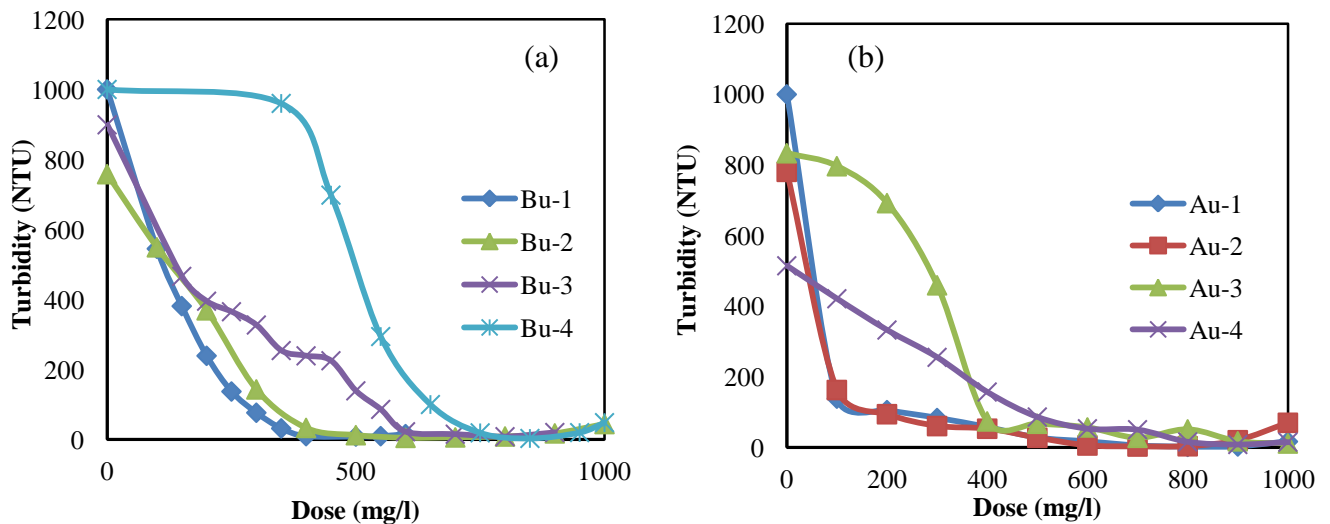
Figure 4-3 Residual turbidity vs. dosage (a) before upgrade (b) after upgrade of WWTP

The detailed results obtained from the coagulation trials are presented in Figure 4-3. All the curves in Figure 4-3 followed a similar trend. Turbidity decreased quickly at low doses in all trials (except for Bu-4) until it essentially levelled off at some dosage value. At this dosage, which was considered to be the optimal dosage, the majority of the

colloidal particles were likely neutralized. Although the average values of the observed optimal dosages were constant before and after upgrade, turbidity decreased quicker at low dosages in trials after the upgrade of the WWTP compared to before the upgrade period. On the basis of the jar test results it was anticipated that the coagulant dose required to remove organic and colloidal compounds from the wastewater would be less after the upgrade.

4.5 Membrane Filtration Results

Once the MBBR process had achieved a pseudo steady-state a series of tests were conducted to assess the impact of coagulant dosing and flux on the performance of the downstream membrane.

4.5.1 Initial Membrane Resistance Changes with Time

After each trial, a CIP was performed to recover the membrane permeability; however, the permeability after cleaning was not constant and changed with time. Figure 4-4 shows the initial membrane resistance versus time after each CIP cleaning. According to figure 4-4, it is apparent that initial membrane resistance (at the beginning of each trial) was almost constant at an average of 6.6E+12 1/m; there was, however, a significant difference for the last three trials, with membrane resistance increasing to 1.3E+13 1/m for the last run. As described in Chapter 3, chemical cleaning was conducted between each trial; however membrane permeability was not restored completely in the later trials. It seems that fouling was mainly caused by pore-blockage and foulants still existed after cleaning. It is unlikely that the presence of either cake or gel fouling layers would result in permanent membrane blockages since they can normally be removed by chemical CIP (Wei *et al*., 2011). Another possible reason for the lack of recovery of permeability (high initial resistance) could be membrane damage that generally happens through exposure to the chemicals during cleaning. The chemicals can increase the pore size of the membrane, therefore small particles more likely block the membrane and cause the permanent fouling. However, damaged membranes are not clearly visible in many cases. Some of the diagnosis methods (i.e. vacuum test) have been developed to monitor

membrane integrity (Lozier, 2004); thus further tests would be required to prove degradation of the membrane unit.
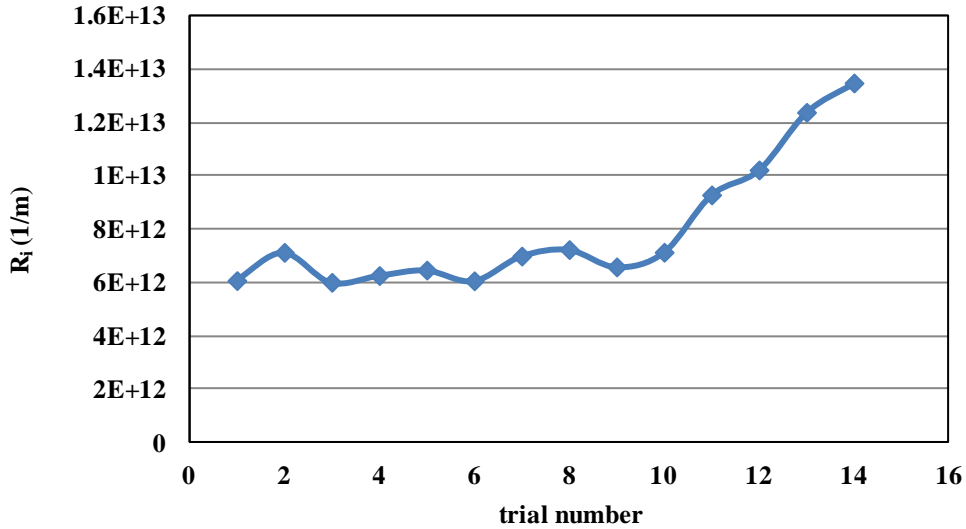
Figure 4-4 Initial membrane resistance for different trials

Since the initial membrane resistance was different at the start of each trial, once a steady state had been reached, the values were averaged and presented as a final membrane resistance. Total resistance was analyzed for each run based on the difference between the final membrane resistance (average data after reaching a plateau) and initial membrane resistance. Hence this was resistance was calculated based on equation 4-1:

$$R_t = R_2 - R_1 \tag{4-1}$$

where R_t is the total resistance, R_2 is the average resistance (plateau) at the end of the 3-day trial period and R_1 is the initial resistance.

A sample of typical flux and TMP data for a specific trial is presented in Table 4-4 to demonstrate how the resistance plots were generated. This table lists the results of the membrane trial which employed an 800 mg/l coagulant dose pre-treatment and a 7.6 LMH permeate flux. The TMP, flow rate and temperature of the permeate were recorded using a data logger. The calculated flux values were based on a membrane active surface

area (20.9 m^2). As can be seen in Table 4-4, TMP increased with time from 122 Kpa (1.7 psi) to 544 Kpa (7.9 psi) by the end of the 3-day period and correspondingly the flux decreased from 7.6 LMH to 4.9 LMH. Since both TMP and flux changed during the trial, the variations of membrane resistance were calculated and performances comparison was done based on the resistance values. The resistance values were calculated using Darcy's law.

Table 4-4 Typical TMP and Flux data for a specific trial

Time (min)	0	1	2	3	4	5	6	…	4320
TMP (Kpa)	12.2	14.4	15.1	15.5	15.5	15.7	16.0	…	54.4
Flux (LMH)	7.6	7.5	7.5	7.4	7.2	7.1	7.0	…	4.9

Figure 4-5 shows an example of a raw resistance plot. Each of the points on the figure was calculated using a pair of TMP and the permeate flux values that were presented in Table 4-4. As seen in Figure 4-5, the resistance was approximately 6.5E+12 1/m at the beginning of the trial and increased to an average value of 4.6E+13 1/m at the end of the 3-day period. As shown in Figure 4-5, membrane fouling demonstrated two different trends. A rapid rise was observed in the resistance when R increased from 6.5E+12 1/m to around 3.0E+13 1/m during the first 18 hours of the operation and then a slow increase from 3.0E+13 to 4.6E+13 for the rest of the 3-day period occurred. The observed behaviour was likely a result of the high concentrations of solids that the membranes were exposed to. These solids likely adsorbed to the majority of available sites on the membrane surface or inside pores due to concentration polarization during the first day (Baker, 2004) and hence contributed to the sharp increase of the membrane resistance for the first day. Once the majority of sites were occupied, the cake resistance became stabilized and the rate of fouling remained relatively constant over the next two days. The

gaps in the data set represent the PFE cleaning cycles which occurred every 4 hours of operation. It should be noted that membrane permeability was recovered after cleaning however; it increased quickly once the operation restarted.
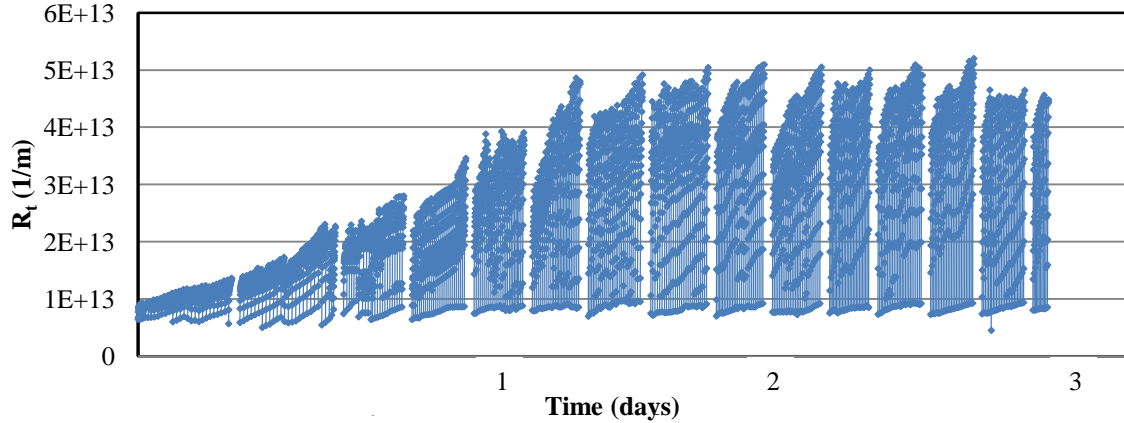
Figure 4-5 Total resistance versus time for a typical membrane trial (800 mg/l ferric chloride and 7.6 LMH permeate flux)

4.5.2 Reproducibility of Membrane Trials

The reproducibility of the UF results was assessed by conducting three replicate trials over the period between April and July 2011. In these tests, the ferric chloride dose was 600 mg/l and the permeate flux was 8.7 LMH. Table 4-5 presents the main characteristics of the bioreactor influent and effluent for the trials.

Table 4-5 Conventional parameter data for replicate membrane testing

Trial	Influent flow (m³/d)	D.O (mg/l)	Influent			Effluent		
			TSS (mg/l)	TCOD (mg/l)	SCOD (mg/l)	TSS (mg/l)	TCOD (mg/l)	SCOD (mg/l)
2-1	10.9	3.5 ± 0.7	1853 ± 1296	3918 ± 789	2779 ± 273	2310 ± 785	2849 ± 414	691 ± 113
2-2	10.9-21.8	3.9 ± 1.8	1300 ± 1255	3928 ± 1070	2092 ± 456	1519 ± 398	2296 ± 694	701 ± 360
2-3	10.9	3.7 ± 1	1197 ± 730	2933 ± 800	1941 ± 333	1280 ± 565	1850 ± 325	312 ± 84

The influent flow and the DO of the MBBR effluent are given in Table 4-5. In addition, the table shows the concentrations of TSS, TCOD, and SCOD in the influent and effluent streams. The influent flow was generally adjusted to 2 GPM (10.9 m^3/d), however, in trial 2-2, the influent flow increased to 4 GPM (21.8 m^3/d) overnight and was returned to approximately 1.8 GPM (10.4 m^3/d) in the early morning. The DO was above 2 mg/l during all trials, therefore the oxygen concentration was not likely to have impacted upon the biomass properties in the MBBR and hence this was not expected to impact the membrane performance.

From Table 4-5 it can be seen that there was substantial variability between replicate runs due to fluctuations in the influent wastewater. The TSS of the raw wastewater varied from a minimum of 600 mg/l to a maximum of 3280 mg/l during this period of time. The TSS values of the influent and effluent were the lowest for trial 2-3 (1197 ± 730 mg/l and 1280 ±565 mg/l), while the trial 2-1 experienced the highest concentration of solids. The TCOD of the wastewater ranged from 2072 to 5147 mg/l. Trial 2-3 had the lowest TCOD concentrations with values of 2933 ± 800 mg/l and 1850 ±325 mg/l for the influent and effluent streams, respectively. The SCOD concentrations were similar for the first two trials. The third trial had the lowest effluent SCOD concentrations (312 ± 84 mg/l) and this was attributed to lower concentrations in the raw wastewater at that period. Although the properties of the bioreactor influent and effluent would not directly impact the membrane performance, they would impact upon the characteristics of the solids that the membrane was exposed to in the membrane tank.

Table 4-6 Steady state resistances observed in replicate tests (600 mg/l and 8.7 LMH)

Trials	Trial # 2-1	Trial # 2-2	Trial # 2-3
Average R_t (1/m)	4.70E+13	4.62E+13	4.79E+13
Standard Deviation (1/m)	1.6E+12	8.9E+11	1.0E+12

Total membrane resistances were calculated for each trial, based on Equation 4-1. Table 4-6 lists the values of R_t that were calculated as the average of (R_2-R_1) after reaching

steady state for the replicates. In order to examine reproducibility of the trials, an ANOVA table for membrane resistance was constructed as shown in Table 4-7. From Table 4-7 it was concluded that the difference between trials was not significant and that the membrane performance results were reproducible even when tests were conducted some time apart. This was important to establish as it increased the confidence of the subsequent comparisons of membrane performance under differing operating conditions.

Table 4-7 ANOVA for the replicate trials

Source of variation	Sum of Squares	df	Mean Square	F	Fcrit
Between Groups	1.0495E+25	2	5.2476E+24	3.3020	3.4928
Within Groups	3.1784E+25	20	1.5892E+24		
Total					

4.5.3 Effect of Coagulant Dose on pH and Soluble COD Removal

This section addresses the effect of coagulant dose on pH and SCOD removal through the membrane. Figure 4-6 presents the pH of samples taken from the bioreactor effluent and the UF tank at different dosages. The pH of the MBBR effluent during all the membrane trials was essentially constant at 7.6 ± 0.3. Hence, variations in the pH of the membrane tank contents were attributed to the coagulant addition. As can be seen in Figure 4-6, the pH of the membrane tank decreased with increasing coagulant dose; however, addition of extremely high coagulant doses (1000 mg/l) resulted in an increase of the pH to 6.6 ± 0.2. This may have been due to the high alkalinity of the wastewater (560 ± 180 mg/l $CaCO_3$) during this run. High alkalinity acts to resist pH decreases and is desirable for coagulation, since it tends to have more positively charged ions to interact with the negatively charged colloids (O'Melia *et al*., 1999).
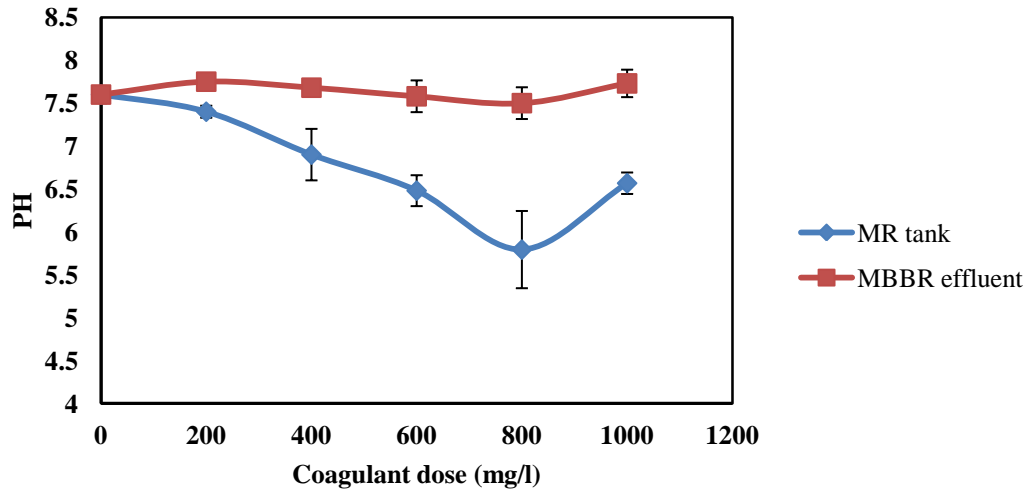
Figure 4-6 pH of samples at different coagulant dosage

pH is an important parameter in the coagulation process since it controls the presence of hydrolysis species. When a coagulant, such as aluminum or ferric salt, is added to water, a series of soluble hydrolysis species are formed. These hydrolysis species can have positive or negative charges depending on the water pH. Species are positively charged at low pH (< 6) and negatively charged at high pH. The positively charged hydrolysis species can absorb onto the surface of colloidal particles and destabilize the stable colloidal particles. This mechanism is called 'charge neutralization'. In addition, precipitates of aluminum and ferric hydroxide are formed at an adequately high coagulant dosage. These precipitates can physically sweep the colloidal particles from suspension. This mechanism is called 'sweep-floc coagulation' (Kim *et al*., 2001). In this study, following $FeCl_3$ coagulant addition, it would appear that sweep-floc coagulation was active due to the relatively high pH (6.6 ± 0.7) observed in all trials.

Colloidal particles are aggregated to form flocs, when coagulant is added; therefore it would be expected that SCOD would decrease upon addition of coagulant. Different coagulant doses may have different affects on floc formation and SCOD removal. Figure 4-7 presents a summary of the SCOD removal data for all the membrane trials at various coagulant doses. Samples were taken before and after the coagulation process occurred. As the ferric chloride dose increased, the organic removal efficiency increased, however

a significant change in the value of SCOD removal was not observed for extremely high doses (1000 mg/l), as SCOD removal only increased from 65% to 68.3%. However, the overall COD removal by the pilot plant (based on MBBR effluent and the final permeate product) was in the range of $97 \pm 1.2\%$, indicating high organic removal.
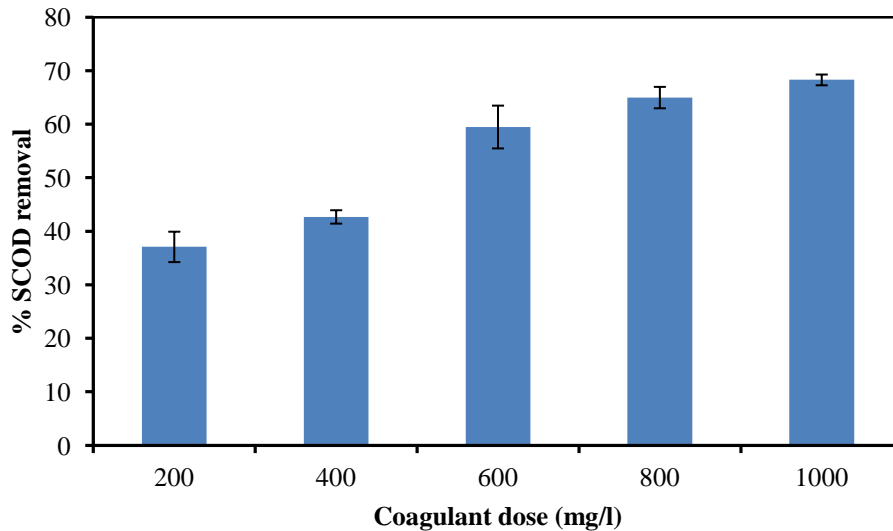
Figure 4-7 SCOD removal for different coagulant dose

4.5.4 Impact of Coagulant Dose on Membrane Fouling

The objective of this portion of the study was to evaluate the impact of ferric chloride pre-coagulation of the MBBR effluent on the subsequent ultra-filtration process. The effect of the coagulant dose on membrane fouling was investigated by varying the concentration of ferric chloride that was added to the coagulation tank. As mentioned previously, there were two phases of this experiment: before upgrades to the wastewater facility took place (Phase I) and after upgrades were completed (Phase II). The following sections present the results of the membrane trials for both phases along with a comparison of the results of the two phases.

4.5.4.1 Phase I

During this phase, four trials were performed at a constant flux of 7.6 LMH to determine the effect of coagulant dose on membrane fouling behaviour. Figure 4-8 shows the total resistance versus time for the different doses that were employed.
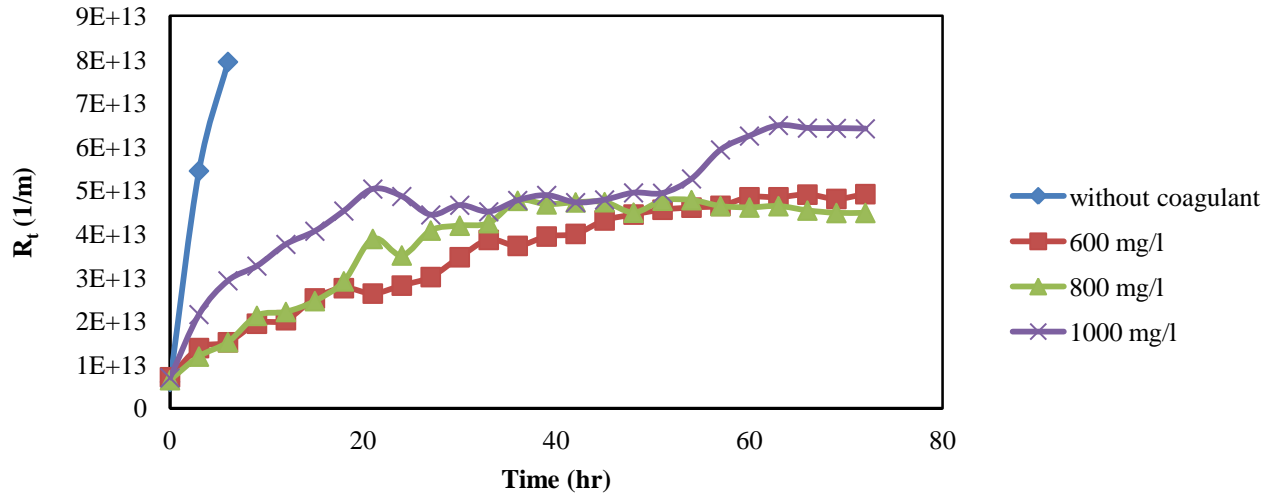
Figure 4-8 Impact of ferric chloride dose on total resistance over duration of Phase I trials (7.6 LMH flux)

As shown in Figure 4-8, the resistance in the non-dosed trial increased sharply during the first hours of operation and reached over 8E+13 1/m after 6 hours of operation. However, in the trials with coagulant addition, the filtration time was extended to over 3 days with a lower resistance (R) value. The trials with doses of 600 and 800 mg/l showed a similar increasing trend during the 3-day period, reaching average resistances of 4.7E+13 and 4.6E+13 1/m, respectively. The trial conducted with a 1000 mg/l dose experienced a higher fouling rate as compared to the test runs with 600 and 800 mg/l. It should be noted that during the 3-day period for the 1000 mg/l trial, a decreasing trend of fouling in the second day and a fairly rapid increase in the membrane resistance during the last day of operation were observed. In order to investigate the reasons for these changes, some characteristics of the samples obtained at different locations during the three continuous days of operation are shown in Table 4-8.

Table 4-8 Characteristics of process streams versus time for 1000 mg/l dose

Trial	TSS (mg/l)			TCOD (mg/l)			SCOD (mg/l)	
Day	MBBR effluent	MR feed	concentrate	MBBR effluent	MR feed	Permeate	MR tank	Colloidal COD
1 st	1185	1980	10180	1779	2000	90	180	90
2 nd	1190	1860	11360	1522	1700	75	97	22
3 rd	4100	4700	14390	2490	3500	70	200	130

As shown in Table 4-8, there was a substantial increase in the solids concentration of the MBBR effluent during the last day of operation that caused an increased solids concentration in the feed stream (around 3.5 times higher as compared to the first two days) as well. The solids concentration in the concentrate stream also increased with time. In addition, the COD concentrations of the MBBR effluent and feed line experienced a considerable increase on the third day. On the second day, the SCOD of the membrane tank was almost half of that experienced on the other days, exhibiting a concentration of 97 mg/l as compared to 180 and 200 mg/l for the first and third days, respectively. The colloidal matter portion of the COD was lowest on the second day (22 mg/l compared to 90 and 130 mg/l). Therefore it was concluded that elevated solids and colloid concentrations were responsible for the observed fouling pattern at the 1000 mg/l dose.

Table 4-9 presents the total resistance values along with their standard deviations at steady state versus coagulant dose. The total resistance values were calculated based on the average of the differences between the resistances at the beginning of trial and after it reached steady state. With the exception of the 1000 mg/l dose, all of the trials reached steady state after the second day of operation. In the 1000 mg/l trial, the steady state condition was established in the last 18 hours of operation. An ANOVA test was conducted to statistically determine whether the means of the trials were different. The ANOVA is summarized in Table 4-10.

Table 4-9 Impact of ferric chloride dose on membrane resistance

Trial	Non dosed	600 mg/l	800 mg/l	1000 mg/l
R_t	7.3E+13	4.0E+13	3.9E+13	5.6E+13
Standard Deviation		1.7E+12	1.1E+12	2.1E+12

Table 4-10 ANOVA for the different ferric chloride doses trials (phase I)

Source of variation	Sum of Squares	df	Mean Square	F	Fcrit
Between Groups	1.20618E+27	2	6E+26	229.8691	3.4668
Within Groups	5.50959E+25	21	2.6E+24		
Total					

The results of the ANOVA indicated that the means were significantly different however, the ANOVA did not identify which means were different. Therefore, a multiple comparisons test was performed to identify the differences between the trials. According the results of a Tukey test, there was no significant difference between trials with doses of 600 and 800 mg/l; however the trial with a dose of 1000 mg/l exhibited a significant difference with respect to other two trials (Tables B-9 in Appendix B). From table 4-9 it can be seen that adding 600 or 800 mg/l of coagulant reduced resistance by more than 45% as compared to the non-dosed sample, while the 1000 mg/l dose only decreased total resistance by 20% as compared to the non-dosed trial. The reduced effectiveness of the 1000 mg/l coagulant dose may have been due to charge reversal under these conditions. This change can cause re-stabilization of the colloid complex (Wu *et al*., 2009). Therefore, they have a potential to become foulants through formation of a cake layer on the membrane surface.

In order to understand the possible causes of fouling the effect of the wastewater characteristics are discussed here. Samples were taken from different locations of the pilot plant each day of the trials for analysis of pH, solids and COD and the average values along with standard deviations are presented in Table 4-11. It can be seen from the data in Table 4-12 that the pH values of the samples for the 800 mg/L trial were the lowest of the three trials. The reduction in pH could enhance NOM removal and also

lower the concentration of NOM in the feed line for membrane filtration, resulting in mitigation of fouling (Dong *et al.* 2007). During the third trial, although the concentration of ferric chloride that was added was extremely high (1000 mg/l), the pH did not drop, instead remaining in the range of 6.5. This may have been due to the high alkalinity of wastewater (560 ± 180 mg/l $CaCO_3$) during this run.

Table 4-11 Results of sample analysis for different dose trials

Trial	Ferric Chloride Dose		
	600 mg/l	**800 mg/l**	**1000 mg/l**
pH Membrane tank	6.5 ± 0.3	5.8 ± 1.2	6.5 ± 0.2
TCOD MBBR effluent (mg/l)	2311 ± 96	2231 ± 305	1930 ± 501
TCOD Membrane feed (mg/l)	2525 ± 158	2398 ± 366	2400 ± 964
SCOD Membrane tank (mg/l)	152 ± 19	120 ± 35	159 ± 54
COD Permeate (mg/l)	74 ± 5	65 ± 12	78 ± 10
Colloidal COD MR (mg/l)	78 ± 15	55 ± 14	80 ± 54
TSS Membrane feed (mg/l)	2430 ± 10	2767 ± 336	2847 ± 1606
TSS Concentrate (mg/l)	7033 ± 660	7180 ± 1870	11643 ± 2616

From Table 4-11 it can be seen that the properties of the streams were changed with coagulant dose. As the coagulant dose increased, the solids concentration in the membrane feed increased. Consequently, an increase in the concentration of solids at the concentrate stream was observed too. There was not a significant difference in the TSS of the concentrate stream for the 600 mg/l and 800 mg/l trials (Refer to ANOVA and Tukey tests presented in Tables B-10 and B-11, Appendix B); however, the concentration of

TSS was higher (11643 mg/l) in the 1000 mg/l trial. The higher solids concentrations in the membrane tank could have been partially responsible for intensive fouling of the membrane in this condition.

Table 4-11 presents values for the colloidal COD for the various process streams for each coagulant dose. As seen in Table 4-11, the concentration of colloidal organic matter was the similar for all trials. An ANOVA test was performed and it confirmed this observation (Table B-12 Appendix B). In contrast, the colloidal COD concentration for the non-dosed trial was 235 mg/l, which was about three times higher than that for other trials. It would appear that pore blockage by colloidal matter was a significant contributor to fouling of the membrane when operated without coagulant. The fouling was mitigated with ferric chloride addition due to removal of colloidal matters. It was concluded that the dominant fouling mechanism when coagulant was added was cake layer formation, since the colloidal concentrations were almost the same for the dosed trials. The large value of TSS concentrations at the 1000 mg/l dose likely increased the cake layer thickness and this lead to the higher fouling rate in contrast to other trials.

4.5.4.2 Phase II

There was an upgrading of the wastewater treatment plant at the facility part way through the study and therefore phase II of the experimental work was performed to investigate the effects of coagulant dose and plant upgrading on the membrane performance. It was previously demonstrated in the preliminary coagulation jar tests (Section 4.4) that with the enhancement of the wastewater treatment processes at the facility, smaller doses of coagulant were required to reduce the turbidity. Hence, considering the improvements made to the pre-treatment system at the factory, a lower range of coagulant dosages (200, 400 and 600 mg/l) was employed in Phase II. Figure 4-9 illustrates the results of the trials for the selected doses at a constant permeate flux of 7.6 LMH.
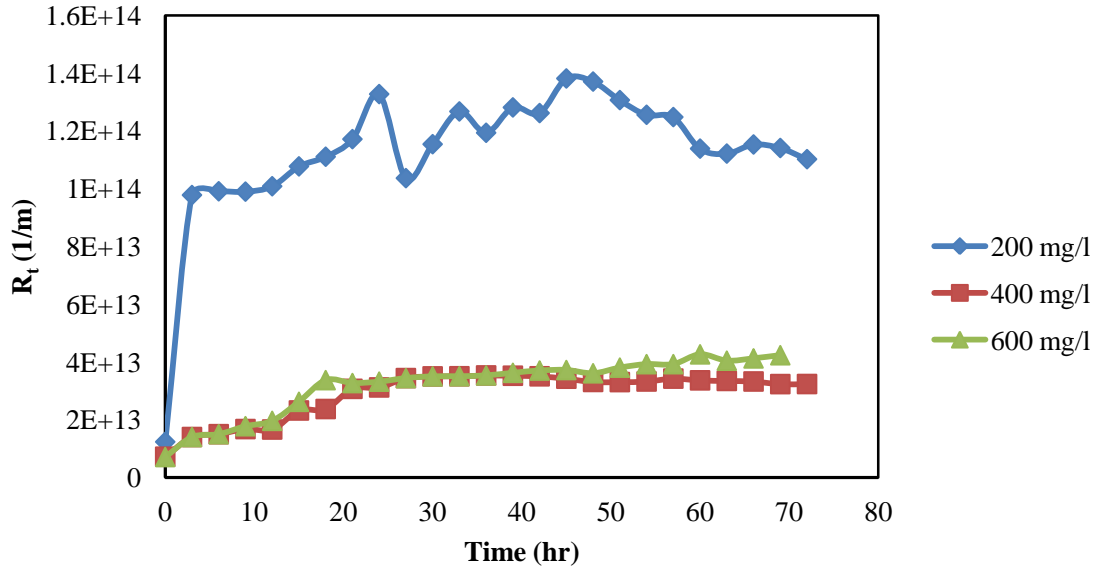
Figure 4-9 Impact of coagulant dose on development of resistance after upgrade

As shown in Figure 4-9, the total resistance of the trials with doses of 400 and 600 mg/l increased during the first day of operation and this was followed by only a slight increase for the rest of the 3-day period. The final resistance values were approximately 3.3E+13 and 4.1E+13 1/m for the 400 and 600 mg/l doses, respectively. There was a very significant increase in the membrane resistance (9.8E+13 1/m) when using a 200 mg/l dose of coagulant, especially during the first hours of operation. However, only a gradual increase in resistance with some fluctuations was observed after about 3 hours and it reached steady state (1.1E+14 1/m) at the very end of operation (approximately the last 15 hours). Table 4-12 summarizes the membrane resistances at steady state for the various coagulant doses. The average resistances and their standard deviations were obtained according to the procedure explained in section 4.5.4.1. An ANOVA test was conducted to statistically compare the resistances (Table 4-13).

71

Table 4-12 Impact of ferric chloride dose on membrane performance after pre-treatment upgrade

Trial	Ferric Chloride Dose		
	200 mg/l	400 mg/l	600 mg/l
R_t	1.0E+14	2.6E+13	3.4E+13
Standard Deviation	2.0E+12	5.9E+12	1.7E+12

Table 4-13 ANOVA for the different ferric chloride doses trials (phase II)

Source of variation	Sum of Squares	df	Mean Square	F	Fcrit
Between Groups	2.0E+28	2	9.915E+27	4781.5	3.5219
Within Groups	3.94E+25	19	2.074E+24		
Total					

The results of the ANOVA test indicated that there was a significant difference between the resistances that were observed at the different coagulant doses and hence Tukey-tests were also performed to compare the mean values (Table B-13 in Appendix B). Based on the Tukey test results, it was concluded that all the trials had different resistance values. Based on the data shown on Table 4-12, the 400 mg/l trial was found to perform the best at reducing membrane fouling, reaching a total membrane resistance of only 2.6 E+13 1/m, while this value was 3.4E+13 1/m for the trial employing 600 mg/l. The total membrane resistance was the highest for the 200 mg/l trial with a value of 1.0E+14 and a standard deviation of 2.0E+12 1/m. It should be noted that the initial membrane resistance (at the beginning of operation) was extremely high (1.2E+13 1/m) for the 200 mg/l trial as compared to 400 and 600 mg/l trials (7.2E+12 1/m, 7.1E+12 1/m). This run was one of the three last runs in this study and even a CIP cleaning did not recover the membrane permeability. The presence of the residual foulants after cleaning may have caused the rapid initial fouling of the membrane during the 200 mg/l trial however it is apparent that a steady state developed for this condition and its resistance was considerably higher than the others. The initial membrane resistances were very similar in the 400 and 600 mg/l trials.

72

Table 4-14 Selected characteristics of process streams versus coagulant dose

Trial	Ferric Chloride Dose		
	200 mg/l	400 mg/l	600 mg/l
pH Membrane tank	7.4 ± 0.1	6.7 ± 0.3	6.6 ± 0.2
TCOD Membrane feed (mg/l)	1793 ± 139	1447 ± 169	2867 ± 375
SCOD Membrane tank (mg/l)	220 ± 23	120 ± 20	152 ± 39
COD Permeate (mg/l)	75 ± 7	65 ± 23	51 ± 11
Colloidal COD MR (mg/l)	145 ± 20	55 ± 18	101 ± 29
TSS MBBR influent (mg/l)	835 ± 35	310 ± 60	893 ± 93
TSS MBBR effluent (mg/l)	1250 ± 200	1263 ± 165	1313 ± 272
TSS Membrane feed (mg/l)	1523 ± 42	1633 ± 246	1917 ± 74
TSS Concentrate (mg/l)	3217 ± 797	3577 ± 455	5823 ± 984

Table 4-14 shows a number of characteristics of the process streams at different locations of the MBBR-MR as a function of coagulant dose. The subsequent discussion is based upon the results of ANOVA and Post-Hoc tests (Tukey tests) that were conducted to compare means (Table B-14 to 17 in Appendix B). The TSS concentrations in the membrane feed and the concentrate stream were not significantly different between the 200 mg/L and 400 mg/L doses. However, the TSS concentrations had the highest values at the 600 mg/l dosage. The higher solids concentration at the 600 mg/l dosage may have caused the formation of a denser cake layer on the membrane surface that would have increased membrane fouling.

The COD concentration had the highest value for the feed streams of the membrane in the third trial with an average TCOD concentration of 3867 mg/l as compared to 1793 and 1447 mg/l for the first and second trials, respectively. Although, the TCOD of the membrane feed for the 600 mg/l trial was higher than that for 200 mg/l trial, the 200 mg/l trial had the highest soluble COD (220 ± 23 mg/l) as compared to the other trials. The

SCOD concentrations of the 400 and 600 mg/l trials were not significantly different as determined by a t-test (Table B-18, Appendix B).

Table 4-14 shows that the estimated colloidal COD concentrations in the membrane tank had the highest values for the 200 mg/l trial, approximately three times of the concentration of the 400 mg/l trials (t-test in Table B-19, Appendix B). It should be noted that the concentration of solids present in the membrane feed and the concentrate line had the lowest value for trial 200 mg/l; however the soluble and colloidal COD of the membrane experienced a higher value than the other trials. It is interesting to note that the greatest fouling corresponded to these higher concentrations.

A possible reason behind this observation is that employing a low coagulant dose as a pre-treatment resulted in low SCOD removal by the coagulant (around 37%). The low coagulant dose probably caused incomplete aggregation of colloidal particles such that internal fouling and pore-blockage of the membrane occurred. Therefore, it was concluded that a higher concentration of colloidal solids remained un-coagulated during the low coagulant dose trials. In these cases, the colloids occupied sites on the membrane surface and inside the pores, causing the more severe fouling impact. There are several studies that observed the higher fouling rate of the membrane with addition of low coagulant dose for water treatment purposes (Judd and Hillis, 2001; Guigui *et al*., 2002). Guigui *et al*. (2002) observed an increase of the resistance even in quasi-stable hydrodynamic operating conditions when the coagulant dose was reduced.

4.5.4.3 Impact of Wastewater Treatment Upgrade on UF Performance

The impacts of upgrading the WWTP on the raw wastewater and MBBR performance were described in Section 4.3. As it was mentioned, enhancement of the WWTP reduced the COD and solids loading on the MBBR by 22% and 31%, respectively. Membrane filtration performance in terms of flux, backwash frequency and chemical cleaning is highly dependent on the raw water quality (Crozes *et al*., 1997). It was therefore expected that upon upgrading pre-treatment, the quality of the raw wastewater, and consequently the effluent of the bioreactor and the feed to the membrane system, would experience some changes. In order to assess the effect of upgrading pre-treatment on membrane

fouling, trials employing a 600 mg/l coagulant dose with two different fluxes were conducted before and after enhancement of the WWTP.

Table 4-15 Total resistance before and after upgrade

Trial	Before upgrade		After upgrade	
	7.6 LMH	**8.7 LMH**	**7.6 LMH**	**8.7 LMH**
R_t	4.01E+13	4.70E+13	3.36E+13	3.97E+13
Standard Deviation	1.69E+12	1.60E+12	1.73E+12	1.85E+12

Table 4-15 illustrates average total resistances that were observed at steady state for the selected trials. Table 4-15 shows that the fouling resistance decreased when the pre-treatment facilities were upgraded, as there was approximately a 16% reduction in membrane fouling for both fluxes. The total resistances decreased from 4.01E+13 to 3.36E+13 (1/m) and 4.70E+13 to 3.97E+13 (1/m) for the flux of 7.6 and 8.7 LMH, respectively. To confirm the significance of the results, an ANOVA tests was performed and the results are presented in Table 4-16.

Table 4-16 ANOVA for 600 mg/l doses trials (phase I and II)

Source of variation	Sum of Squares	df	Mean Square	F	Fcrit
Between Groups	7.64E+26	3	2.55E+26	86.42657	2.911334
Within Groups	9.14E+25	31	2.95E+24		
Total					

On the basis of the ANOVA it was concluded that the R_t values were significantly different between the trials. A Tukey-test was performed to compare the mean values of the R_t data (see Tables B-20 in Appendix B). It was concluded that all the trials except the first (7.6 LMH, before upgrade) and last (8.7 LMH, after upgrade) trials were significantly different. These two trials had the resistance values of 4.01E+13 and 3.97E+13 1/m, respectively. Therefore it was concluded that the membrane could be

operated at a higher permeate flux (at a constant dose) with the upgraded wastewater treatment plant.

Table 4-17 Characteristics of process streams before and after upgrading WWTP

Analysis	Location	Before upgrade WWTP		After upgrade WWTP	
		Trial 7.6 LMH	Trial 8.7 MH	Trial 7.6 LMH	Trial 8.7 MH
PH	MR	6.5 ± 0.3	6.4 ± 0.2	6.6 ± 0.2	6.4 ± 0.1
TSS (mg/l)	Membrane feed	2430 ± 10	2813 ± 832	1917 ± 74	1360 ± 355
	Concentrate	7033 ± 660	7633 ± 1114	5823 ± 984	5200 ± 290
SCOD (mg/l)	Membrane tank	152 ± 19	293 ± 54	152 ± 39	216 ± 162
	Permeate	74 ± 5	85 ± 4	51 ± 11	82 ± 25
	Colloidal COD	78 ± 15	208 ± 51	101 ± 29	134 ± 67
O&G (mg/l)	MBBR influent	83.1 ± 127		27.0 ± 32	

The composition of the process streams with respect to conventional parameters was assessed to obtain insight into the underlying mechanisms responsible for membrane fouling and this data is shown in Table 4-17. As shown in Table 4-17, the pH of the wastewater in the membrane tank remained nearly constant for all runs and hence it did not contribute to the differing fouling behaviour.

The suspended solids concentrations of the membrane feed for the high flux trial decreased by 50%, from 2813 to 1360 mg/l when the WWTP was upgraded. As a result, the solids concentration in the concentrate stream decreased by approximately 30% (from 7633 mg/l to 5200 mg/l). In addition, there was approximately a 20% reduction of solids concentration in the membrane feed with upgrading for the flux of 7.6 LMH. The reduced concentrations were statistically significant (Tables B-21 through B-23 in Appendix B). The reduced solids concentrations in the membrane feed stream would be expected to result in less adsorption on the membrane surface and reduced formation of cake layers. Therefore, it would lower the possibility of fouling.

The soluble and colloidal COD of the membrane tank contents were assessed to evaluate whether they had a significant effect on observed fouling. On the basis of statistical tests, it was found that there was not a significant change in the concentration of soluble and colloidal particles for all these trials (Tables B-24 and B-25 in Appendix B) and the overall average concentration was 118 ± 51 mg/l. Therefore, it can was concluded that the colloidal organic matter did not play a major role in the observed fouling reduction upon upgrade of WWTP. It was therefore concluded that pre-treatment had a significant effect on MBBR-MR performance by reducing the solids loading and probably the O&G concentration in the feed stream upon installation of a DAF system upstream of the WWTP. Suspended solids concentration decreased by 30-50% in the membrane tank. This reduction likely reduced build-up of foulants on the membrane surface.

Wastewaters that are generated in food processing may contain significant quantities of oil and grease. Therefore, it was interesting to investigate whether the oil and grease (O&G) concentration changed after upgrading of the WWTP and also if it affected fouling of the membrane. O&G are insoluble in water (Tchobanoglous *et al*., 2003) and could adsorb on the membrane surface or within the pores to cause an intensive fouling and membrane permeability deterioration. As shown in Table 4-17, the O&G concentration decreased by 67%, from 83.1 ± 127 mg/l to 27.0 ± 32 mg/l, after the plant upgrading was completed. Therefore it was concluded that that the reduction of O&G concentrations may have also contributed to the fouling reduction after the system was upgraded. There are several studies that have observed a significant adverse effect of O&G concentrations on fouling (Kim *et al*., 2006; Wu *et al*., 2010; Yang *et al*., 2012).

4.5.5 Impact of Permeate Flux on Membrane Fouling

In order to investigate the effect of permeate flux on membrane fouling, trials were performed at the same coagulant dose with different fluxes (7.6, 8.7 and 9.8 LMH). The flux was changed by varying the permeate flow rate using the manual valve on the permeate stream line. A two-way factorial approach was chosen to consider the effects of flux and dose simultaneously (Table 4-18).

Table 4-18 Factorial design for flux and dose

Dose / Flux	7.6 LMH	8.7 LMH	9.8 LMH
200 mg/l	x	x	-
400 mg/l	x	-	x
600 mg/l	x	x	x
800 mg/l	x	-	x

The trends with respect to resistance versus time in the trials were examined prior to conducting statistical tests. Figure 4-10 shows a summary of the three trials conducted using a coagulant dose of 600 mg/l for three different permeate fluxes: 7.6, 8.7 and 9.8 LMH.
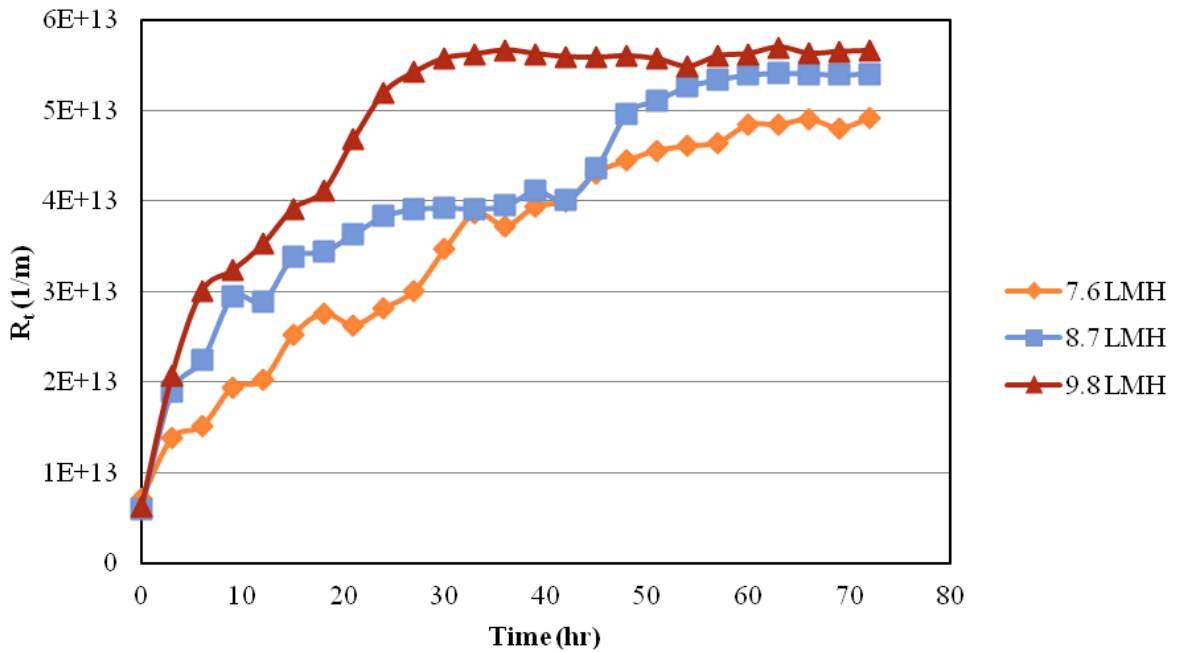
Figure 4-10 3-day trials for 600 mg/l coagulant dose

From Figure 4-10 it can be observed that when the flux was higher membrane fouling occurred more quickly. Operation at higher fluxes had higher fouling rates at the beginning of operation, and then they levelled off to achieve a steady state condition. There were some fluctuations in the data that may be attributed to changes in the characteristics of the wastewater. As shown in Figure 4-10, in the trial with a flux of 8.7 LMH there was a considerable increase in fouling (approximately 34%) in the last day of operation. Table 4-19 presents some selected characteristics of wastewater for the three days of testing.

Table 4-19 Process conditions versus time for operation with 600 mg/l dose and 8.7 LMH flux

Flux: 8.7 LMH	1st day	2nd day	3rd day
TSS Concentrate (mg/l)	6980	7000	9000
SCOD MR Tank (mg/l)	241	289	350
Colloidal COD MR Tank (mg/l)	158	207	260

The values of the TSS of the concentrate stream, SCOD and colloidal COD of the membrane tank are shown in the Table 4-19. The rapid increase in fouling on the third day of operation might have been due to the high solids concentration (9000 mg/l) in the membrane tank and/or the high concentrations of colloidal and SCOD of the membrane tank (350 mg/l) as they all increased substantially. Suspended solids with smaller particle size distributions and dissolved solids such as soluble and colloidal solids (which may include extracellular polymeric substances and soluble microbial products) are prone to blocking membrane pores and also forming a gel structure on the membrane surface (Cho and Fane, 2002, Guglielmi *et al*., 2007, Wang *et al*., 2009, and Rosenberger *et al*., 2006).
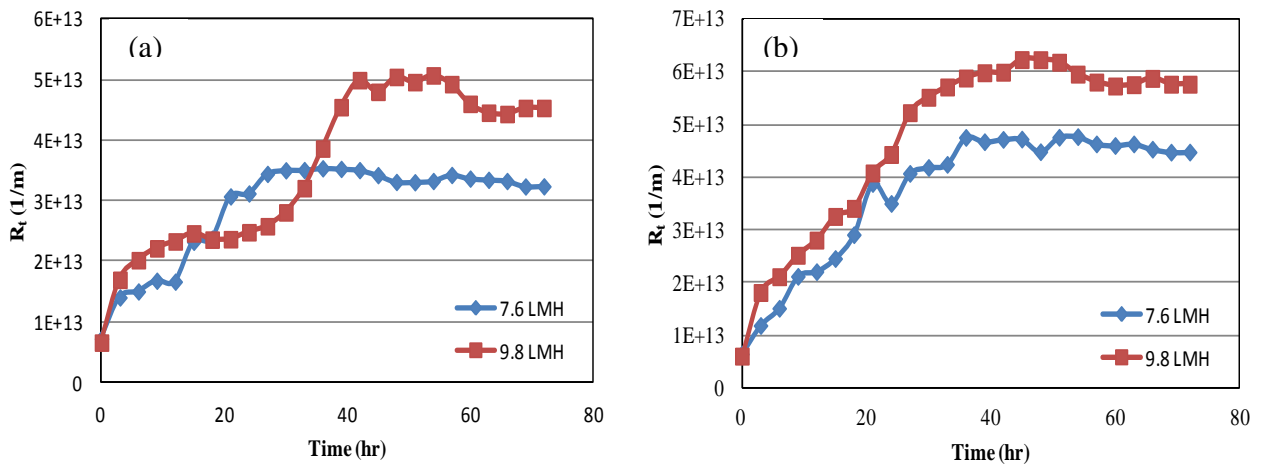
Figure 4-11 Membrane resistance versus time and flux for trials for 400 mg/l (a) and 800 mg/l dose (b)

Figure 4-11 presents the development of resistance for fluxes of 7.6 and 9.8 LMH when employing 400 mg/l and 800 mg/l of coagulant dose. The trials using 800 mg/l had a sharp increasing trend at the beginning and reached a plateau with some small fluctuations during the last day of operation. The same pattern was observed for the 400 mg/l dose and a flux of 7.6 LMH. As demonstrated in Figure 4-13 (a), there was a considerable rise in membrane resistance for the membrane trial with a dosage of of 400 mg/l and a flux of 9.8 LMH during the second day of operation, increasing from 2.5E+13 to approximately 5.0E+13 1/m. It should be noted that the concentrate line was clogged for a period of time during the second day of operation and the TSS concentration in the concentrate stream and SCOD of the membrane tank reached 6020 mg/l and 290 mg/l as compared to 2890 mg/l and 100 mg/l on the first day, respectively. The operation resumed after draining a portion of the wastewater from the tank. Considering the presence of high concentrations of organic matter and suspended solids in the membrane feed and concentrate streams it was concluded that the rapid fouling was mainly caused by these elevated concentrations and their interaction with the membrane.

Table 4-20 Total resistance of two factors (flux and dose)

Dosage	Flux	7.6 LMH	8.7 LMH	9.8 LMH
200 mg/l	Average (1/m)	1.00E+14	1.51E+14	-
	Standard Deviation (1/m)	1.98E+12	6.40E+12	-
400 mg/l	Average (1/m)	2.60E+13	-	4.07E+13
	Standard Deviation (1/m)	5.93E+11	-	2.66E+12
600 mg/l	Average (1/m)	4.01E+13	4.70E+13	4.99E+13
	Standard Deviation (1/m)	1.69E+12	1.60E+12	6.11E+11
800 mg/l	Average (1/m)	3.95E+13	-	5.30E+13
	Standard Deviation (1/m)	1.14E+12	-	1.90E+12

Table 4-21ANOVA table for two factors

Source of variation	Sum of Squares	df	Mean Square	F	Fcrit
Dose	5.621E+28	3	1.874E+28	2612.350	2.53
Flux	8.131E+27	2	4.065E+27	566.797	3.15
Dose * Flux	3.655E+27	3	1.218E+27	169.856	2.53
Error	4.877E+26	68	7.173E+24		
Total	3.742E+29	77			

The steady state resistance of the membrane was assessed using an ANOVA test that considered three levels of flux (7.6, 8.7, and 9.8 LMH) and four different doses (200, 400, 600, and 800 mg/l) (Tables 4-20 and 4-21). On the basis of the ANOVA it was concluded that both factors and the interaction between them significantly affected the

steady state resistance. At all dosages, the resistances were higher at the higher flux. Since the interaction between dosage and flux was significant, it was concluded that effect of dose on resistance depended on the value of flux.

Table 4-22 Characteristics of sample for different dose and flux

Dose (mg/l)	Flux (LMH)	TCOD MR feed (mg/l)	SCOD MR (mg/l)	Colloidal COD MR (mg/l)	TSS MR feed (mg/l)	TSS Concentrate (mg/l)
200	7.6	1793 ± 139	220 ± 23	145 ± 20	1523 ± 42	3217 ± 797
	8.7	1827 ± 91	173 ± 10	126 ± 10	2113 ± 136	3243 ± 1096
400	7.6	1447 ± 169	120 ± 20	55 ± 18	1633 ± 246	3577 ± 455
	9.8	1900 ± 174	90 ± 10	29 ± 9	1710 ± 882	4893 ± 824
600	7.6	2525 ± 158	152 ± 19	78 ± 15	2430 ± 10	7033 ± 660
	8.7	3027 ± 704	293 ± 54	208 ± 51	2813 ± 832	7633 ± 1114
	9.8	4045 ± 650	348 ± 92	265 ± 77	3803 ± 774	7640 ± 505
800	7.6	2398 ± 366	120 ± 35	55 ± 14	2767 ± 336	7180 ± 1870
	9.8	2431 ± 304	235 ± 44	147 ± 22	5100 ± 680	16000 ± 175

Table 4-22 summaries the properties of the membrane feed and the concentrate streams in these trials. Based on statistical tests, it was found that there were no significant differences between the COD and TSS concentrations for both fluxes of the 200 mg/l trial. Therefore, it was concluded that the higher fouling for the higher flux was not related to the feed characteristics, since the colloidal and solids concentrations were the same for both fluxes. The resistance was likely due to increased solids adsorption and cake formation on the membrane surface, since an increase in the flux would increase the rate of movement of solids towards the membrane.

As Table 4-22 shows, for the 400 mg/l trials, the TCOD concentrations of the feed to the membrane were higher for the flux of 9.8 as compared to those for the 7.6 LMH flux.

Despite this observation, the estimated colloidal COD concentration of the wastewater in the membrane tank was similar for both fluxes. There was not a significant difference between the TSS values of the feed and the concentrate line for both fluxes. Statistical tests shown in Tables B-26 through B-29 (Appendix B) confirmed these observations. As colloidal COD and TSS of the feed were almost same for both trials, it can be concluded that feed characteristics did not contribute to fouling and higher fouling occurred at the higher flux only due to flux changes.

In the 600 mg/l trial, the SCOD and colloidal COD concentrations in the membrane tank had higher values for the 9.8 LMH flux as compared to the 7.6 and 8.7 LMH. The same trend was observed for TCOD of the membrane feed. However, the solids concentration in the membrane feed and concentrate were similar for all fluxes (Table B-30 to B-36, Appendix B). The increase in resistance that was observed with the higher flux was likely due to both the increased flux and the presence of more colloidal particles that would contribute to the formation of a denser cake layer.

As shown in Table 4-22, the solids concentrations of the feed stream for the 800 mg/l trial and the 9.8 LMH flux was two times higher than that of the 7.6 LMH flux which could have resulted in the high TSS concentration in the concentrate stream. In addition, SCOD and estimated colloidal COD were two and three times higher for the higher flux, respectively (statistical tests were performed and presented in Table B-37 and B-38, Appendix B). It was concluded that both feed characteristics (colloidal particles and suspended solids concentration) and flux may have caused the increased resistance (26%).

4.5.6 Effect of Process Conditions on Membrane Fouling

Membrane fouling can occur in three general forms: (1) build-up of the constituents in the feedwater on the membrane surface, (2) chemical precipitation (scaling) due to the chemistry of the feedwater or (3) damage to the membrane due to presence of chemical substances that can react with the membrane (Tchobanoglous *et al*., 2003). There are three accepted mechanisms for the first form of membrane fouling, namely pore narrowing, pore plugging and gel/cake formation. Cake formation occurs when the

majority of the solid matter in the feed is larger than the pore size of the membrane. Concentration polarization can be described as the build-up of solid matter close to or on the membrane surface that causes an increase in resistance to solvent transport across the membrane. The formation of a gel or cake layer, is an extreme case of concentration polarization where a large amount of matter has accumulated on the membrane surface, forming a gel or cake layer (Tchobanoglous *et al*., 2003).

It was hypothesized that there would be a relationship between cake formation and the TSS concentrations in the membrane tank. Figure 4-18 illustrates the observed total resistance versus the concentration of suspended solids in the membrane tank. It should be noted that samples were taken at both the top and bottom (concentrate) zones of the membrane, and that average values were used to plot the TSS concentrations. Each line presents the relationship between TSS and resistance at a specific flux. As shown in Figure 4-12, there were significant relationships between solids concentration and resistance (except for at the low coagulant dose of 200 mg/l where two points deviated away from the lines). In general, greater fouling was observed for conditions that had higher TSS concentrations in the membrane tank. All three regressions were significant based on ANOVA tests (Table 4-24). The regression information including R^2 values and slopes are shown in Table 4-23. As shown in Table 4-23 ,all the lines had relatively high R^2 (above 0.95) values which showed very good fits.

Table 4-23 Regression information

Flux	**7.6 LMH**	**8.7 LMH**	**9.8 LMH**
R Square	0.9667	0.9897	0.9580
Intercept	4.20E+12	3.03E+13	3.79E+13
Slope	8.81E+9	2.70E+9	1.76E+9
Standard Error	2.35E+12	5.01E+11	1.85E+12

Table 4-24 ANOVA table for different lines

7.6 LMH	Sum of Squares	df	Mean Square	F	Significance F
Regression	4.79E+26	1	4.79E+26	86.69	0.0026
Residual	1.66E+25	3	5.53E+24		
Total	4.96E+26	4			

8.7 LMH	Sum of Squares	df	Mean Square	F	Significance F
Regression	4.81E+25	1	4.81E+25	192.05	0.0052
Residual	5.01E+23	2	2.51E+23		
Total	4.86E+25	3			

9.8 LMH	Sum of Squares	df	Mean Square	F	Significance F
Regression	7.78E+25	1	7.78E+25	22.82	0.1314
Residual	3.41E+24	1	3.41E+24		
Total	8.12E+25	2			

As shown in Figure 4-12, the TSS concentration appeared to affect fouling behaviour with an increase in resistance as TSS concentration increased. Qualitatively, this phenomenon could be explained by the deposition rate of particles onto the membrane surface. A higher TSS concentration will result in a higher particle density on the membrane surface, accounting for the lower permeability. However, for the operations under higher permeate fluxes (more than 7.6 LMH), this effect was observed to be reduced as the slopes of the line 69% and 79% less for fluxes of 8.7 and 9.8 LMH as compared to the 7.6 LMH flux. Hence, there was a greater dependence of fouling on TSS concentration at low fluxes than at high fluxes. The observed responses were likely due to the factors that affect the formation of a cake layer which was responsible for membrane fouling. From Figure 4-12 it is apparent that a maximum resistance was observed for all fluxes and this value was the same for all fluxes. At a high flux this

maximum value was achieved at the lowest TSS concentrations while for lower fluxes the maximum resistance was only attained at higher TSS concentrations.
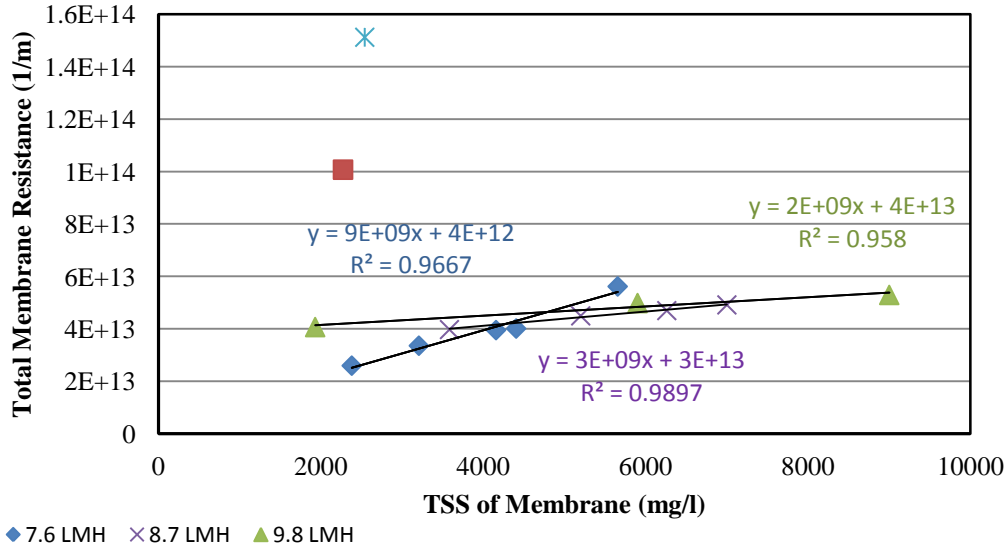
Figure 4-12 Total Membrane resistance vs. TSS concentration in membrane tank

The trials with coagulant doses of 200 mg/l did not exhibit the same dependence upon TSS concentration as those with higher coagulant doses. Although the solids concentration in the membrane tank was approximately 2000 mg/l (which was generally low when compared to the other trials), a very large membrane resistance was observed (1.0E+14 1/m). It was hypothesized that fouling in the 200 mg/l dose trials was due to pore plugging rather than cake formation. Uncoagulated colloidal particles which were smaller than the pore size of the membrane may have plugged the pores or attached themselves to the interior surface of the pores, resulting in a narrowing of the pores. Hence, the relationship between colloidal material and fouling was investigated.

As mentioned in Section 4-7 the colloidal COD was estimated to be the difference between the soluble COD of the membrane (as determined with a glass fibre filter with a pore size of 1.2μm and the permeate COD where the pore size was 0.03 μm). Figure 4-13 presents the relationship between colloidal COD and resistance of the membrane for the

7.6 , 8.7 and 9.8 LMH fluxes. The figure shows regressions between the concentration of colloidal particles and membrane resistance.

A statistical analysis of the regression and the associated ANOVA tables are presented for all regressions in Tables 4-25 and 4-26. It is shown in Table 4-26 that regression between colloidal COD of the membrane tank and resistance was only significant for 7.6 LMH. The R^2 values for the fluxes of 7.6, 8.7 and 9.8 LMH were approximately 0.94, 0.37 and 0.54, respectively. The magnitudes of R^2 again demonstrated that the regressions between colloidal COD and resistance were not significant for the fluxes of 8.7 and 9.8 LMH. The results indicate that there was a greater dependence of resistance on colloidal COD at lower fluxes. It appears that high flux values caused solids to migrate to the membrane surface at a higher rate and therefore the formation of a cake is enhanced thereby reducing the blocking of pores. As a consequence, higher concentrations of colloidal COD did not affect the membrane and would be trapped by the cake layer.
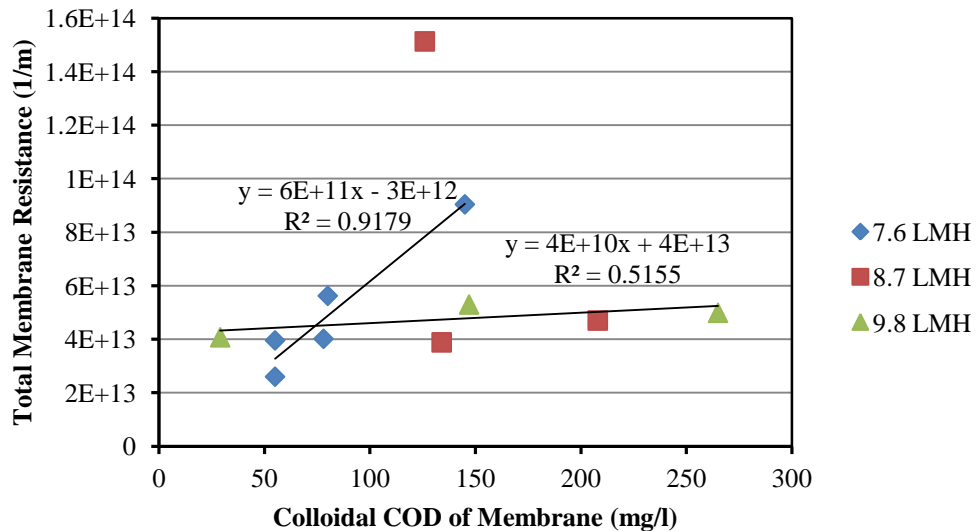
Figure 4-13 Total Membrane resistance versus concentration of colloidal COD

Table 4-25 Regression statistics

Flux	**7.6 LMH**	**8.7 LMH**	**9.8 LMH**
R Square	0.938649	0.26979	0.515533
Intercept	-1.0E+13	1.89E+14	4.21E+13
Slope	7.62E+11	-7.1E+11	3.88E+10
Standard Error	8.30E+12	7.47E+13	6.27E+12

Table 4-26 ANOVA for colloidal COD

7.6 LMH	Sum of Squares	df	Mean Square	F	Significance F
Regression	3.16E+27	1	3.16E+27	45.89888	0.006572
Residual	2.07E+26	3	6.88E+25		
Total	3.37E+27	4			

8.7 LMH	Sum of Squares	df	Mean Square	F	Significance F
Regression	2.06E+27	1	2.06E+27	0.369468	0.652301
Residual	5.59E+27	1	5.59E+27		
Total	7.65E+27	2			

9.8 LMH	Sum of Squares	df	Mean Square	F	Significance F
Regression	4.19E+25	1	4.19E+25	1.064124	0.49011
Residual	3.93E+25	1	3.93E+25		
Total	8.12E+25	2			

In summary, was concluded that for operation under lower fluxes, both suspended solids and colloidal matter concentrations affected the membrane fouling through pore blockage or/and cake layer formation. However, as flux increased, the dominant fouling mechanism was formation of a cake layer by deposition of solids on the membrane surface. In terms of fouling mechanisms, soluble and colloidal materials are assumed to

be responsible for the pore blockage of the membrane, while suspended solids account mainly for the cake layer resistance (Itonaga *et al.*, 2004)

4.5.7 Permeate Quality

In order to investigate the effects of pre-coagulation treatment on permeate quality, the COD of the permeates that were generated at different coagulant doses and different fluxes was examined. Figure 4-14 presents the mean and standard deviations of the observed COD values. From Figure 4-14 it can be seen that the treatment efficiency was consistently high with a COD value of 75 ± 25 mg/l, regardless of coagulant dose and permeate flux. To support the above finding, statistical tests were performed to investigate the effect of coagulant dose on the permeate quality. Table 4-27 presents the ANOVA table which lists the statistical parameters and on the basis of these results it was concluded that the effect of dose on COD was insignificant. The value of COD measured in the permeate represents the inert and non-biodegraded COD present in the inlet wastewater. Leiknes *et al*. (2006) reported lower permeate COD concentrations when the bioreactor was operated under a low rate condition as compared to a high rate condition. This was probably a result of more slowly biodegradable COD being removed during low rate operation which has a higher HRT. Therefore, a somewhat lower COD concentration in the permeate might have been achieved if the HRT of the MBBR were increased.

Table 4-27 ANOVA for COD of permeate

Source of variation	Sum of Squares	df	Mean Square	F	F crit
Between Doses	2979.105	5	595.8209	0.919545	2.558127
Within Doses	18142.65	28	647.9517		
Total	21121.75	33			
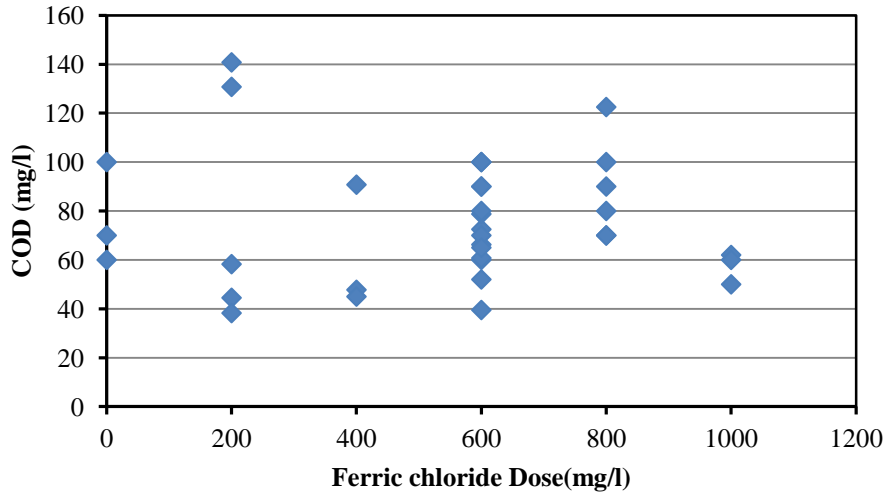
Figure 4-14 COD of permeate for different coagulant doses

The wastewater treatment process was found to provide overall average removal efficiencies of 99 ± 1.0% for suspended solids (~0) and turbidity (20 ± 14 NTU), and 97 ± 1.2% for COD. The method of operation of the membrane reactor did not affect these results. The biodegradable components were removed in the MBBR while the particulate substances were removed in the membrane reactor. The average TCOD of the MBBR influent was in the range of 3023 ± 740 mg/l during the UF trials. Also, the average value of SCOD and TCOD of the wastewater at the concentrate stream were 378 ± 372 mg/l and 4206 ± 1116 mg/l, respectively. Therefore, it can be concluded that approximately 86% of organic compound was biodegradable and removed by the MBBR, while 14% was directed to the waste stream in this process.

Occasionally, the permeate stream was observed to possess a slightly yellow colour which was hypothesized to be due to the presence of iron residuals. To determine if there were Fe^{+3} ions present in the permeate solution, a simple test was performed by adding sodium sulphide to the permeate solution. If any iron residuals were present, they would react with the sodium sulphide (Na_2S) to form ferric sulphide (Fe_2S_3). The ferric sulphide would precipitate as a layer at the bottom of the beaker and change the colour of the water from yellow to white. Figure 4-15 shows the permeate samples which were tested. Beaker (a) shows the yellowish permeate sample and beaker (b) presents the permeate

sample after addition of sodium sulphide. As it can be seen from the Figure 4-15, a precipitate layer formed at the bottom of the beaker, and permeate colour changed to white. While this is only an indirect measurement of the presence of iron residuals in solution, it is hypothesized that their presence may have an adverse effect on the UF membrane by deposition and degradation of the membrane surface. Gabelich *et al*. (2002) investigated the effects of aluminum sulphate and ferric chloride coagulant residuals on polyamide membrane performance. They observed that the presence of residual iron in the pre-treatment effluent caused a chlorination reaction on the membrane surface, leading to membrane degradation. Hence, it would be desirable to not overdose with coagulant in this type of application to avoid membrane deterioration. It was observed earlier that overdosing with ferric (i.e. 1000 mg/l) increased fouling.
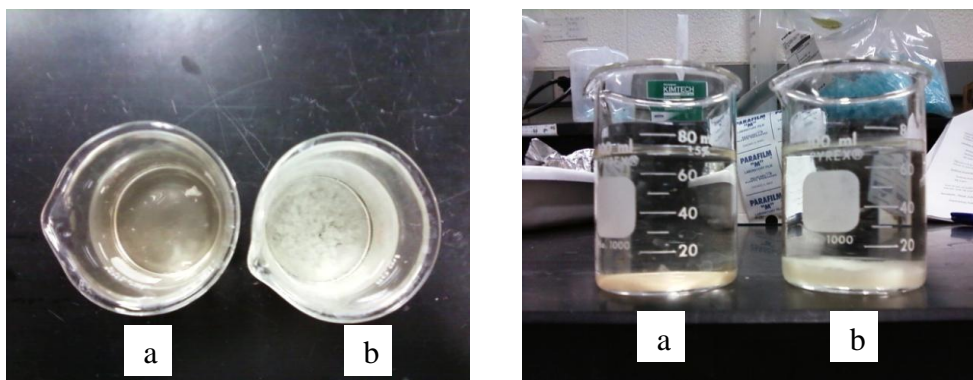
Figure 4-15 Sample of permeate (a) and permeate with sodium sulphide (b)

4.5.8 Effect of Using Defoamer in the MBBR on Membrane Fouling

As discussed in Chapter 3, to prevent over-foaming in the MBBR, a silicon- based defoamer was initially used to reduce foaming. Since rapid fouling was observed, the use of the defoamer was discontinued and a sprinkler system was employed to spray wastewater on top of the bioreactor. Silicon-based defoamers usually contain oil and grease (O&G) substances. O&G are organic substances that are insoluble in water and are often found in water as an emulsion. Certain surface-active chemicals (i.e. surfactants)

91

react with O&G to form colloid-size droplets that are typically very stable in water. O&G foulants coat membrane surfaces and reduce the permeability of membranes significantly (Yang *et al.*, 2012). To investigate the effect of the silicon based defoamer on the UF performance, trials that employed 800 mg/l of coagulant dose and a 9.8 LMH permeate flux were conducted with and without defoamer addition.

Figure 4-16 compares the total resistance observed in these two trials. It can be seen that the total membrane resistance increased significantly during the 27 hours of operation for the trial with defoamer. The rate of fouling was approximately four times higher for the defoamer trial than for the trial with no defoamer (2.2E+14 compared to 5.8E+13 1/m). This finding supports the finding of Kim *et al.* (2006) who noted that the inadvertent use of silicon-based defoamer significantly decreased the flux.
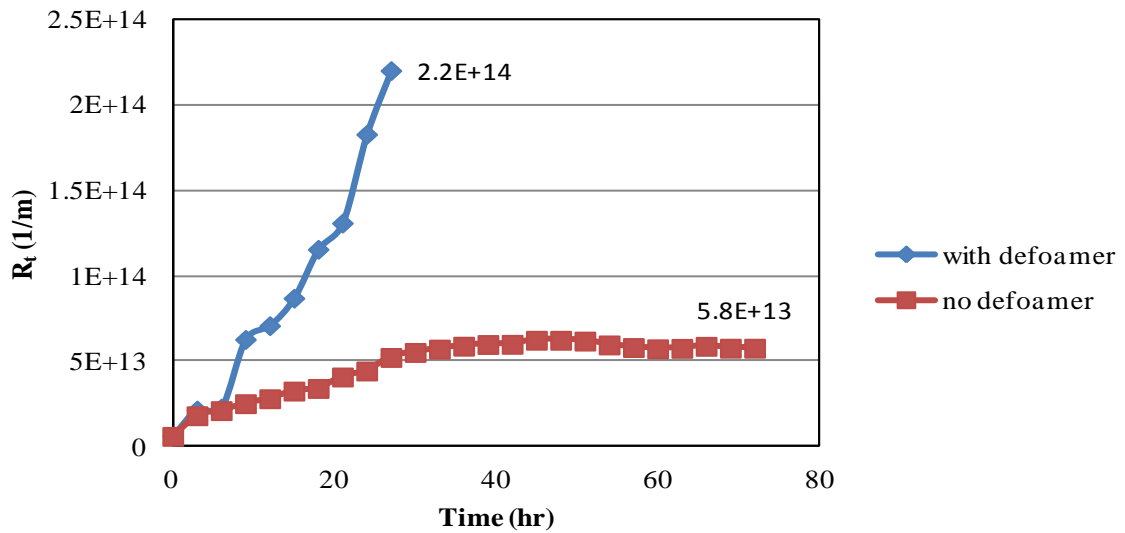
Figure 4-16 Effect of defoamer on membrane fouling

CHAPTER 5

CONCLUSIONS AND RECOMMENDATIONS

5.1 Conclusion

There are limited studies on MBBR-MR configurations and only few publications have been performed on enhancement of MBBR-MR performance by pre-coagulation. In this study the feasibility and potential of the MBBR-MR process for industrial wastewater treatment was investigated with respect to membrane fouling and COD removal efficiency. The effect of pre-coagulation of the MBBR effluent with different doses of coagulant (ferric chloride) on fouling of membrane and COD removal efficiency was investigated. In addition, the effect of permeate flux on fouling of the membrane was assessed. Finally pilot operation with wastewater after primary settling as pre-treatment was compared to operation with the wastewater after enhanced primary settling and dissolved air flotation on the basis of membrane fouling as well as MBBR performance. The findings of this research can be summarized as follows:

1- Over the operating period the MBBR effluent had considerable variability that corresponded to influent feed fluctuations. Although these fluctuations affected fouling of the membrane, a consistent high quality permeate that could be suitable for water reuse purposes was obtained at a relatively high loading rate.

2- Silicon base defoamer had a significant effect on membrane fouling and caused severe fouling.

3- Fouling of the membrane by the wastewater was found to be substantially reduced by coagulation as pre-treatment.

4- The extent of the pre-coagulation effect on membrane fouling was found to strongly dependent on the dosage of the coagulant and the MBBR effluent

93

characteristics. A coagulant dose of 400 mg/l with a permeate flux of 7.6 LMH performed the best at reducing membrane fouling.

5- Colloidal fouling was found to be a significant fouling mechanism at low coagulant dose (e.g. 200 mg/l), while cake formation appeared to be mainly responsible for fouling at higher coagulant doses.

6- Permeate flux was found to have a significant effect on fouling of the membrane especially during the first day of operation, however a change in the flux was not significant near the end of three day period.

7- The presence of colloidal matters at low fluxes and TSS at higher fluxes were responsible for fouling of the membrane by blocking the pores and formation of the cake layer on the membrane surface, respectively.

8- Pre-coagulation did not affect permeate quality. The permeate was consistently free of suspended solids with a COD of 75 ± 25 mg/l.

9- Upgrading WWTP (adding DAF) improved wastewater characteristics in terms of lowering COD (22%) and TSS (31%) and consequently reduced the fouling of the membrane.

10- Soluble COD removal by coagulant increased by increasing coagulant dosage, however overall COD removal by the pilot was $97\% \pm 1.2\%$.

5.2 Recommendations

The combination of MBBR and ultra-filtration system for treatment of food processing wastewater showed promising results. Recommendations for further studies of the MBBR-MR system include:

1- Operation of the MBBR at lower HRT than 4 hrs (Which would also require improved air supply) to investigate removal efficiency of MBBR and its effect on membrane fouling.

2- Investigation of the effect of backwash frequency and its duration on membrane fouling and final effluent quality.

3- Analysis of particle size distribution and characteristics (such as Zeta potential/ hydrophobicity) of MLSS constituents to provide insight into membrane fouling.

4- Evaluation of membrane fouling using more recent membranes (i.e. Turbo clean) that do not need process tanks (reduced chance of accumulation of flocs in the tank).

5- Installation of a flowmeter that does not get clogged by particles for MBBR influent

References

Ahl R.M., Leiknes T., Odegaard H. (2006) Tracking particle size distributions in a Moving Bed Biofilm Membaren Reactor for treatment of municipal wastewater, *Water Science and Technology*, 53(7): 33-42.

APHA. (1996) Clesceri, L.S., Eaton A.D., Greenberg A.E., Franson M.A.H., American Public Health Association., American Water Works Association., and Water Environment Federation, Standard methods for the examination of water and wastewater: 19th edition supplement. Washington, DC.

AWWA. (1999) Water quality and treatment: A handbook of community water supplies, fifth Edition, Raymond Letterman (Technical editor), McGraw-Hill Inc., Washington, D.C.

AWWA. (2005) Microfiltration and ultrafiltration membranes for drinking water, 1st edition, American Water Works Association, Denver, Colorado.

Bae T.H., Tak T.M. (2005) Interpretation of fouling charactersistics of ultrafiltration membranes during the filtration of membrane bioreactor mixed liquor, *Membrane Science*, 264: 151-160.

Baker R.W. (2004) Membrane technology and applications, Second edition,John Wiley & Sons, Chichester, England.

Belfort G., Davis R.H., Zydney A.L. (1994) The behaviour of suspensions and macromolecular solution in cross flow microfiltration, *Membrane Science*, 96: 1-58.

Berthold W., Kempken R. (1994) Interaction of cell-culture with downstream purification- A case-study, *Cytotechnology*, 15(1-3): 229-242.

Bouhabila E.H., Ben-Aim R., Buisson H. (2001) Fouling characterisation in membrane bioreactors, *Separation and Purification Technology*, 22(23): 123–132.

Bowen W.R., Gan Q. (1991) Properties of microfiltration membranes: flux loss during constant pressure permeation of bovine serum albumin, *Biotechnology and Bioengineering*, 38: 688- 696.

Bowen W.R., Hughes D.T. (1990) Properties of microfiltration membranes: Adsorption of bovine serum albumin at aluminium oxide membranes, *Membrane Science*, 51: 189-200.

Bratby J. (2006) Coagulation and Flocculation in Water and Wastewater Treatment, 2nd edition, IWA publishing, Alliance House, London, UK.

Brookes A., Jefferson B., Guglielmi G., Judd S.J. (2006) Sustainable flux fouling in a membrane bioreactor: impact of flux and MLSS, *Separation Science and Technology*, 41: 1279-1291.

Bruggen B.V.D., Vandecasteele C., Gestel T.V., Leysen R. (2003) A review of pressure-driven membrane processes in wastewater treatment and drinking water production, *Environmental progress*, 22 (1): 46-56.

Chang I., Clech P. L., Jefferson B., Judd S. (2002) Membrane fouling in membrane bioreactors for wastewater treatment, *Environmental Engineering* , 128(11): 1018-1029.

Chen W., Liu J. (2012) The possibility and applicability of coagulation –MBR hybrid system in reclamation of dairy wastewater, *Desalination*, 285: 226-131.

Cherkasov A.N., Tsareva S.V., Polotsky A.E. (1995) Selective properties of ultrafiltration membranes from the sandpoint of concentration polarization and adsorption phenomena, *Membrane Science*, 104: 157-165.

Cho B.D., Fane A.G. (2002) Fouling transients in nominally sub- critical flux operation of a membrane bioreactor, *Membrane Science*, 209: 391-403.

Choi H., Zhang K., Dionysiou D.D., Oerther D.B., Sorial G.A. (2005) Effect of permeate flux and tangential flow on membrane fouling for wastewater treatment, *Separation and Purification Technology*, 45: 68-78.

Choo K.H., Choi S.J., Hwang E.D. (2007) Effect of coagulant type on textile wastewater reclamation in a combined coagulation/ultrafiltration system, *Desalination*, 202: 262-270.

Cicek N., Suidan M.T., Ginestet P., Audic J.M. (2003) Impact of soluble organic compounds on permeate flux in an aerobic membrane bioreactor, *Environmental Technology*, 24: 249-256.

Combe C., Molis E., Lucas P., Riley R., Clark, M. (1999) The effect of CA membrane Properties on adsorptive fouling by humic acid, *Membrane Science*, 154:73- 87.

Crozes G.F., Jacangelo J.G., Anselme C., Laine J.M. (1997) Impact of ultrafiltration operating conditions on membrane irreversible fouling, *Membrane science*, 124: 63-76.

Defrance L., Jaffrin M.Y. (1999) Comparison between filtration at fixed transmembrane pressure and fixed permeate flux: application to a membrane bioreactor used for wastewater treatment, *Membrane Science*, 152: 203-210.

Defrance L., Jaffrin M.Y., Gupta B., Paullier P., Geaugey V. (2000) contributions of various constituents of activated sludge to membrane bioreactor fouling, *Bioreactors Technology*, 73: 105-112.

Defrise D., Gekas V. (1988) Microfiltration membranes and the problem of microbial adhesion- A literature survey, *Process Biochemistry*, 23: 105-116.

Dong B.Z., Chen Y., Gao N.Y., Fan J.C. (2007) Effect of coagulation pretreatment on the fouling of ultrafiltration membrane, *Environmental science*, 19: 278-283

EEA. (2001) European Environment Agency, Copenhagen, Denmark. "Indicator: Biochemical oxygen demand in rivers".

Erbil H.Y. (2000) Vinyl acetate emulsion polymerization and copolymerization with acrylic Monomers, CRC Press LLC, Boca Raton, Florida.

Faibish R.S., Elimelech M., Cohen Y. (1998) Effect of interparticle electrostatic double layer interactions on permeate flux decline in crossflow membrane filtration of colloidal suspensions: An experimental investigation, *Colloid and Interface Science*, 204: 77-86.

Farahbakhsh K., Svrcek C., Guest R.K., Smith D.W. (2004) A review of the impact of chemical pre-treatment on low-pressure water treatment membranes. *Environmental and Engineering Science*, 3: 237-253.

Field R. (2010) Fundamentals of Fouling, in Membrane Technology: Membranes for Water Treatment, Volume 4 (eds K.-V. Peinemann and S. Pereira Nunes), Wiley-VCH Verlag GmbH & Co. KGaA, Weinheim, Germany.

Field R.W., Wu D., Howell J.A., Gupta B.B. (1995) Critical flux concept for microfiltration fouling, *Membrane Science*, 100: 259-272.

Frenander U., Jonsson A.S. (1996) cell harvesting by cross-flow microfiltration using a shear-enhanced module, *Biotechnology and Bioengineering*, 52: 397- 403.

Gabelich C.J. Yun T.I., Coffey B.M., Suffet M. (2002) Effects of aluminum sulphate and ferric chloride coagulant residuals on polyamide membrane performance, *Desalination*, 150: 15-30.

Gander M.A., Jefferson B., Judd S. J. (2000) Membrane bioreactors for use in small wastewater treatment plants: membrane materials and effluent quality, *Water Science and Technology*, 41 (1): 205-211.

Grady C.P.L., Daigger G.T., Lim H.C. (1999) Biological wastewater treatment, Marcel Dekker Inc., New York, NY.

Gregory J., Duan J. (2001) Hydrolyzing metal salts as coagulants, *Pure and Applied Chemistry*, 73(12): 2017-2026.

Guglielmi G., Chiarani D., Judd S.J., Andreottola G. (2007) Flux criticality and sustainability in a hollow fibre submerged membrane bioreactor for municipal wastewater treatment. *Membrane Science*, 289: 241-248.

Guigui C., Rouch J.C., Durand-Bourlier L., Bonnelye V., Aptel P. (2002) Impact of coagulation conditions on the in-line coagulation/UF process for drinking water production, *Desalination*, 147: 95-100.

Haberkamp J., Ruhl A. S., Ernst M., Jekel M. (2007) Impact of coagulation and adsorption on DOC fractions of secondary effluent and resulting fouling behaviour in ultrafiltration, *Water Research* ,41, (17): 3794-3802.

Harscoat C., Jaffrin M., Bouzerar R., Courtois J. (1999) Influence of fermentation conditions and microfiltration processes on membrane fouling during recovery of glucuronane polysaccharides from fermentation brooths, *Biotechnology and Bioengineering*, 65: 500- 511.

Hlavacek M., Bouchet F. (1993) Constant flow-rate blocking laws and an example of their application to dead end microfiltration of protein solutions, *Membrane science*, 82: 285-295.

Hong S.P., Bae T.H., Tak T.M., Hong S., Randall A. (2002) Fouling control in activated sludge submerged hollow fiber membrane bioreactors, *Desalination*, 143: 219–228.

Howe K.J., Clark M.M. (2002) Coagulation pretreatment for membrane filtration, AWWA Research Foundation Report, Denver, CO.

Howell J.A. (1995) Sub-critical flux operation of microfiltration, *Membrane Science*, 107: 165-171.

Huang X., Gui P., Qian Y. (2001) Effect of sludge retention time on microbial behaviour in a submerged membrane bioreactor, *Process Biochemistry*, 36: 1001-1006.

Itonaga T., Kimura K., Watanable Y. (2004) Influence of suspension viscosity and colloidal particles on permeability of membrane used in membrane bioreactor (MBR), *Water Science & Technology*, 50: 301-309.

Ivanovic I., Leiknes T.O., Odegaard H. (2008) Fouling control by reduction of submicron particles in a BF-MBR with an integrated flocculation zone in the membrane reactor, *Separation Science and Technology* 43(7): 1871-1883.

Jarusutthirak C., Amy G., Croué J. (2002) Fouling characteristics of wastewater effluent organic matter (EfOM) isolates on NF and UF membranes, *Desalination*, 145 (1-3): 247-255.

Jefferson B., Laine A.L., Judd S.J., Stephenson T. (2000) Membrane bioreactors and their role in wastewater reuse, *Water Science and Technology*, 41(1): 197-204.

Jiang J. (2001) Development of coagulation theory and pre-polymerized coagulants for water treatment, *Separation and Purification Methods,* 30(1): 127-141.

Jiang T., Kennedy M.D., Guinzbourg B.F., Vanrolleghem P.A., Schippers J.C. (2005) Optimising the operation of a MBR pilot plant by quantitative analysis of the membrane fouling mechanism, *Water Science and Technology*, 51: 19–25.

Jördening H.J., Winter J. (2005) Environmental Biotechnology: Concepts and Applications, WILEY-VCH Verlag GmbH & Co. KGaA, Weinheim.

Judd S. (2011) The MBR book: Principles and Applications of Membrane Bioreactors for Water and Wastewater Treatment, 2nd edition, Elsevier Ltd., London.

Judd S. J., Hillis P. (2001) Optimisation of combined coagulation and microfiltration for water treatment, *Water Research*, 35: 2895- 2904.

Kabsch-Korbutowicz M., Majewska-Nowak K., Winnicki T. (1999) Analysis of membrane fouling in the treatment of water solutions containing humic acids and mineral salts, *Desalination*, 126: 179-185.

Kerry J.H., Marwah A., Chiu K.P., Adham S.S. (2006) Effect of coagulation on the size of MF and UF membrane foulants, *Environmental Science and. Technology*, 40: 7908-7913.

Kim B.R., Anderson J.E., Muller S.A., Gaines W.A., Szafranski M.J., Bremmer A.L., Yarema G.J., Guciardo C.D., Lnden S., Doherty T.E. (2006) Design and start up of a membrane biological rector system at a ford-engine plant for treating oily wastewater, *Water Environmental Research*, 78(4): 362-371.

Kim S.H., Moon B.H., Leeb H. I. (2001) Effects of pH and dosage on pollutant removal and floc structure during coagulation, *Microchemical Journal*, 68 (2-3): 197-203.

Kim S.H., Moon S.Y., Yoon C.H., Yim S.K., Cho J.W. (2005) Role of coagulation in membrane filtration of wastewater for reuse, *Desalination*, 173: 301-307.

Kimura K., Hane Y., Watanabe Y. (2005) Effect of Pre-coagulation on mitigating irrervisble fouling during microfiltration of a surface water, *Water Science and Technology*, 51(6-7): 93-100.

Kwon D.Y., Vigneswaran S., Fane A.G, Ben Aim R. (2000) Experimental determination of critical flux in cross flow microfiltration, *Separation and Purification Technology*, 19: 169-181.

Laboussine-Turcaud V., Wiesner M.R., Bottero J.Y., Mallevialle J. (1990) Coagulation pretreatment for ultrafiltration of surface water, American Water Works Association, 82(12): 76-81.

Le- Clech P., Chen V., Fane T.A.G. (2006) Fouling in membrane bioreactors used in wastewater treatment, *Membrane Science*, 284: 17-53.

Lee W.N., Kang I.J., Lee C.H. (2006) Factor affecting filtration characteristics in membrane coupled Moving Bed Biofilm Reactor, *Water Research*, 40: 1827-1835.

Leiknes T., Ivanovic I., Odegard H. (2006) Investigating the effect of colloids on the performance of a biofilm membrane reactor (BF-MBR) for treatment of municipal wastewater, *Water South African*, 32(5): 708-714.

Leiknes T., Odegaard H. (2007) The development of a biofilm membrane bioreactor, *Desalination*, 202: 135-143.

Li H., Fane A.G., Coster H.G.L.,Vigneswaran S. (1998) Direct observation of particle deposition on the membrane surface during crossflow microfiltration, *Membrane Science*, 149: 83-97.

Li N.N., Fane A.G., Ho W.S.W., Matsuura T. (2008) Advanced membrane technology and applications, John Wiley & Sons, Inc., Hoboken, New Jersey.

Li X., Gao F., Hua Z., Du G., Chen J. (2005) Treatment of synthetic wastewater by a novel MBR with granular sludge developed for controlling membrane fouling, *Separation and Purification Technology*, 46 (1-2): 19-25.

Liu S., Xu Y., Bing W., Wei W. (2011) Test Study on Domestic Wastewater Treatment by Coagulate-MBR, International Conference on Multimedia Technology.

Lozier J. (2004) Microbial removal and integrity monitoring of high -pressure membranes, JWA, London, UK.

Maiorella B., Dorin G., Carion A., Harano D. (1991) Crossflow microfiltration of animal cells, *Biotechnology and Bioengineering*, 37: 121-126.

Melin E., Leikness H., Rasmussen V., Odegarard H. (2005) Effect of the organic loading rate on a wastewater treatment process combining Moving Bed Biofilm and Membrane Reactors, *Water Science and Technology*, 51(6-7): 421-430.

Mulder M. (1996) Basic principles of membrane technology, 2nd edition, Kluwer Academic, Dordrecht, The Netherlands.

MWH. (2005) Water treatment- Principles & Design, 2 nd edition, John Wiley & Sons, Inc, NY.

Newcombe G., Dixon D. (2006) Interface science in drinking water treatment: theory and application, Elsevier Ltd.

O'Melia C.R., Becker W.C., Au K.K. (1999) Removal of humic substances by coagulation, *Water Science and Technology*, 40(9): 47-54.

Odegaard H. (2006) Innovations in wastewater treatment: The Moving Bed Biofilm Process, *Water Science and Technology*, 53(9): 17-33.

Odegaard H., Glsvold B., Strickland J. (2000) The influence of carrier size and shape in the Moving Bed Biofilm Process, *Water Science and Technology*, 41(4-5): 383-391.

Odegaard H., Rusten B., Siljudalen J. (1999) The development of the moving bed biofilm process–from idea to commercial product, European Water Management, 2(2).

Odegaard H., Rusten B., Westrum T. (1994) A New Moving Bed Biofilm Reactor-Appliations And Results, *Water Science and Technology*, 29 (10-11): 157-165.

Ognier S., Wisnieswski C., Grasmick A. (2001) Biofouling in membrane bioreactors: phenomenon analysis and modelling, in: Proceedings of the MBR 3, Cranfield University, UK.

Pervissian A., Parker W.J., Legge R. (2011) Combined MBBR-MF for industrial wastewater treatment, *AIChE*, In press.

Pilutti M., Nemeth J. (2003) Technical and cost review of commercially available MF/UF membrane products, *Desalination*.

Pollice A., Brookes A., Jefferson B., Judd S. (2005) Sub-critical flux fouling in membrane bioreactors: a review of recent literature, *Desalination*, 174: 221–230.

Psoch C., Schiewer S. (2006) Resistance analysis for enhanced wastewater membrane filtration, *Membrane Science*, 280: 284–297.

Rahimi Y., Torabian A., Mehrdadi N., Habibi-Rezaie M., Pezeshk H., Nabi-Bidhendi G.R. (2011), Optimizing aeration rates for minimizing membrane fouling and its effect

on sludge characteristics in a Moving Bed Membrane Bioreactor, *Hazardous Materials*, 186: 1097-1102.

Randtke S.J. (1988) Organic contaminant removal by coagulation and related process combinations, *American Water Works Association*, 80(5): 40-56.

Richens D.T. (1997) The Chemistry of Aqua Ions, John Wiley & Sons Ltd., Chichester, England.

Rosenberger S., Laabs C., Lesjean B., Gnirss R., Amy G., Jekel M., Schrotter J.C. (2006) Impact of colloidal and soluble organic material on membrane performance in membrane bioreactors for municipal wastewater treatment, *Water Research*, 40: 710-720.

Ross C.C., Smith B.M., Valentine G.E. 2000. Rethinking Dissolved Air Flotation (DAF) design for industrial pretreatment, WEF and Purdue University Industrial Wastes Technical Conference, Environmental Treatment System, Inc., Atlanta, Georgia.

Russotti G., Goklen K.E. (2001) Crossflow membrane filtration of fermentation broth, Membrane Seperation in Biotechnology (Wang W.K., ed), pp 85-159, Marcel Dekker Inc., New york.

Rusten, B., McCoy M., Proctor R., Siljudalen J.G. (1998) The innovative Moving Bed Biofilm Reactor/solids contact reaeration process for secondary treatment of municipal wastewater, *Water Environment Research*, 70(5): 1083-1089.

Schäfer A.I., Fane A.G., Waite T.D. (2005) Nanofiltration: Principles and applications. Elsevier Ltd., NY.

Sethi S., Wiesner M.R. (2000) Simulated cost comparisons of hollow fiber and integrated nanofiltraton configurations, *Water Research,* 34(9): 2589-2597.

Sharp E.L., Parson S.A., Jefferson B. (2006) Coagulation of NOM: linking character to treatment, *Water Science and Technology*, 53(7): 67-76.

Tardieu E., Grasmick A., Geaugey V., Manem J. (1999) Influence of hydrodynamics on fouling velocity in a recirculated MBR for wastewater treatment, *Membrane Science*, 156: 131-140.

Taylor J.S. Wiesner M. (1999) Membranes, 5 [th] eddition, Letterman R.D. ed. ,Water Quality and Treatment, New York, McGraw Hill, Inc., 11 (1) 71.

Tchobanoglous G., Burton F.L., David Stensel H.(2003) Watewater engineering: Treatment and Reuse, Metcalf & Eddy Inc., New York, NY.

Tu S-C., Ravindran V., Den W., Pirbazari M. (2001) Predictive membrane transport model for nanofiltration processes in water treatment, *AIChE*, 47(6): 1346-1362.

Vyas H.K. Bennett R.J., Marshall A.D. (2002) Performance of crossflow microfiltration during constant transmembrane pressure and constant flux operations, *International Dairy*, 12: 473-479.

Wang Z., Wu Z., Tang S. (2009) Characterization of dissolved organic matter in a submerged membrane bioreactor by using three-dimensional excitation and emission matrix fluorescence spectroscopy, *Water Research*, 43(6): 1533-1540.

Wei C.H., Huang X., Aim R.B., Yamamoto K., Amy G. (2011). Critical flux and chemical cleaning- in- place during the long term operation of a pilot-scale submerged membrane bioreactor for municipal wastewater treatment, *Water Research*, 45(2): 863-871.

Wisniewski C., Grasmick A. (1998) Floc size distribution in a membrane bioreactor and consequences for membrane fouling, *Colloids and Surfaces A: Physicochemical and Engineering Aspects*, 138(2-3): 403-441.

Wu B., An Y., Li Y., Wong F.S. (2009) Effect of adsorption /coagulation on membrane fouling in microfiltration process post-treating anaerobic digestion effluent, *Desalination* ,242: 183-192.

Wu Z., Zhou Z., Wang Z., Tian L., Pan Y., Wang X. (2010) The Application of Membrane Bioreactor Technology to the Treatment of Wastewater from a Multifunctional Supermarket, *Environmental Progress and Sustainable Energy* , 29(1): 52-59.

Yamamoto K., Hiada M., Mahmood T., Matsue T. (1989) Direct solid-liquid separation using hollow fiber membrane in an activated sludge aeration tank, *Water Science and Technology*, 21 (4-5) : 43-54.

Yang B., Chen G., Chen G. (2012) Submerged membrane bioreactor in treatment of simulated restaurant wastewater, *Separation and Purification Technology*, 88: 184-190.

Yoon S. H, Collins J. H., Musale D., Sundararajan S., Tsai S. P, Hallsby G. A., Kong J. F., Koppes J., Cachia P. (2005) Effects of flux enhancing polymer on the characteristics of sludge in membrane bioreactor process, *Water Science and Technology,* 51(6-7): 151-7.

Yoon S., Collins J. H. (2006) A novel flux enhancing method for membrane bioreactor (MBR) process using polymer, *Desalination*, 191(1-3): 52-61.

Zeman L.J., Zydney A.L. (1996) Microfiltration and ultrafiltration: principles and applications, Marcel Dekker.

Zhang J., Chuan C.H., Zhou J., Fane A.G. (2006) Effect of sludge retention time on membrane bio-fouling intensity in a submerged membrane bioreactor, *Separation Science and Technology*, 41: 1313–1329.

Appendices

Appendix A

ACTIVECELL AREAL BIOMASS DENSITY TEST (AGTS)

Purpose:

While suspended growth may be readily measured, the amount of attached growth is more difficult to quantify on a daily basis. The procedure to determine the mass of biomass on the ActiveCell biofilm carriers is termed the biomass areal density test.

Materials:

- sample carrier pieces (minimum of 10, recommended 20)
- two beakers
- tweezers
- distilled water
- crucible (or large aluminum weigh dishes)
- oven (100 °C)
- desiccator
- 100 mL vials
- bleach
- weigh scale
- strainer

Procedure:

1. Use a clean beaker to scoop water (with carrier) from the bioreactor (suggested minimum # of carrier pieces = 10, recommended 20).
2. Using gloved hands, extract the carrier pieces, being careful not to dislodge any significant amount of biofilm (touch the exteriors of the carrier only) and place the pieces into a large beaker with fresh water. Let stand for 5 minutes (this should dislodge any loose biofilm that may cling to the carrier)
3. Touching only the exterior of the carrier, remove the carrier pieces from the beaker, place them in a pre-weighed crucible (or aluminum weigh dish) and place the crucible in an oven at a temperature of 100°C for 24 hours.
4. Remove the dried carrier pieces from the oven and put in a desiccator for > 1 hour and note the weight (in grams) (A).
5. Put the dried carrier pieces in individual 100 mL vials/beaker (5 pieces/vial) or all pieces in a larger vial, fill the vials with domestic bleach and cap them tightly.

6. Shake the contents of each vial 4-5 times for 1-2 minutes each. Place a stir bar in the vial/beaker and let them stir overnight.

7. Use a strainer to thoroughly wash the carrier pieces under running tap water and dry the carrier pieces on a towel paper for 15 minutes.

8. Put the carrier pieces in a pre-weighed crucible and place the crucible in an oven at a temperature of 100°C for 24 hours.

9. Remove the dried carrier pieces from the oven and put in a desiccator for 1 hour and note the weight (in grams) (B).

Calculations:

The results of the test and the calculation of the biomass density are shown below:

Weight of dried carrier = A

Weight of dried and cleaned carrier = B

# of test pieces = N

Weight of biomass = A − B

Weight of biomass per unit of carrier = (A − B) / (N)

Surface area per unit of carrier = 0.003792 m^2

Biomass Areal Density (g/m^2) = weight per unit carrier / surface area per unit carrier

Reference:

Headworks Bio Canada Inc. Victoria, BC

Appendix B

STATISTICAL ANALYSIS OF THE RESULTS

Table B-1: ANOVA Table to compare pH of MBBR effluent before and after upgrade

	Sum of Squares	df	Mean Square	F	Sig.
Between Groups	.050	1	.050	.328	.569
Within Groups	10.485	69	.152		
Total	10.534	70			

Table B-2: t-test to compare TKN of MBBR effluent before and after upgrade

	Sum of Squares	df	Mean Square	F	Sig.
Between Groups	5303.724	1	5303.724	4.936	.045
Within Groups	13969.284	13	1074.560		
Total	19273.008	14			

Table B-3: t-test too compare TCOD of MBBR influent before and after upgrade

	Sum of Squares	df	Mean Square	F	Sig.
Between Groups	6803609.452	1	6803609.452	13.801	.000
Within Groups	35002666.981	71	492995.310		
Total	41806276.433	72			

Table B-4: t-test to compareTSS of MBBR influent before and after upgrade

	Sum of Squares	df	Mean Square	F	Sig.
Between Groups	4692005.556	1	4692005.556	4.067	.048
Within Groups	70375685.714	61	1153699.766		
Total	75067691.270	62			

Table B-5: t-test to compare TP of MBBR influent before and after upgrade

	Sum of Squares	df	Mean Square	F	Sig.
Between Groups	45.893	1	45.893	.710	.411
Within Groups	1099.462	17	64.674		
Total	1145.355	18			

Table B-6: t-test to compare NH_3 of MBBR influent before and after upgrade

	Sum of Squares	df	Mean Square	F	Sig.
Between Groups	367.607	1	367.607	4.462	.043
Within Groups	2636.126	32	82.379		
Total	3003.734	33			

Table B-7: t-test to compare %SCOD removal of MBBR before and after upgrade

	Sum of Squares	df	Mean Square	F	Sig.
Between Groups	314.786	1	314.786	4.489	.038
Within Groups	4137.244	59	70.123		
Total	4452.030	60			

Table B-8: ANOVA to compare TSS of concentrate streams of replicates (600 mg/l, 8.7 LMH)

	Sum of Squares	df	Mean Square	F	Sig.
Between Groups	26165660.417	2	13082830.208	3.235	.101
Within Groups	28309002.083	7	4044143.155		
Total	54474662.500	9			

Table B-9: Tukey test to compare total resistances of trials 600, 800, and 1000 mg/l

(I) Dose	(J) Dose	Mean Difference (I-J)	Std. Error	Sig.	95% Confidence Interval	
					Lower Bound	Upper Bound
600.00	800.00	6.00067E+11	7.63558E+11	.716	-1.3245E+12	2.5247E+12
	1000.00	-1.6061E+11	8.53684E+11	.000	-1.8213E+13	-1.3909E+13
800.00	600.00	-6.0007E+11	7.63558E+11	.716	-2.5247E+12	1.3245E+12
	1000.00	-1.6661E+13[*]	8.53684E+11	.000	-1.8813E+13	-1.4509E+13
1000.00	600.00	1.6061E+13[*]	8.53684E+11	.000	1.3909E+13	1.8213E+13
	800.00	1.6661E+13[*]	8.53684E+11	.000	1.4509E+13	1.8813E+13

*. The mean difference is significant at the 0.05 level.

Table B-10: ANOVA to compare TSS of the concentrate streams of 600, 800, and 1000 mg/l trials (7.6 LMH)

	Sum of Squares	df	Mean Square	F	Sig.
Between Groups	47466066.667	2	23733033.333	8.230	.019
Within Groups	17301533.333	6	2883588.889		
Total	64767600.000	8			

Table B-11: Tukey test to compare TSS of the concentrate streams (600, 800, 1000 mg/l)

(I) Dose	(J) Dose	Mean Difference (I-J)	Std. Error	Sig.	95% Confidence Interval	
					Lower Bound	Upper Bound
600.00	800.00	-146.66667	1386.50373	.994	-4400.8409	4107.5075
	1000.00	-4943.33333*	1386.50373	.028	-9197.5075	-689.1591
800.00	600.00	146.66667	1386.50373	.994	-4107.5075	4400.8409
	1000.00	-4796.66667*	1386.50373	.031	-9050.8409	-542.4925
1000.00	600.00	4943.33333*	1386.50373	.028	689.1591	9197.5075
	800.00	4796.66667*	1386.50373	.031	542.4925	9050.8409

*. The mean difference is significant at the 0.05 level.

Table B-12: ANOVA to compare Colloidal COD of trial 600, 800 and 1000 mg/l (7.6 LMH)

	Sum of Squares	df	Mean Square	F	Sig.
Between Groups	1448.767	2	724.383	.719	.520
Within Groups	7054.833	7	1007.833		
Total	8503.600	9			

Table B-13: Tukey- tests to compare total resistances of trials 200,400, and 600 mg/l

(I) Dose	(J) Dose	Mean Difference (I-J)	Std. Error	Sig.	95% Confidence Interval	
					Lower Bound	Upper Bound
200.00	400.00	7.4780E+13*	8.03203E+11	.000	7.2740E+13	7.6821E+13
	600.00	6.7168E+13*	8.20935E+11	.000	6.5083E+13	6.9254E+13
400.00	200.00	-7.4780E+13*	8.03203E+11	.000	-7.6821E+13	-7.2740E+13
	600.00	-7.6120E+12*	6.99722E+11	.000	-9.3896E+12	-5.8344E+12
600.00	200.00	-6.7168E+13*	8.20935E+11	.000	-6.9254E+13	-6.5083E+13
	400.00	7.6120E+12*	6.99722E+11	.000	5.8344E+12	9.3896E+12

*. The mean difference is significant at the 0.05 level.

Table B-14 ANOVA to compare TSS concentration of MR feed streams of 200, 400, and 600 mg/l

	Sum of Squares	df	Mean Square	F	Sig.
Between Groups	247088.889	2	123544.444	5.450	.045
Within Groups	136000.000	6	22666.667		
Total	383088.889	8			

Table B-15 Tukey test to compare TSS concentration of MR feed streams of 200, 400, and 600 mg/l

(I) Dose	(J) Dose	Mean Difference (I-J)	Std. Error	Sig.	95% Confidence Interval	
					Lower Bound	Upper Bound
200.00	400.00	-110.00000	122.92726	.663	-487.1746	267.1746
	600.00	-393.33333*	122.92726	.043	-770.5079	-16.1587
400.00	200.00	110.00000	122.92726	.663	-267.1746	487.1746
	600.00	-283.33333	122.92726	.131	-660.5079	93.8413
600.00	200.00	393.33333*	122.92726	.043	16.1587	770.5079
	400.00	283.33333	122.92726	.131	-93.8413	660.5079

*. The mean difference is significant at the 0.05 level.

Table B-16 ANOVA to compare TSS concentration of concentrate streams of 200, 400, and 600 mg/l

	Sum of Squares	df	Mean Square	F	Sig.
Between Groups	11971822.222	2	5985911.111	9.914	.013
Within Groups	3622800.000	6	603800.000		
Total	15594622.222	8			

Table B-17 Tukey test to compare TSS concentration of concentrate streams of 200, 400, and 600 mg/l

(I) Dose	(J) Dose	Mean Difference (I-J)	Std. Error	Sig.	95% Confidence Interval	
					Lower Bound	Upper Bound
200.00	400.00	-360.00000	634.45515	.842	-2306.6826	1586.6826
	600.00	-2606.66667*	634.45515	.015	-4553.3493	-659.9840
400.00	200.00	360.00000	634.45515	.842	-1586.6826	2306.6826
	600.00	-2246.66667*	634.45515	.028	-4193.3493	-299.9840
600.00	200.00	2606.66667*	634.45515	.015	659.9840	4553.3493
	400.00	2246.66667*	634.45515	.028	299.9840	4193.3493

*. The mean difference is significant at the 0.05 level.

Table B-18: t- tests to compare SCOD of the membrane of 400 and 600 mg/l trials

	600 mg/l	400 mg/l
Mean	151.75	120
Variance	1536.438	400
Observations	3	3
Hypothesized Mean Difference	0	
df	3	
t Stat	1.249691	
P(T<=t) one-tail	0.150014	
t Critical one-tail	2.353363	
P(T<=t) two-tail	0.300028	
t Critical two-tail	3.182446	

Table B-19: t-test to compare Colloidal COD of MR for trials of 200 and 400 mg/l

	200 mg/l	400 mg/l
Mean	144.9167	55
Variance	393.2708	325
Observations	3	3
Hypothesized Mean Difference	0	
df	4	
t Stat	5.811078	
P(T<=t) one-tail	0.002182	
t Critical one-tail	2.131847	
P(T<=t) two-tail	0.004364	
t Critical two-tail	2.776445	

Table B-20: Tukey test to compare resistances of 600 mg/l (7.6 and 8.7 LMH) before and after upgrade

(I) Trials	(J) Trials	Mean Difference (I-J)	Std. Error	Sig.	95% Confidence Interval	
					Lower Bound	Upper Bound
1.00	2.00	-6.8324E+12*	8.09431E+11	.000	-9.0293E+12	-4.6355E+12
	3.00	6.5553E+12*	8.3434E+11	.000	4.2909E+12	8.8198E+12
	4.00	3.92356E+11	8.0943E+11	.962	-1.8045E+12	2.5892E+12
2.00	1.00	6.8324E+12*	8.0943E+11	.000	4.6355E+12	9.0293E+12
	3.00	1.3388E+13*	8.3434E+11	.000	1.1123E+13	1.5652E+13
	4.00	7.2248E+12*	8.09431E+11	.000	5.0279E+12	9.4216E+12
3.00	1.00	-6.5553E+12*	8.34342E+11	.000	-8.8198E+12	-4.2909E+12
	2.00	-1.3388E+13*	8.34342E+11	.000	-1.5652E+13	-1.1123E+13
	4.00	-6.1630E+12*	8.34342E+11	.000	-8.4274E+12	-3.8985E+12
4.00	1.00	-3.9236E+11	8.09431E+11	.962	-2.5892E+12	1.8045E+12
	2.00	-7.2248E+12*	8.09431E+11	.000	-9.4216E+12	-5.0279E+12
	3.00	6.1630E+12*	8.34342E+11	.000	3.8985E+12	8.4274E+12

*. The mean difference is significant at the 0.05 level.

Table B-21: t-test to compare TSS of the membrane feed for 600 mg/l, 8.7 LMH before and after upgrade

	8.7 BU	8.7 AU
Mean	2813.333	1360
Variance	692233.3	126100
Observations	3	3
Hypothesized Mean Difference	0	
df	3	
t Stat	2.782664	
P(T<=t) one-tail	0.034419	
t Critical one-tail	2.353363	
P(T<=t) two-tail	0.068838	
t Critical two-tail	3.182446	

Table B-22: t-test to compare TSS of the membrane feed for 600 mg/l, 7.6 LMH before and after upgrade

	7.6 BU	*7.6 AU*
Mean	2430	1916.667
Variance	100	5433.333
Observations	3	3
Hypothesized Mean Difference	0	
df	2	
t Stat	11.95272	
P(T<=t) one-tail	0.003463	
t Critical one-tail	2.919986	
P(T<=t) two-tail	0.006927	
t Critical two-tail	4.302653	

Table B-23: t-test to compare TSS of the concentrate stream for 600 mg/l, 8.7 LMH before and after upgrade

	8.7 BU	*8.7 AU*
Mean	7633.333	5200
Variance	1241733	84400
Observations	3	3
Hypothesized Mean Difference	0	
df	2	
t Stat	3.659895	
P(T<=t) one-tail	0.033608	
t Critical one-tail	2.919986	
P(T<=t) two-tail	0.067216	
t Critical two-tail	4.302653	

Table B-24: ANOVA to compare SCOD of the membrane for 600 mg/l, 7.6/ 8.7 LMH before and after upgrade

	Sum of Squares	df	Mean Square	F	Sig.
Between Groups	20911.81	3	6970.602	1.266601	0.357167
Within Groups	38523.75	7	5503.393		
Total	59435.56	10			

Table B-25: ANOVA to compare colloidal COD of the membrane for 600 mg/l, 7.6/ 8.7 LMH before and after upgrade

	Sum of Squares	df	Mean Square	F	Sig.
Between Groups	12938.84	3	4312.946	2.317305	0.162231
Within Groups	13028.33	7	1861.19		
Total					

Table B-26: t-test to compare TCOD of membrane feed for 400 mg/l trials

	9.8 LMH	*7.6 LMH*
Mean	1898.667	1446.667
Variance	30405.33	28633.33
Observations	3	3
Hypothesized Mean Difference	0	
df	4	
t Stat	3.222039	
P(T<=t) one-tail	0.016109	
t Critical one-tail	2.131847	
P(T<=t) two-tail	0.032218	
t Critical two-tail	2.776445	

Table B-27: t-test to compare colloidal COD of membrane tank for 400 mg/l trials

	7.6 LMH	*9.8 LMH*
Mean	55	29
Variance	325	73
Observations	3	3
Hypothesized Mean Difference	0	
df	3	
t Stat	2.257316	
P(T<=t) one-tail	0.054598	
t Critical one-tail	2.353363	
P(T<=t) two-tail	0.109196	
t Critical two-tail	3.182446	

Table B-28: t-test to compare TSS of membrane feed for 400 mg/l trials

	9.8 LMH	*7.6 LMH*
Mean	1710	1633.333
Variance	777100	60833.33
Observations	3	3
Hypothesized Mean Difference	0	
df	2	
t Stat	0.145065	
P(T<=t) one-tail	0.44898	
t Critical one-tail	2.919986	
P(T<=t) two-tail	0.897959	
t Critical two-tail	4.302653	

Table B-29: t-test to compare TSS of concentrate stream for 400 mg/l trials

	9.8 LMH	*7.6 LMH*
Mean	4893.333	3576.667
Variance	679033.3	206633.3
Observations	3	3
Hypothesized Mean Difference	0	
df	3	
t Stat	2.423267	
P(T<=t) one-tail	0.046947	
t Critical one-tail	2.353363	
P(T<=t) two-tail	0.093894	
t Critical two-tail	3.182446	

Table B-30: ANOVA to compare SCOD of MR feed stream for 600 mg/l trials for all fluxes

	Sum of Squares	df	Mean Square	F	Sig.
Between Groups	61224.042	2	30612.021	7.830	.021
Within Groups	23456.083	6	3909.347		
Total	84680.125	8			

Table B-31: Tukey tests to compare SCOD of MR feed stream for 600 mg/l trials for all fluxes

(I) Flux	(J) Flux	Mean Difference (I-J)	Std. Error	Sig.	95% Confidence Interval	
					Lower Bound	Upper Bound
7.60	8.70	-140.91667	51.05126	.073	-297.5560	15.7226
	9.80	-195.83333[*]	51.05126	.020	-352.4726	-39.1940
8.70	7.60	140.91667	51.05126	.073	-15.7226	297.5560
	9.80	-54.91667	51.05126	.562	-211.5560	101.7226
9.80	7.60	195.83333[*]	51.05126	.020	39.1940	352.4726
	8.70	54.91667	51.05126	.562	-101.7226	211.5560

*. The mean difference is significant at the 0.05 level.

Table B-32: ANOVA to compare colloidal COD of MR feed stream for 600 mg/l trials for all fluxes

	Sum of Squares	df	Mean Square	F	Sig.
Between Groups	54967.792	2	27483.896	9.400	.014
Within Groups	17543.083	6	2923.847		
Total	72510.875	8			

Table B-33: Tukey tests to compare colloidal COD of MR feed stream for 600 mg/l trials for all fluxes

(I) Flux	(J) Flux	Mean Difference (I-J)	Std. Error	Sig.	95% Confidence Interval	
					Lower Bound	Upper Bound
7.60	8.70	-130.08333	44.15010	.058	-265.5480	5.3813
	9.80	-186.66667[*]	44.15010	.013	-322.1313	-51.2020
8.70	7.60	130.08333	44.15010	.058	-5.3813	265.5480
	9.80	-56.58333	44.15010	.454	-192.0480	78.8813
9.80	7.60	186.66667[*]	44.15010	.013	51.2020	322.1313
	8.70	56.58333	44.15010	.454	-78.8813	192.0480

*. The mean difference is significant at the 0.05 level.

Table B-34: ANOVA to compare TCOD of MR feed stream for 600 mg/l trials for all fluxes

	Sum of Squares	df	Mean Square	F	Sig.
Between Groups	3599503.125	2	1799751.563	5.727	.041
Within Groups	1885462.500	6	314243.750		
Total	5484965.625	8			

Table B-35: Tukey tests to compare TCOD of MR feed stream for 600 mg/l trials for all fluxes

(I) Flux	(J) Flux	Mean Difference (I-J)	Std. Error	Sig.	95% Confidence Interval	
					Lower Bound	Upper Bound
7.60	8.70	-501.25000	457.70715	.551	-1905.6212	903.1212
	9.80	-1520.00000*	457.70715	.037	-2924.3712	-115.6288
8.70	7.60	501.25000	457.70715	.551	-903.1212	1905.6212
	9.80	-1018.75000	457.70715	.145	-2423.1212	385.6212
9.80	7.60	1520.00000*	457.70715	.037	115.6288	2924.3712
	8.70	1018.75000	457.70715	.145	-385.6212	2423.1212

*. The mean difference is significant at the 0.05 level.

Table B-36: ANOVA to compare TSS concentration of concentrate stream for 600 mg/l trials for all fluxes

	Sum of Squares	df	Mean Square	F	Sig.
Between Groups	728088.889	2	364044.444	.566	.596
Within Groups	3860533.333	6	643422.222		
Total	4588622.222	8			

Table B-37: t-test to compare TSS of concentrate stream for 800 mg/l trials

	9.8 LMH	*7.6 LMH*
Mean	16016.67	7180
Variance	30833.33	3500800
Observations	3	3
Hypothesized Mean Difference	0	
df	2	
t Stat	8.144441	
P(T<=t) one-tail	0.007372	
t Critical one-tail	2.919986	
P(T<=t) two-tail	0.014743	
t Critical two-tail	4.302653	

Table B-38: t-test to compare colloidal COD of the membrane for 800 mg/l trials

	9.8 LMH	*7.6 LMH*
Mean	147.0833	55
Variance	481.7708	212.6667
Observations	3	4
Hypothesized Mean Difference	0	
df	3	
t Stat	6.298265	
P(T<=t) one-tail	0.004043	
t Critical one-tail	2.353363	
P(T<=t) two-tail	0.008086	
t Critical two-tail	3.182446	